EVALUATION OF THE GROUND CONTROL DISTRICTS CLASSIFICATION AND SUPPORT METHODOLOGY AT KOPANANG MINE

Fezekile Pearl Mosiane

0305916R

A research report submitted to the Faculty of Engineering and the Built Environment, University of the Witwatersrand, in partial fulfilment of the requirements for the degree of Master of Science in Engineering.

Johannesburg, 2021

Evaluation of the Ground Control Districts Classification and Support Methodology at Kopanang Mine

Name: Fezekile Pearl Mosiane

Student ID: 0305916R

Supervisor: Professor Rudrajit Mitra

Department: School of Mining Engineering

University: University of the Witwatersrand, Johannesburg, South Africa

Degree: Master of Science in Engineering (Mining)

DECLARATION

I declare that this research report is my own, unaided work. It is being submitted for the Degree of Master of Science in Engineering at the University of the Witwatersrand, Johannesburg. It has not been submitted before for any degree or examination in any other University.

Fezekile Pearl Mosiane

October 2021

In Johannesburg

ABSTRACT

This research project aims to review the classification of ground control districts at Kopanang mine. A ground control district (GCD) is defined as a portion of the mine in which a given set of geological conditions, with associated rock-related hazards, permits a common set of rock engineering strategies to be employed to minimize the risks.

Ground control districts at Kopanang mine are currently delineated to address those areas that display a measurable and unique response to mining, either in the form of mining induced seismicity, or some other measurable rock mass response such as closure rate, geological structures or rock mass fracturing. However, there have been recent concerns regarding the unstable footwall behaviour in some portions of the mine and the inability of the current support system to address this instability. The factors driving this kind of footwall behaviour are currently not well understood at the mine. It is envisaged that if these factors can be understood, then the ground control districts can be re-delineated. This will ensure that specific support strategies are applied to precisely address specific ground control or rock mass problems.

This research aims to establish a method to delineate these ground control districts to ensure that, ultimately, suitable mining and support strategies are being utilized in the relevant areas.

To achieve this, rock mass classification methods were used to determine the quality of the rock mass and to establish the influence of lateral variation in the Vaal reef package across the mine. Results of numerical modelling analysis were also used to evaluate the influence of stress on the rock mass quality across the mine. Lastly, a comparison was done between the actual support installed in the different regions or zones of the mine and the requirements as determined by rock mass classification methods and numerical modelling.

Conclusions were then drawn, and recommendations made on the proposed classification or delineation of the ground control districts at Kopanang mine.

DEDICATION

This research is dedicated to:

My late father, Isaac Nhlapo and late sister, Brenda Nhlapo

ACKNOWLEDGEMENTS

In completing this research, many people generously dedicated their time and to them I will forever be grateful, “To all of you, thank you for your part in my journey”.

First and foremost, I would like to thank God, the Almighty from whom all good things come, “Daddy God, thank you for waking me up every morning, for keeping me together when I was falling apart and for giving me the strength to keep going”.

My most sincere gratitude to my research supervisor, Professor Rudrajit Mitra for his academic guidance and support, it has been said, “Teaching is the greatest act of optimism”.

Special thanks to the Management Team at Kopanang mine and Open House Management Solutions for allowing me to conduct this research. I will be forever indebted to the Geology department, particularly Wendy Chabangu and Vusi Luphahla for always taking the time to entertain my questions. To Pule Molisalife, for those underground visits and data collection that seemed to take forever.

Many thanks to my mom, for agreeing to babysit for weeks on end, and finally yet importantly, to my son, Neo, “Dodo, thank you for your understanding when mommy’s work took up your time as well”.

TABLE OF CONTENTS

LIST OF FIGURES

LIST OF TABLES

CHAPTER 1: INTRODUCTION

A ground control district (GCD) is defined as a portion of the mine in which a given set of geological conditions, with associated rock-related hazards, permits a common set of rock engineering strategies to be employed to minimize the risks (Jager & Ryder, 1999).

Ground control districts at Kopanang mine are delineated to address those areas that display a measurable and unique response to mining, either in the form of mining-induced seismicity, or some other measurable rock mass response such as closure rate, geological structures or rock mass fracturing. However, there have been recent concerns regarding the unstable footwall behaviour in some portions of the mine and the inability of the current support system to address this instability. The factors driving this kind of footwall behaviour are currently not well understood at the mine. A proper understanding of these driving factors can lead to better re-delineation of ground control districts. This will ensure that tailor-made support strategies are applied to address specific ground concerns.

In general mining terminology, the footwall is defined as the mass of rock below the reef plane (Spearing, 1995). In intermediate-depth mines, which according to Jager and Ryder (1999) typically range from mining depths of 1000m to 2250m, access to the ore deposit is predominantly gained via a shaft system and a network of haulages, crosscuts, reef drives and stope gullies. At this depth, stress conditions range from low to moderately high, with k-ratios being less than 1.The excavations are usually surrounded by an envelope of fractured rock and closure rates vary but are generally high (Jager & Ryder, 1999). In this type of environment, scattered mining is the preferred method of mining.

In scattered mining, access development is generally located in the footwall of the reef and the stability and longevity thereof is very much dependant on the competence and ability of the footwall to withstand the various mining factors and conditions to which it might be subjected.

Premature loss of access ways often leads to costly re-development and/or rehabilitation costs. The effects can be more catastrophic, leading to multiple injuries and loss of lives if such failures occur abruptly and without warning. It is for this reason that a proper understanding of the factors driving failure in footwall development is necessary. By narrowing down the driving factors, it is possible to ultimately derive mining and support strategies that present a specific solution to a specific problem.

By analysing data from Kopanang Mine, this research endeavours to improve the current understanding of the footwall behaviour and to provide reasons and possible mitigation for the undesired rock mass behaviour and failure currently experienced.

1.1. Background

Kopanang mine is situated immediately south of the Vaal River in the Free State province. It is located east of Orkney and southeast of Klerksdorp and forms part of the Vaal River operations as indicated by the black arrow in Figure 1.

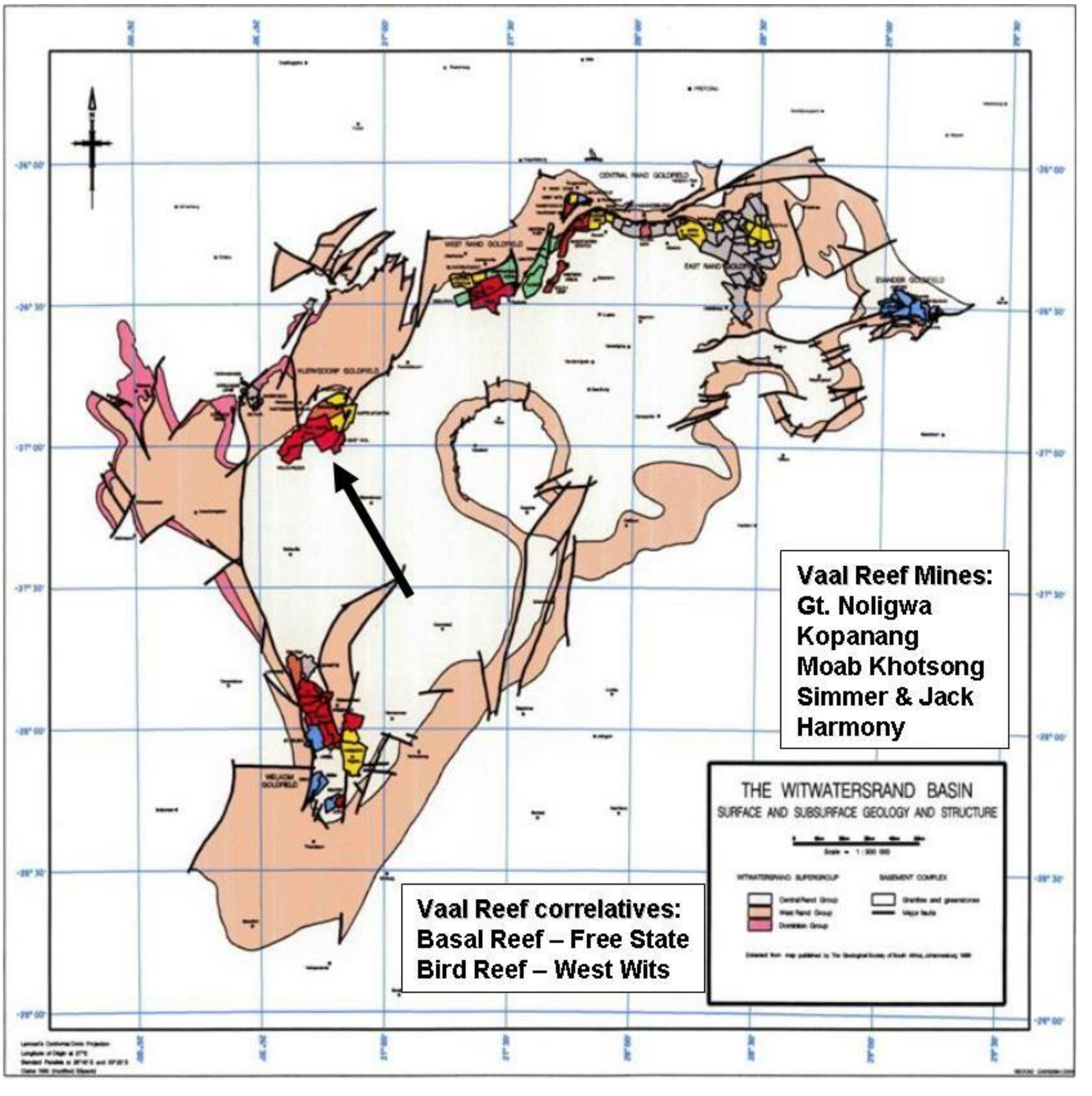

Figure 1: Location of Kopanang mine relative to the Witwatersrand Basin (COP, 2017)

The mine forms part of the Johannesburg subgroup of the Central Rand Group of the Witwatersrand Supergroup. Kopanang mine exploits the Vaal and Crystalkop reefs of the Klerksdorp Goldfield at mining depths ranging between 1200m and 2100m below the surface and can thus be classified as an intermediate depth to deep level mine.

1.2. Geological Setting

Mining in the Klerksdorp Goldfields exposes rocks of the Gold Estates (GE) and Main Bird (MB) formations. The Vaal reef occurs at the base of the MB4 unit, which is underlain by the MB5 to MB10 units of which only the MB5, MB6 and MB7 units are routinely exposed in underground workings. The Vaal reef is the principal reef being mined at Kopanang mine.

The Vaal reef footwall haulages are developed predominantly in competent MB6 quartzite with a uniaxial compressive strength (UCS) ranging between 180MPa and 220MPa. Generally, crosscuts are driven through the MB6 quartzite to approximately 50m below reef before the MB5 quartzite, which forms the immediate footwall to the Vaal reef, is intersected. The MB5 unit is a heterogeneous package of medium-grained argillaceous and siliceous quartzite with occasional grit bands and shale partings with an average UCS of 172MPa (COP, 2017). Figure 2 shows the stratigraphy of the Witwatersrand basin.

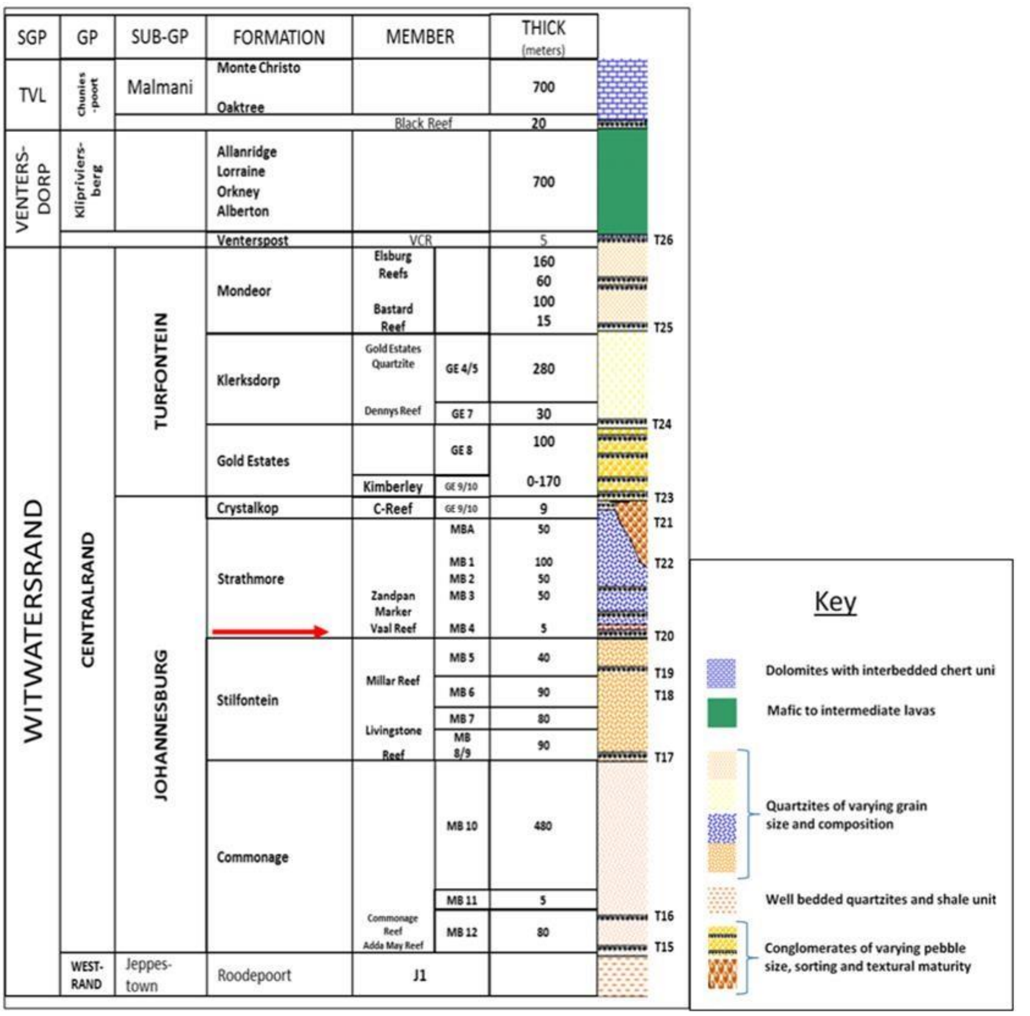

Figure 2: Generalized stratigraphic column of the Witwatersrand Basin (Watts, 2006)

1.3. Seismological and Geotechnical Setting

Mining at Kopanang mine can be divided into three main areas namely Vaal reef, C reef and off-reef mining. The three main areas, in turn, translate into the three-ground control districts defined for the mine. The mine is regarded as being moderately seismically active with the largest seismic event ever recorded by the mine's seismic monitoring system being an M3.4 in 2005 (COP, 2017). The main seismic emission sources are identified and grouped as follows:

- Geological features (faults and dykes), particularly at their intersections
- Intersections of geological features close mining operations and
- Pillars, particularly when intersected by geological features.

The geotechnical environment of the mine is characterized by the following:

- **Moderate closure rates and the possibility of damaging seismic emissions**
  All the workings on Kopanang Mine can be classified as being low to moderately seismically active. Seismic activity varies in terms of rates and locations.
- **The presence and complexity of low angle joints and faulting**
  The entire lease area on Kopanang Mine is traversed by numerous geological structures and zones of weakness could be intersected in any of the mining blocks as mining progresses. These give rise to potential gravity induced structural failure due to block release along planes of weakness.
- **The thickness, relative strengths and local distribution of the hanging wall and footwall lithologies**
  These could have an overriding influence on the behaviour of the peripheral rock mass. The reef horizon and surrounding lithologies are relatively uniform in nature and generally exhibit a similar rock mass response during mining.
- **The presence of shale or cross bedding in the immediate hanging wall beams**
  These often impact on local rock mass stability within the workings.
- **Back break / beam failure**
  This failure is geologically driven where potential unstable wedges are formed due to geological structures dipping in opposite directions in the absence of horizontal stress.

1.4. Problem Statement

Instability in footwall development may manifest itself as catastrophic falls of ground with the potential to induce multiple injuries and fatal accidents. Premature collapse and closure of access development may not only lead to costly re-development and rehabilitation costs but may in many cases lead to premature sterilization and loss of otherwise profitable ore reserves.

A lack of proper understanding of the behaviour of the footwall and the factors that lead to this kind of behaviour leads to the inability to prescribe the correct design methodology as well as the correct support measures for these conditions.

At Kopanang mine, the failure mode in the footwall, as well as the factors that influence and govern this failure are not properly understood. Instead, a one-size fits all approach has been utilized over the years to successfully manage rock mass response in the different ground control districts of the mine.

The consequence of this ill-fitting approach has been uncontrolled footwall development failure and premature loss of accesses. The incidents pose a threat to the safety of underground workers and the economic extraction of the orebody.

An understanding of a reliable methodology for delineation of ground control districts is thus necessary to ensure that the support systems utilized across the mine are suitable for the conditions in which they are applied.

1.5. Research Objectives

The proposed research aims to investigate the factors influencing the behaviour of the footwall at Kopanang mine and based on these factors, to re-classify the ground control districts at the mine. The research will evaluate the contributing factors in terms of the influence of the:

- Differences in rock mass quality across the mine by applying rock mass characterization
- Mining induced stress; and
- Support systems currently in use at Kopanang mine

Once the influencing factors have been determined, the research aims to determine the support requirements for the footwall at Kopanang mine and to make conclusions and recommendations to that effect.

1.6. Research Methodology

The method of research employed in this study involved primarily a comprehensive review of available literature on the subject. The purpose of the literature review was to establish what work had previously been done on the subject matter. The second reason for reviewing of literature was to evaluate methods previously used by other researchers to get to certain conclusions on the matter.

The literature review was followed by underground visits to the concerned areas and the logging of core from underground boreholes. The purpose for the logging of the core was to determine the rock mass properties such as the quality, frequency, and nature of the discontinuities as well as the influence of groundwater, if any.

The information from the core-logging was then used in the application of various rock mass classification systems. This was done to obtain an understanding of the strength of the rock mass. The core-logging would also assist in determining whether the behaviour of the rock mass is influenced by the rock mass composition, failure mechanism or by lateral and/or vertical variations.

The influence of stress on the rock mass behaviour was then assessed using numerical modelling. Tunnels subjected to the same mining conditions in terms of mining extent, mining span, geological complexity but different depths were modelled, and the results compared.

Lastly, a comparison was done in terms of the support currently installed in these areas and the support recommended by the various classification systems and the numerical modelling results.

From this study, conclusions were drawn, and recommendations were made in terms of the re-classification of the ground control districts and the most suitable support strategies for the prevailing conditions.

1.7. Contents of the Research Report

This chapter of the research report presented a brief background on Kopanang mine. This entailed a description of the location, geological nature and geotechnical setting of the mine. The problem statement, which provided insight into the footwall development challenges currently experienced by the mine, was also discussed.

Factors governing footwall instability were listed. Lastly, the methodology employed for the research was briefly discussed.

Chapter 2 of this research report reviews the literature applicable to this study. Rock mass classification systems, particularly, ones deemed to be the most appropriate for the mining environment at Kopanang mine are reviewed. Rock mass failure mechanisms are also reviewed with special emphasis on the Mohr-Coulomb, Hoek Brown, Griffith’s cracks analysis and the Extension Strain Criterion. In-situ rock mass parameters are reviewed with an understanding that reliable estimates of the strength and deformation of rock masses are required for almost any form of underground excavation design. Furthermore, Chapter 2 evaluates analytical design methods with special emphasis on support design methodology and the mechanisms of support based on rock-support system interaction.

Chapter 3 gives a comprehensive study approach used by the author to meet the research objectives. Chapter 4 presents the findings and discussion on the rock mass classification conducted by applying the Q-system, the modified Q-system and the Geomechanics classification on 20 borehole core samples obtained at the mine.

Chapter 5 presents the results and discussion on the numerical modelling analysis for the different areas of the mine. This analysis was conducted to understand the influence of stress variation on excavations. This influence is explained through a case study which considers the behaviour of tunnels subjected to varying conditions. An evaluation for the selection of suitable support for the various conditions is discussed in Chapter 6. Chapter 7 outlines the conclusions drawn from the research and discusses the recommendations emanating from the research.

CHAPTER 2: LITERATURE REVIEW

2.1 Introduction

This chapter reviews fundamental knowledge on the research and critically assesses previous literature. This is done to gain an understanding of the research problem and to come up with effective solutions. The research looks at the application of rock mass classification systems as well as their shortcomings. The importance of these systems is emphasised in that it allows one to relate a set of conditions to that already encountered by others and thus forms an integral part of the design process.

An overview of the failure mechanisms is also conducted to get an understanding of the processes involved with and the factors that usually influence different failure modes.

Lastly, with the aid of numerical modelling, a review of support mechanisms is conducted where different types of support and their mode of application is assessed.

2.2 Overview of Rock Mass Classification Systems

Rock mass classification systems and their application in rock mechanics and mine design have been investigated and studied by various authors. Hoek and Brown (1980) state that the beauty of rock mass classifications lies in their ability to enable one to relate one's set of conditions to conditions encountered by others.

With rock mass classification systems, it is possible to relate the experience on rock conditions and support requirements gained in other areas to a specific problem, particularly when it is necessary to make a design decision where engineering judgement and practical experience must play an important part. Bieniawski (1989) lists the objectives of rock mass classifications as:

- To identify the most significant parameters influencing the behaviour of a rock mass
- To divide a rock mass formation into areas of similar behaviour, that is, rock mass classes of varying quality
- To provide a basis for understanding the characteristics of each rock mass class
- To relate the experience of rock conditions at one site to the conditions and experiences encountered at others
- To derive quantitative data and guidelines for engineering design
- To provide a common basis for communication between engineers and geologists.

According to Jager and Ryder (1999), rock mass classification systems attempt to define the characteristics of the rock mass based on a simplified assessment of critical rock mass parameters. It is further mentioned by Jager and Ryder (1999) that rock mass classification systems cater well for low-stress environments where geological discontinuities control the instabilities involved. They also stress the usefulness and application of these systems when the level of available data is insufficient to conduct a detailed structural analysis of the rock mass and potential failure mechanisms.

In general, rock mass classifications work by assigning a numerical value to those properties or features of the rock mass considered likely to influence its behaviour, and to combine the individual values into one overall classification rating for the rock mass (Brady & Brown, 1993).

The parameters most employed by rock mass classification systems are described by Swart (2005) to include:

- Rock material strength
- Rock quality designation (RQD)
- Spacing of discontinuities
- Condition of discontinuities (roughness, continuity, separation, joint wall weathering, infilling)
- Orientation of discontinuities
- Groundwater conditions and in situ stresses.

Brady and Brown (1993) continue to list the aspects of rock mass behaviour that have been studied using rock mass classifications to include, stable spans of unsupported excavations, stand up times of given unsupported spans and support requirements for various spans.

While recognizing the importance and usefulness of rock mass classification systems, Brady and Brown (1993) caution against their shortcomings and the reason why they must be used with extreme care. It is further stated that it is important to realize that classification systems give reliable results only for the rock masses and circumstances for which the guidelines were originally developed.

Potvin and Wesseloo (2012) caution against the pitfalls and misuse of rock mass classification systems and further state that they are not meant to be accurate and precise. There are many potential pitfalls to be avoided and sources of uncertainty to be controlled when applying rock mass classification methods. Experience and training can be used to reduce the risk associated with these potential sources of inaccuracy. Palmstrom and Broch (2006) emphasise the importance of understanding the limitations of rock mass classification schemes and that their use cannot replace some of the more elaborate design procedures.

Hoek and Brown (1980) have reviewed a considerable number of rock mass classification systems that have been developed for a variety of purposes. Ryder and Jager (2002) state that the most widely used classification systems are the Q-system, and the Geomechanics classification or Rock Mass Rating system, which also forms the basis of the Modified (or Mining) Rock Mass Rating system. The following sections will review some of the rock mass classification systems.

2.2.1 Terzaghi's Rock Load Classification

This classification system was proposed by Terzaghi in 1946 and was intended for use in estimating the loads to be supported by steel arches in tunnels. The system works by assigning ranges of rock loads for various ground conditions. In using this classification system, it is important to know about the defects to be expected in the type of rock being analysed (Hoek & Brown, 1980). Barton (1988) however states that this classification system is unsuitable for modern tunnelling methods in which rock bolts and shotcrete are used.

2.2.2 Classifications of Stini and Lauffer

In his classification system, Stini (1950) also stressed the importance of structural defects in the rock mass and the need to avoid tunnelling parallel to the strike of steeply dipping structures. Lauffer (1958) suggested that the stand-up time for any given active span is related to the rock mass characteristics (Hoek & Brown, 1980). According to Barton (1988), this classification system appears to be excessively conservative when compared with present-day tunnelling methods.

2.2.3 Rock Quality Designation (RQD)

This system was developed by Deere in 1964 and it is a quantitative index of rock mass quality based upon core recovery by diamond drilling (Figure 3). The Rock Quality Designation (RQD) is defined as the ratio of the sum of core of length > 100mm to the total length of the hole. The Q-system which was developed by Barton further refines the RQD system and tries to account for the presence of joints and the stress state (Spearing, 1995).

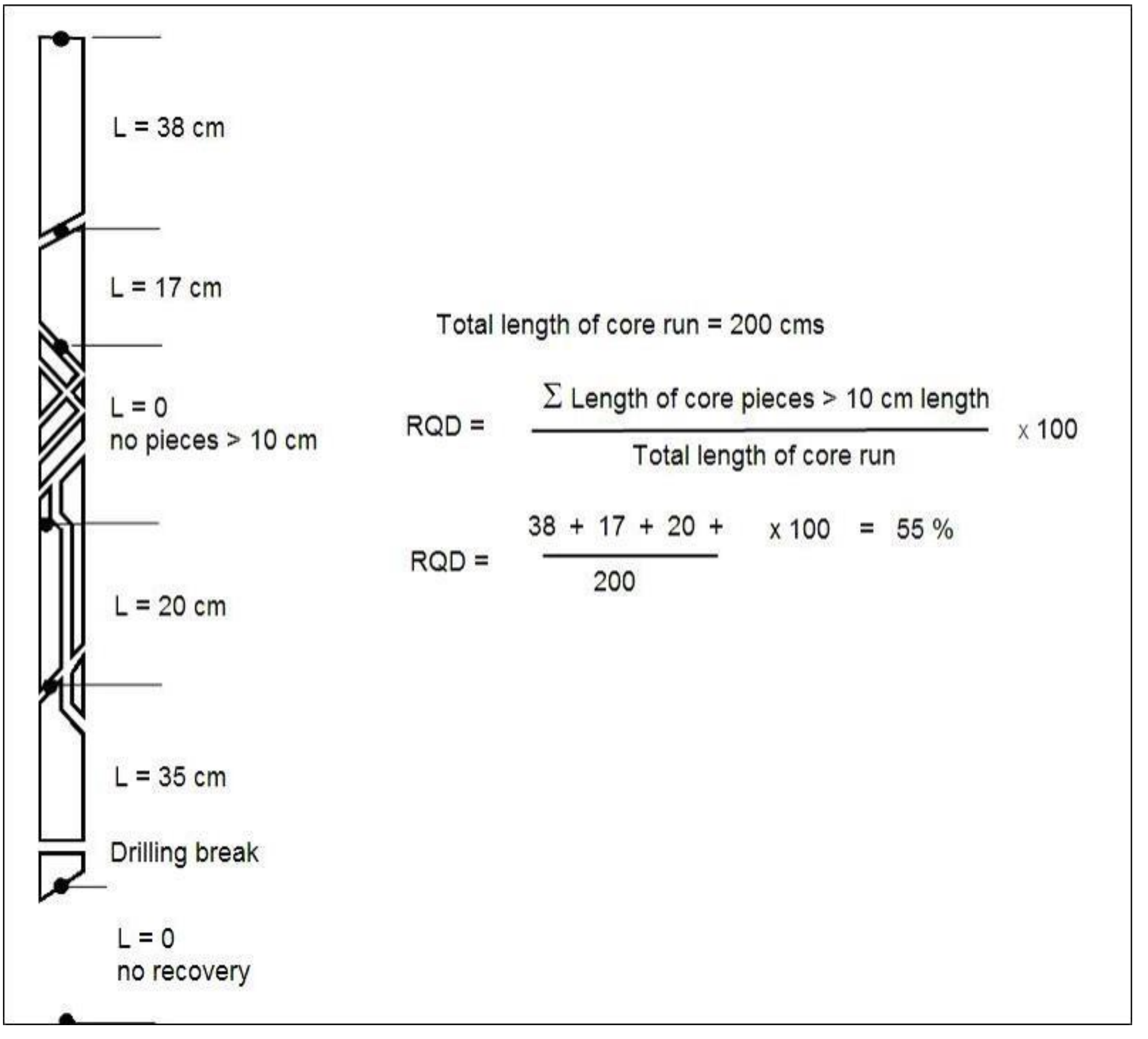

Figure 3: Procedure for measurement and calculation of rock quality designation (Hoek, 1998)

It has been suggested by Palmstrom (1982) that, when no core is available, but discontinuity traces are visible in surface exposures or exploration adits, the RQD may be estimated from the number of discontinuities per unit volume. The suggested relationship for clay-free rock masses is:

$\mathbf{RQD} = \mathbf{115 - 3.3J_v}$ [EQ 1]

where,

J_v is the sum of the number of joints per unit length for all joint (discontinuity) sets known as the volumetric joint count.

The RQD is further explained to be a directionally dependent parameter and its value is influenced by the borehole orientation. The use of the volumetric joint count is suggested as it is useful in reducing the directional dependence. Deere, et al. (1967) mention that, on its own, the RQD fails to account for the condition of joint surfaces and filling materials. It is regarded that the most important use of the RQD is as a component of the Rock Mass Ratings.

2.2.4 Geomechanics Classification

According to Ryder and Jager (2002), the Geomechanics classification or Rock Mass Rating (RMR) was developed by Bieniawski and was based on case studies of civil construction within South Africa. The RMR is stated to be derived from a rating based on the consideration of critical rock mass parameters including the intact rock strength, discontinuity frequency, discontinuity condition and the presence of water within the rock mass.

The details of this classification system were first published by Bieniawski in 1976 and over the years the system has been successfully refined and changes made to the ratings assigned to the parameters.

In his 1989 version, Bieniawski uses the following six parameters to classify a rock mass using the RMR system:

- Uniaxial compressive strength of rock material (UCS)
- Rock Quality Designation (RQD)
- Spacing of discontinuities
- Condition of discontinuities
- Groundwater conditions
- Orientation of discontinuities

In applying this classification system, the rock mass is divided into several structural regions and each region is classified separately. The boundaries of the structural regions usually coincide with a major structural feature such as a fault or with a change in rock type. In some cases, significant changes in discontinuity spacing or characteristics, within the same rock type, may necessitate the division of the rock mass into several small structural regions.

2.2.5 Mining Rock Mass Rating

The Mining Rock Mass Rating (MRMR) was developed by Laubscher in 1975 as a modification to the Rock Mass Rating. According to Ryder and Jager (2002), the MRMR modifications were intended to cater for the differences in support between the original civil environment and the mining environment.

This system assigns a rating to the in-situ mass based on measurable geological parameters. This system essentially describes the same parameters as Bieniawski's classification system, but the individual parameters are weighted differently. Each geological parameter is weighted according to its importance, and the total maximum rating is 100.

Swart (2005) states that Laubscher's in-situ rock mass rating is adjusted to assess the behaviour of the rock mass in a specified mining environment, and the adjusted rating is referred to as the Mining Rock Mass Rating (MRMR). The adjustments include:

- Weathering
- Mining induced stress
- Joint orientation and
- Blasting effects

The adjusted rock mass rating is then used to determine the support requirements for the excavation. This is achieved by using Laubscher's series of tables, in which the rating is described in terms of a rock mass class and support techniques are recommended for each class.

2.2.6 The Q-System

The Q-System was developed by Barton (1974) and is explained to have been built extensively on the RQD method of Deere, et al. (1967). The method was based on an analysis of 212 case records and introduces five additional parameters to modify the RQD value to account for the number of joint sets, the joint roughness and alteration (filling), the amount of water, and the various adverse features associated with loosening, high stress, squeezing and swelling.

The Q-system describes the rock mass quality by combining six parameters as follows:

$$\mathbf{Q} = (\mathbf{RQD}/\mathbf{J_n}) \cdot (\mathbf{J_r}/\mathbf{J_a}) \cdot (\mathbf{J_w}/\mathbf{SRF}) \qquad \text{[EQ 2]}$$

where,

RQD is the Rock Quality Designation (Deere, et al., 1967)

J_n is the joint set number

J_r is the joint roughness number (of least favourable discontinuity or joint set)

J_a is the joint alteration number (of least favourable discontinuity or joint set)

J_w is the joint water reduction factor, and

SRF is the Stress Reduction Factor.

The three ratios (RQD/J_n), (J_r/J_a) and (J_w/SRF) represent block size, minimum inter block shear strength and active stress, respectively. Barton (1988) elaborates that the values of J_r and J_a relate to the joint set or discontinuity most likely to allow failure to initiate and that the important influence of orientation relative to the tunnel axis is implicit in this method.

The Q-system is further described as being more detailed than any of the other methods as it regards the factors, joint roughness, joint alteration, and relative orientation. The classification of "least favourable features" represents one of the strongest features of the method, and this seems to be a factor that is ignored by all the other classification schemes.

Barton (1988) states that the two classification methods that are widely used in tunnelling and which do not rely on performance monitoring are the RMR and the Q-System. Barton (1988) continued to compare these two classification methods and concluded that both methods used Deere's RQD as a common parameter. The RMR includes joint spacing and orientation, while the Q-system considers the number of joint sets. Orientation is said to be implicitly included in the Q-system by classifying the joint roughness and alteration of only the most unfavourably orientated joint set or discontinuity.

A further description of both systems is given in Table 1. The table highlights the main differences between RMR and Q-system in terms of characterization, project purpose and empirical relations. The challenges and practical limitations that exist in each method highlight the need to use more than one single method to classify the site (Ongoje, 2017).

Table 1: Comparison of the RMR and Q system in terms of characterization, project purposes and empirical relations (Ongoje, 2017)

Parameter	**RMR**	**Q-System**
Characterization	Jointing patterns described except anisotropic rocks.	Describes the mechanical properties of discontinuities and in-situ stresses.
Project Purpose	Orientation for axis structure. Bolt lengths are easily determined. Stand-up time (conservative). Not helpful to choose excavation method.	Not relevant to orientation. Bolt lengths usually inaccurate. Easily choose roof support. Helpful to choose excavation method.
Empirical Relations	RMR, strength and deformability parameters.	Q, physical and mechanical parameters.

2.2.7 The Modified Q-system by Kirsten

In the work conducted by Dunn and Hungwe (2002), it is mentioned that rock mass classification systems have not been widely applied on South African gold mines due to the perception that they do not cater for stress effects, which are the dominant factors in rock mass conditions in South African gold mines.

Piper (1985) also evaluated five different systems in terms of their application in deep gold mines. He concluded that whilst rock mass classification systems can provide valuable information in the design and support of mining excavations, the systems evaluated had disadvantages, which limit their application in deep mines. Piper (1985) further indicated that whilst rock mass classification systems had been developed to cater for jointed rock masses, further development was required for their application to fractured rock masses encountered in deep and intermediate-depth mines.

Kirsten (1988) as quoted by Dunn and Hungwe (2002) proposed modifications to the Q-system to account for the fracturing of the rock mass. The work done by Dunn and Hungwe (2002) indicated that the Modified Q-system seemed the most appropriate to use as it postulated that the SRF, which is one of the parameters of the Q-system, is not a geological property that varies for different regimes of rock around an excavation. It is a parameter that characterises the loosening of the rock around the excavation. Thus, SRF is dependent on the variation of the maximum and minimum stress relative to rock alteration and the uniaxial compressive strength of the host rock.

Kirsten (1988) modified the Q-system by assigning SRF relationships for homogeneous and non-homogeneous rock masses. These relationships are denoted by SRF_h and SRF_n (Kirsten, 1988).

$$\mathbf{SRF_h = 0.244K^{0.35}(\frac{H}{\delta})^{1.32} + 0.18(\delta)^{1.14}} \quad \text{[EQ 3]}$$

$$\mathbf{SRF_n = 1.81Q^{-0.33}} \quad \text{[EQ 4]}$$

where,

K is the maximum to minimum principal field (absolute) stress ratio H is the head of rock corresponding to maximum field stress (m) δ is the uniaxial compressive strength of the rock (MPa).

2.3 Review and Evaluation of Rock Mass Failure Mechanisms

The failure of rocks has been studied by many, and as such various theories have been formulated which attempt to provide an explanation of the failure mechanisms of rock under the influence of stress. The following section reviews some of these theories and examines the assumptions on which these theories are founded as well as the limitations that govern them.

Failure in rocks is understood to occur when the magnitude of the stress to which the rock is subjected to exceeds the strength of the rock. It can be said that rocks under natural conditions experience different stress conditions.

When rock fails, fractures develop from the coalescence of several micro cracks. The rock may be subjected to varying stress conditions and different failure modes.

Goodman (1989) states that varieties of load configuration in rock are such that no single mode of failure predominates. Goodman (1989) further elaborates that the modes of failure can include but are not limited to:

- Flexure, which refers to failure by bending with development and propagation of tensile cracks. This is explained as tending to form in layers in the hanging wall. The immediate layer detaches from the layer above under gravity and causes a gap to form. A beam of rock then sags down under its weight.
- Direct tension, which occurs on rock layers resting on convex upward slope surfaces. Direct tension is explained as being the mechanism of failure in rock slopes with non-connected, short joint planes. It is explained that the formation of tension cracks severs the rock bridges and allows a complete block of rock to translate downwards. When rock breaks in tension, the surface of rupture is rough and free from crushed rock particles and fragments.
- Crushing or compression failure is explained to occur in rocks penetrated by a stiff punch. The process of crushing is explained to be a complex model, which involves the formation of tension cracks and their growth and interaction through flexure, and shear.
- Shear failure is explained as being the formation of a surface of rupture where the shear stresses have become critical, followed by a release of the shear stress as the rock suffers a displacement along the surface of rupture. Shear failure is said to occur in mines with softer or weaker roofs or floors.

Failure in brittle rocks is explained using a stress-strain curve under uniaxial compression (Figure 4). In this analysis, the curve is divided into several segments with the various phases explained by Ryder and Jager (2002) as follows:

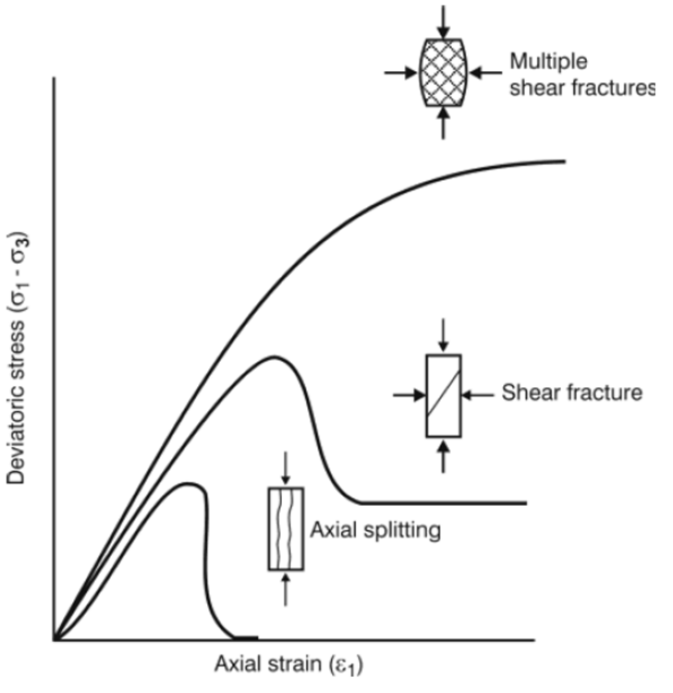

Figure 4: Load deformation curve for various loading conditions (Ryder and Jager, 2002)

The peak strength σ_c under zero confinement is the uniaxial compressive strength (UCS), expressed in MPa or kPa.

For low axial stress, the axial stress: strain characteristics are essentially linear and the slope, is equal to the Young's modulus, E, expressed in units of GPa.

Similar linear behaviour, although over a smaller range is observed in the axial: radial strain behaviour, and this slope is the Poisson's ratio, ν, which is dimensionless.

The deviation of strain from the two straight lines is referred to as the plastic strain, while the deviation of the radial strain from linearity expresses the lateral dilatancy of the rock near and beyond the peak strength point and is expressed in terms of the dilation angle ψ.

Jaeger and Cook (1979) describe the importance of understanding the nature and description of the fractured surface in brittle failure. Jaeger and Cook (1979) continue to describe the various types of failure of brittle rocks at varying confining pressures as follows:

a) Irregular Longitudinal Splitting – This type of failure is observed in unconfined compression. The specimen is described to often split axially into several pieces separated by steeply dipping or near-vertical 'extension fractures'. Ryder and Jager (2002) describes this type of failure as being reminiscent of the spalling on the sidewalls of pillars or abutments, where the overloading/failure of the rock occurs under near uniaxial conditions.

b) Shear Fracture – This type of failure is observed under a moderate amount of confining pressure and is manifest as a single plane of fracture inclined at an angle of less than 45° to the direction of $\sigma 1$. This is explained as being the typical fracture under compression and its characteristic feature is the shearing displacement along the surface of fracture. These are reminiscent of the inclined shear fractures created ahead of the face, commonly seen in deep mining conditions

c) Multiple Shear Fractures – This network of shear fractures accompanied by plastic deformation of the individual crystals appears when the confining pressure is increased such that the material becomes fully ductile. Ryder and Jager (2002) describe these as occurring at extremely high confinements and to be shallow dipping

d) Extension Fracture – This type of fracture occurs in uniaxial tension and is characterised by a clean separation with no offset between the surfaces. Van Aswegen and Stander (2012) divide extension fractures into two categories:

- Near vertical, primary extension fractures that develop some distance ahead of the advancing face.
- Secondary extension fractures that develop close to the face, between the face and primary extension fractures

Van Aswegen and Stander (2012) also describe an assemblage of fractures, which they label as Type III or low-angle and vertical younger fractures as originally described by Adams, et al. (1981). This assemblage of fractures is described as forming close to the stope face within rock that already contains extension and shear fractures. Jager and Ryder (1999) describe these low angled fractures as dipping 20° to 40° towards the face in the hanging wall.

In deep mines, stress fracturing is described by Jager and Ryder (1999) as occurring wherever the magnitude of the stress exceeds the strength of the rock mass. Where fracturing is present, the intensity is such that the stress fractures become the dominant set of discontinuities in the rock mass, with average spacing in the order of 60mm.

Jager and Ryder (1999) explain that several types and sets of stress fractures occur, which are best identified in terms of their orientation. The intersection of stress fractures within the immediate few metres of the hanging wall strata or intersections of fractures and geological discontinuities can result in the formation of unstable blocks, wedges and slabs that require support.

Napier, et al. (1998) mention that if a basic understanding of the underlying failure processes and mechanisms is available, strategies can be refined to reduce the risk of rockburst and rock-fall accidents.

The occurrence of fracturing due to high-stress levels is a major factor in hanging wall stability in deep-level gold mines, however as found by Gumede and Stacey (2007), rockfalls are not as a result of these fractures alone. Rockfalls can result only from the occurrence of unstable blocks defined by the interaction of the stress-induced fractures and naturally occurring geological planes of weakness.

In their investigation, two deep level gold mines were considered, and in comparing the results from the two mines, it was found that:

- Both mines had shallow dipping joints in the hangingwall
- Footwall joints in both mines were consistent in their characteristics and are usually unfilled
- In both mines, a single shallow dipping dominant joint set was observed in tunnels, which represented a cluster of bedding planes.
- Random joints in the footwall made up about 40% of the joints. In both the hanging wall and footwall, the random joints were steeply dipping and this orientation increased the likelihood of unstable block formation.

Gumede and Stacey (2007) concluded that the importance of the natural joints and bedding planes in defining unstable blocks has not been given the required attention. This is unfortunate since, to carry out a satisfactory design of support to cater for the identified potentially unstable blocks, data on joint characteristics is essential.

Other typical rock failure mechanisms include:

- Structurally controlled failure

This type of failure is more prevalent in shallow mining environments, where the rock neither fractures nor dilates and where there is a virtual absence of horizontal clamping forces. In this environment, pre-existing joints and faults intersect to delineate isolated keyblock, which in the absence of stiff support, may dislodge under the influence of gravity.

- Dynamic Failure

This type of rock mass failure is usually unique to deep and ultra-deep mining environments, although there has been cases where such failure has been experienced in intermediate depth environments.

The failure is driven by a high concentration of stress and stored energy, which result in heavy fracturing, dilation and violent strain bursting. This type of failure may be exacerbated by :

- Frequency of occurrence of geological features
- Angle of approach to geological features
- Mining span
- Rate of mining
- Extraction sequence and configuration

- Regional support system characteristics

- Time Dependent Failure

Time dependent failure or "creep" may be described as the failure of rock over time by slow non-terminating movements. Bhoi (2012) attributes the movement to the internal re-arrangement of particles in response to the application of a sustained stress difference. Creep strain is seldom recovered fully when loads are removed, thus it is largely "plastic deformation" (Roy & Rao, 2015). Jager and Ryder (1999) describe the effects of creep as being more noticeable in less competent rock such as argillaceous and bedded quartzites and at elevated stress levels. The effects of creep. The two important consequences of creep are described as being:

- In deep stopes, where the effects lead to deterioration in hangingwall conditions and enhanced amounts of back stope closure
- In tunnels or lifelong service excavations, where support of appropriate quality and yieldability needs to be considered.

As a result of the slow deformation rate, creep behaviour in hard brittle rocks is rare. The effects are only realized at elevated temperatures and pressures. This is in contrast to soft rocks, where the effects are realized at room temperature and atmospheric pressure.

The mechanism of creep behaviour are reported to be affected by the following parameters:

- Stress - creep rate increases with an increase in stress level. The threshold deviatoric stress for brittle crystalline rocks to creep is reported to be 40-60% of its compressive strength.
- Temperature - creep rate increase with an increase in temperature.
- Confining pressure – creep rate decreases with an increase in confining pressure. This is because the confinement acts to supress the tension stresses associated with crack growth and propagation.
- Strain rate - increase in strain rate increases brittleness and higher loss of strength after peak.
- Moisture and humidity – creep deformation increase with an increase in moisture and humidity. This is because water enhances the rate of crack formation under stress (Roy & Rao, 2015).

2.4 Review and Evaluation of Rock Mass Criteria

The stability of an underground excavation depends on both the structural conditions of the rock mass and the relationship between the stresses in the rock and the strength of the rock. To utilize the knowledge of stresses induced around underground excavations, Hoek and Brown (1980) state that it is necessary to have a criterion or set of rules that will predict the response of a rock mass to a given set of induced stresses. The selected rock failure criterion is of significant use if it satisfies the following requirements:

- It adequately describes the response of an intact rock sample to the full range of stress conditions likely to be encountered underground
- It can predict the influence of one or more sets of discontinuities upon the behaviour of a rock sample
- It provides some form of projection, even if approximate, for the behaviour of a full-scale rock mass containing several sets of discontinuities. Four commonly used failure criteria are discussed in this section.

2.4.1 The Mohr-Coulomb Failure Criterion

The Mohr-Coulomb criterion is a mathematical model that describes the response of brittle material to stress. The criterion is represented by a linear envelope that touches all Mohr's circles. The Mohr's circles represent critical combinations for principal stresses as illustrated in Figure 5. The criterion is defined by the equation below:

$$\boldsymbol{\tau = C + \sigma \tan\varphi} \qquad \text{[EQ 5]}$$

where,

C is the cohesion (MPa)

φ is the angle of internal friction (◦)

Mohr's hypothesis initially described the relationship between the normal and shear stress as an envelope around a set of Mohr's circles drawn in the τ: σ plane and corresponding to the results of a set of triaxial tests. The relationship is expressed as a general functional law $\tau = f(\sigma)$ (Ryder & Jager, 2002). *Coulomb*'s classical analysis took a more direct physical view that rock failed once the 'excess shear stress' $\tau - \mu_i\sigma$ across a particular critically-inclined macroscopic plane exceeded a certain inherent 'cohesion' value C_0; where μ_i is an empirical 'coefficient of internal friction', and $\mu_i = \tan\varphi_i$, where φ_i is the 'angle of internal friction' (Jaeger & Cook, 1979).

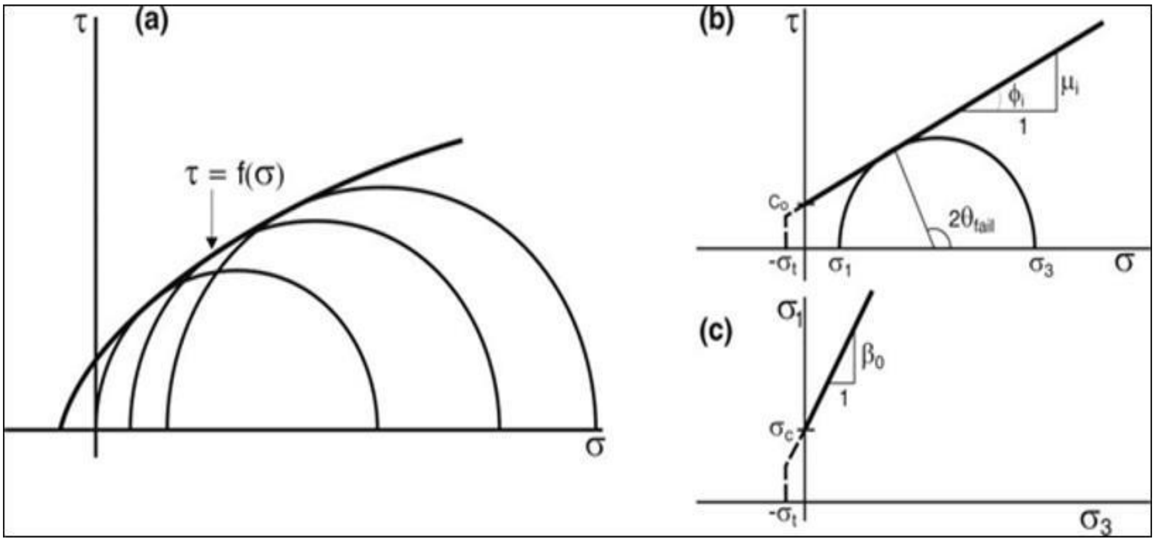

Figure 5: Mohr's hypothesis (Ryder and Jager, 2002)

The Mohr-Coulomb criterion can be used to represent the residual strength and has the merit of simplicity (Goodman, 1989). However, it is not a particularly satisfactory peak strength criterion for rock material (Brady & Brown, 1993). The reasons for this are as follows:

a) It implies that a major shear fracture exists at peak strength. Observations such as those reported to have been made by Wawersik and Fairhurst (1970) show that this is not always the case.

b) It implies a direction of shear failure, which does not always agree with experimental observations.

c) Experimental peak strength envelopes are generally non-linear. They can be considered linear only over limited ranges of σ_n or σ_3.

For these reasons, other peak strength criteria are preferred for intact rock. However, the Mohr-Coulomb criterion can provide a good representation of residual strength conditions, and more particularly, of the shear strengths of discontinuities in rock.

2.4.2 The Griffith's Crack Analysis Theory

According to Jaeger and Cook (1979), Griffith's criteria is based on a theory formulated by Griffith in 1921. In this theory, he stated that fracture is caused by stress concentration at the tips of minute *Griffith's* cracks which are supposed to pervade the material. Fracture is initiated when the maximum stress near the tip of the most favourably orientated crack reaches a value characteristic of the material, according to the equation:

$$(\boldsymbol{\sigma_1 - \sigma_3})^2 = 8T_0(\boldsymbol{\sigma_1 + \sigma_3}) \qquad \text{[EQ 6]}$$

where,

σ_1 is the major principal stress (MPa) σ_3 is the minor principal stress (MPa)

T_0 is the critical tensile strength that starts fracture growth (MPa)

This equation asserts that the uniaxial strength of the material is always eight times larger than its tensile strength (Handley, 2017). The Griffith failure criterion has not found wide application in rock mechanics because it tends to underestimate the strength of rocks in compression when used in its parabolic form.

2.4.3 The Hoek Brown Failure Criterion

Despite all the work carried out by many researchers, there was still no failure criterion, which satisfied all the requirements as set out by Hoek and Brown (1980). According to Hoek and Brown (1980), many of the available failure theories offered excellent explanations for some aspects of rock behaviour but failed to explain others or could not be extended beyond a limited range of stress conditions. It was for this reason that Hoek and Brown embarked on a journey to develop a failure criterion that would meet most of the objectives set above.

The result was, through a process of trial and error, the formulation of the empirical relationship between the principal stresses associated with the failure of rock, known as the Hoek and Brown failure criterion. Hoek and Brown (1980) elaborate that this failure criterion has its basis on Griffith's theory and is defined as:

$$\boldsymbol{\sigma_1 = \sigma_3 + \sigma_{ci}\left(m_b \frac{\sigma_3}{\sigma_{ci}} + S\right)^a} \qquad \text{[EQ 7]}$$

where,

σ_1 is the major principal stress at failure (MPa),

σ_3 is the minor principal stress applied to the specimen (MPa)

σ_{ci} is the uniaxial compressive strength of the intact material in the specimen (MPa)

m_b, s and a are constants which depend upon the properties of the rock and upon the extent to which it has been broken before being subjected to the stresses σ_1 and σ_3.

This failure criterion can also be expressed in terms of the shear and normal stresses acting on the plane inclined on an angle to the major principal stress direction.

Hoek and Brown (1980) presented a series of yield curves for different rock types showing that there is reasonable agreement between laboratory results and fitted curves. By doing so, a range of values for m_b and s were obtained which are subsequently used to estimate rock mass strengths for all stress states given the uniaxial compressive strength and the rock mass quality.

Despite its ability to address some of the problems presented by other failure theories, the Hoek Brown criterion also had its shortcomings. Hoek and Brown (1980) conclude that there are limitations to the use of the Hoek Brown failure criterion, mainly because it assumes that the rock has isotropic strength and for this reason, it should not be applied to anisotropic rocks like shale. It can be used in heavily jointed rock masses where joints/fractures are more or less randomly orientated, because the rock mass as a whole tends to be isotropic (Handley, 2017).

2.4.4 Extension Strain Criterion

The extension strain criterion by Stacey (1981) is a simple criterion, which appears to work well for brittle massive rocks. It automatically considers three-dimensional stresses. The minimum principal strain may be negative (extension) because of the stresses acting, and the criterion simply states that fracture of the rock will initiate when the extension strain exceeds a certain value characteristic of the rock.

For failure, the criterion is:

$$\boldsymbol{\varepsilon_3 \geq \varepsilon_{cr}} \qquad \text{[EQ 8]}$$

where,

ε_{cr} is the critical value of extension strain.

2.4.5 Limitations of Commonly Used Failure Criteria

According to Handley (2017), neither of these commonly used theories adequately predict rock failure over a wide range of stresses. The Mohr-Coulomb tends to underestimate rock strength at low confinements and overestimates it at large confinements, while Griffith's theory underestimates rock strength at large confinements. The theories cannot be accurately fitted to rock failure behaviour due to the following reasons:

- Failure envelopes to rock strength data should be concave downwards, but this concavity lies somewhat between a straight line and a parabola
- Failure envelopes to rock strength data should be concave downwards, but this concavity lies somewhat between a straight line and a parabola
- Both theories assume that the value of the intermediate stress does not affect failure
- The Mohr-Coulomb criterion implies that no processes leading to failure take place in the material until the stress state causes the Mohr circle to touch the failure envelope

- The Mohr-Coulomb failure criteria assumes that failure will take place on an internal plane in shear and that no other mechanism is involved, even though rocks can fail in extension in certain stress conditions.
- The Griffith criterion is based on the physical process of crack opening and extension and implies that no other mechanism is involved.
- The unmodified Griffith criterion cannot account for closing of cracks, crack shear under compression, interactions between cracks and fracture localization
- Modifications to the Griffith theory have made much progress to eliminate the problems with crack closure and shear in compression, although they still fail to take account of interactions between cracks, and crack localization.

2.5 Evaluation of in-situ Rock mass Parameters

The knowledge of the main mechanical constants of a rock mass is one of the fundamental aspects of rock engineering design (Vasarhelyi & Kovacs, 2017). Reliable estimates of the strength and deformation characteristics of rock masses are required for almost any form of analysis used for the design of underground excavations.

Palmstrom and Singh (2001) explain that deformability is characterized by a modulus describing the relationship between the applied load and the resulting strain. According to Palmstrom and Singh (2001), the fact that jointed rock masses do not behave elastically has prompted the usage of the term modulus of deformation rather than the modulus of elasticity or Young's modulus. The Commission of terminology, symbols, and graphic representation of the International Society for Rock Mechanics (ISRM) has given the following definitions.

Modulus of Elasticity or Young's Modulus (E): Ratio of the stress to corresponding strain below the proportionality limit of a material.

Modulus of Deformation of a rock mass (E_m): Ratio of stress to corresponding strain during loading of a rock mass, including elastic and inelastic behaviour.

Modulus of Elasticity of a rock mass (E_{em}): Ratio of stress to corresponding strain during loading of a rock mass, including only the elastic behaviour.

The static modulus of deformation is explained as being among the parameters that best describe the mechanical behaviour of a rock and a rock mass when it comes to underground excavations. Most numerical finite element and boundary element analyses for studies of stress and displacement distribution around underground excavations are based on this parameter. The deformation modulus is therefore a cornerstone of many geomechanical analyses (Palmstrom & Singh, 2001).

Ryder and Jager (2002) state that field measurements constitute the 'bottom line' of rock engineering inferences/predictions of rock mass behaviour and are invaluable in terms of relevance. Unlike other data acquisition methods, field measurements take all variable such as geological weaknesses into account and for this reason; they serve as an irreplaceable final observation/check for real rock behaviour.

Like many other authors, Ryder and Jager (2002) attest to the fact that field observations tend to be relatively expensive, often are deficient in determination or control of important experimental variables, and short in accuracy or completeness of measurement of various ancillary variables.

Palmstrom and Singh (2001) describe three methods of in situ deformation modulus (E_m) measurements of rock masses:

- Plate jacking tests (PJT) – which is achieved by simultaneously loading two diametrically opposite areas
- Plate loading tests (PLT) – which measures the displacements at the loading surface of the rock
- Radial jacking tests (Goodman jack test) – in which two transducers mounted at either end of the 20cm long bearing plates measure the displacement.

In situ measurements are time-consuming and imply notable costs and operational difficulties. For this reason, deformation modulus and other rock mass input parameters are often estimated indirectly from classification systems (Palmstrom & Singh, 2001).

Cai, et al. (2004) confirm that where access to underground is limited, the practical way to obtain these parameters is to apply a rock mass classification system to characterize the rock mass and estimate the rock mass properties.

This section of the research report reviews and evaluates the empirical relationships between the mechanical properties of rock masses and rock mass classification systems. These properties include the uniaxial compressive strength and the modulus of deformation, both of which are frequently related to laboratory data characteristics of intact rock samples and the classical rock classification methods (e.g. RQD, Q, RMR or GSI) (Vasarhelyi & Kovacs, 2017).

2.5.1 Estimation of Elastic Properties

The first linear relationship between the deformation modulus of the rock mass and the RMR value was suggested by Bieniawski in 1978. Bieniawski studied seven projects and assumed that the deformation modulus of the rock mass is independent of the deformation modulus of intact rock, according to:

$\mathbf{E_M = 2RMR - 100}$ (MPa) [EQ 9]

It is further reported that this equation does not give modulus values for RMR<50, thus it cannot be used for poorer rock masses.

Following this, Serafim and Pereira (1983) proposed the more known expression which can be used from poor to very good rock mass quality:

$$\mathbf{E_M = 10}^{\left[\frac{(\mathbf{RMR-10})}{\mathbf{40}}\right]} \text{ (MPa)} \qquad \text{[EQ 10]}$$

Vasarhelyi and Kovacs (2017) explain that when the relationship proposed by Serafim and Pereira (1983) was compared with in situ measurements, it was found that it could be used for good quality rocks. However, for poor quality rocks, it appeared to predict too high values. Based upon practical observations and back analysis of excavation behaviour in poor rock masses, the relationship proposed by Serafim and Pereira (1983) was modified such that:

$$\mathbf{E_M = 10}\left[\frac{(\mathbf{GSI-10})}{\mathbf{40}}\right] \text{ (MPa)} \qquad \text{[EQ11]}$$

In equation 11, the GSI has been substituted for the RMR and the modulus E_M is reduced progressively as the value of σ_c falls below 100MPa. This reduction is based upon the fact that the deformation of better-quality rock masses is controlled by discontinuities while, for poorer quality rock masses, the deformation of the intact rock parts contributes to the overall deformation process (Vasarhelyi & Kovacs, 2017).

Hoek (1998) further modified the equation initially proposed by Serafim and Pereira (1983) and suggested the use of the following equations to determine Young's modulus (E_M) for the rock mass.

$$\boldsymbol{E_M = \sqrt{\frac{\sigma}{100}\mathbf{10}^{\frac{(GSI-10)}{40}}}} \quad \text{for } \sigma_c > 100 \text{ MPa} \qquad \text{[EQ 12]}$$

$$\boldsymbol{E_M = \mathbf{10}^{\frac{(GSI-10)}{40}}} \quad \text{for } \sigma_c \leq 100 \text{ MPa} \qquad \text{[EQ 13]}$$

where,

σ_c is the uniaxial compressive strength of the intact rock (MPa)

GSI is the Geological Strength Index as described by Hoek (1998)

The Geological Strength Index (GSI) is a characterization method which uses properties of intact rock and jointing to determine or estimate the rock mass deformability and strength. Cai, et al. (2004) explain that GSI values can be estimated based on the geological description of the rock mass and this is well suited for rock mass characterization without direct access to the rock mass from tunnels. Figure 6 shows a depiction of the original GSI characterization chart.

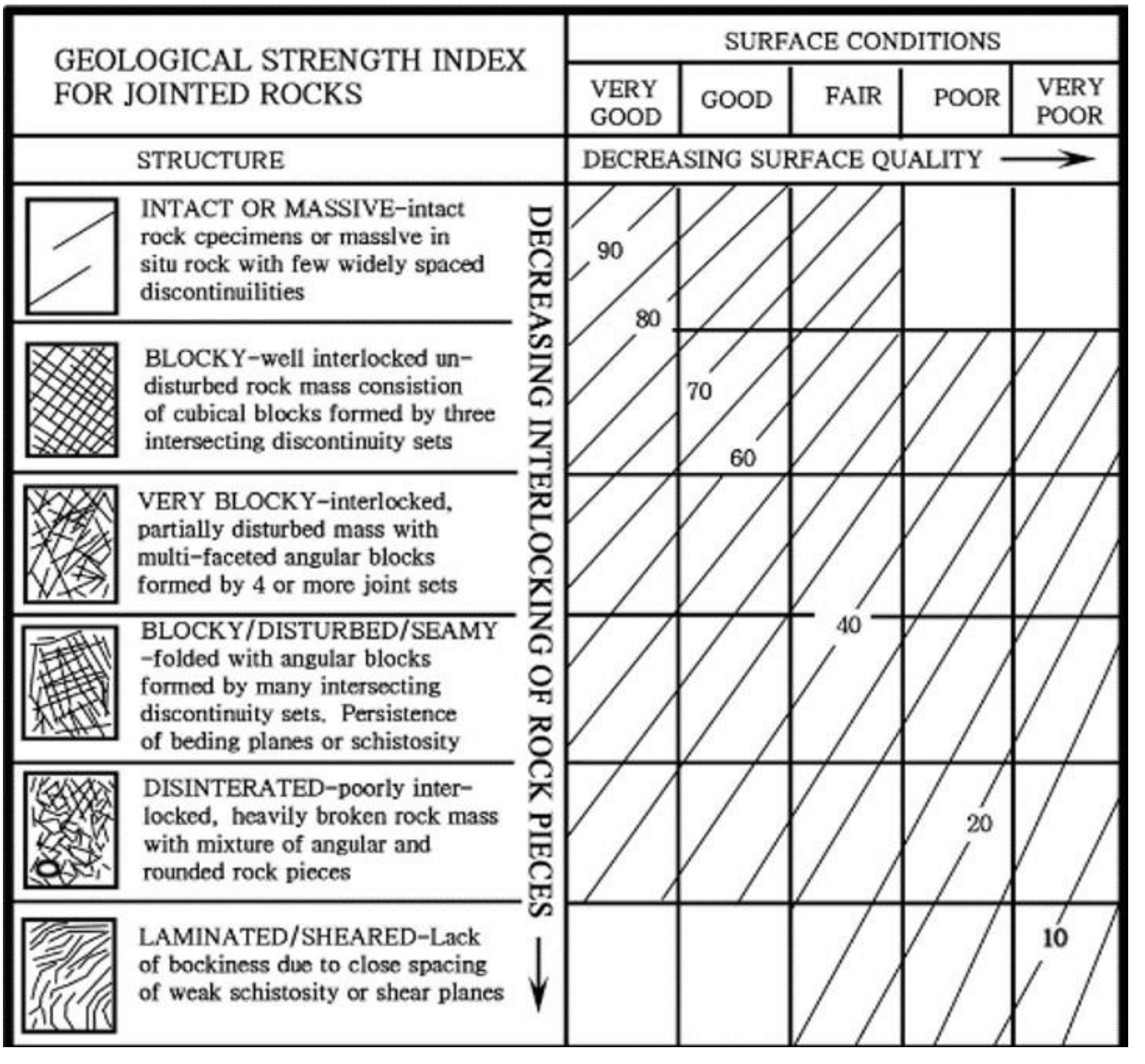

Figure 6: The Geological strength index (GSI) chart (Hoek, 1998)

Cai, et al. (2004) state that, although imperfect, the GSI system is the only system that provides a complete set of mechanical properties (Hoek-Brown strength parameters or the equivalent Mohr-Coulomb strength parameters as well as the elastic modulus) for design purpose. The use of the GSI enables a rock mass to be considered as a mechanical continuum without losing the influence that geology has on its mechanical properties. It also provides a field method for characterizing difficult-to-describe rock masses (Marinos, et al., 2006).

For generally competent rock masses with GSI>25, the value of GSI can be related to the Rock Mass Rating (RMR) using the relationship:

$$\mathbf{GSI = RMR - 5} \qquad \text{[EQ 14]}$$

For very poor-quality rock masses, the value of RMR is difficult to estimate and the correlation between RMR and GSI is no longer reliable. It is for this reason that RMR classification must not be used for estimating GSI values for poor quality rock masses.

2.5.2 Estimation of Rock Mass Strength Properties - Hoek-Brown Method

Hoek (1998) defined the generalized Hoek-Brown failure criterion for jointed rock masses as:

$$\boldsymbol{\sigma_1 = \sigma_3 + \sigma_{ci}(m_i \frac{\sigma_3}{\sigma_{ci}} + S)^{0.5}} \quad \text{[EQ 15]}$$

where:

σ_1 and σ_3 are the maximum and minimum effective stress at failure (MPa)

m_i is the value of the Hoek-Brown constant m for the rock mass

s is a constant which depends upon the rock mass characteristics

σ_{ci} is the uniaxial compressive strength of the intact rock pieces (MPa)

To use the Hoek-Brown criterion for estimating strength and deformability, the following three properties of the rock mass have to be estimated (Hoek, 1998):

- Uniaxial compressive strength (σci, MPa) of the intact rock pieces
- Hoek-Brown constant (mi) for these intact rock pieces
- Geological Strength Index (GSI) for the rock mass

Cai, et al. (2004) state that whenever possible, the values of the uniaxial compressive strength and the Hoek-Brown constant m_i should be determined by statistical analysis of the results of a set of triaxial tests on carefully prepared core samples, with the uniaxial strength alone determined from uniaxial compressive tests. When rock testing is not performed or when the number of tests is limited, these parameters can be estimated from published tables as shown in Table 2 (field estimates of UCS) and Table 3 (constant m_i for intact rock).

Table 2: Field estimates of the uniaxial compressive strength (Hoek, 1998)

Grade*	Term	Uniaxial Comp. Strength (MPa)	Point Load Index (MPa)	Field estimate of strength	Examples
R6	Extremely strong	>250	>10	Specimen can only be chipped with a geological hammer	Fresh basalt, chert, diabase, gneiss, granite, quartzite
R5	Very strong	100-250	4-10	Specimen requires many blows of a geological hammer to fracture it	Amphibolite, sandstone, basalt, gabbro, gneiss, granodiorite, limestone, marble, rhyolite, tuff
R4	Strong	50-100	2-4	Specimen requires more than one blow of a geological hammer to fracture it	Limestone, marble, phyllite, sandstone, schist, shale
R3	Medium strong	25-50	1-2	Cannot be scraped or peeled with a pocketknife, the specimen can be fractured with a single blow from a geological hammer	Claystone, coal, concrete, schist, shale, siltstone
R2	Weak	5-25	**	Can be peeled with a pocketknife with difficulty, shallow indentation made by a firm blow with point of a geological hammer	Chalk, rock salt, potash
R1	Very Weak	1-5	**	Crumbles under firm blows with the point of a geological hammer, can be peeled by a pocketknife	Highly weathered or altered rock
R0	Extremely Weak	0.25-1	**	Indented by thumbnail	Stiff fault gouge
*Grade according to Brown (1981)					
** Point load test on rocks with uniaxial compressive strength less than 25 MPa likely to yield highly ambiguous results					

Table 3: Values of the constant mi for intact rock (Hoek, 1998)

Rock type	Class	Group	Texture			
			Coarse	Medium	Fine	Very Fine
SEDIMENTARY	Clastic		Conglomerate * (21±3) Breccias (19±5)	Sandstone 17±4	Siltstone 7±2 Graywackes (18±3)	Claystones 4±2 (7±2) Shales (6±2)
	Non-Clastic	Carbonates	Chrytsalline Limestone (12±3)	Sparitic Limestones (10±2)	Micritic Limestones (9±2)	Dolomites (9±3)
		Evaporites		Gypsum 8±2	Anhydrite 12±2	
		Organic				Chalk 7±2
METAMORPHIC	Non-Foliated		Marble 9±3	Hornfels (19±4)	Quartzite 20±3	
				Metasandstone (19±3)		
	Slightly Foliated		Migmatite (29±3)	Amphibolites 26±6		
	Foliated**		Gneiss 28±5	Schists 12±3	Phyllites (7±3)	Slates 7±4
IGNEOUS	Plutonic	Light	Granite 32±3	Diorite 25±5		
				Granodiorite (29±3)		
		Dark	Gabbro 27±3	Dolerite (16±5)		
				Norite 20±5		
	Hypabyssal		Pophryies (20±5)		Diabase (15±5)	Periodite (25±5)
	Volcanic	Lava		Rhyolite (25±5)	Dacite (25±3)	Obsidian (19±3)
				Andesite (25±5)	Basalt (25±5)	
		Pyroclastic	Agglomerate (19±3)	Breccia (19±5)	Tuff (13±5)	

*Conglomerates and Breccias may present a wide range of m_1 values depending on the nature of the cementing material and the degree of cementation, so they may range from m values like sandstone to values used for fine-grained sediments.

**These values are for intact rock specimens tested normal to bedding or foliation. The values of m_1 will be significantly different if the failure occurs along a weakness plane.

Values in parenthesis are estimates

According to Cai, et al. (2004), material parameters for jointed rock mass could be estimated from the modified 1976-version of Bieniawski's RMR, assuming completely dry and a favourable joint orientation. However, because this did not work for very poor rock masses with RMR less than 25, a new index called GSI was introduced. The GSI system consolidates various Hoek-Brown versions into a single, simplified and generalized criterion that covers all of the rock types normally covered in underground engineering (Cai, et al., 2004). For rocks yielding in a ductile manner and if the GSI is known, the rock parameters in equation 15 can be determined from the following:

$$\boldsymbol{m_b = m_i \exp(\frac{GSI-100}{28-14D})} \qquad \text{[EQ 16]}$$

$$\boldsymbol{s = \exp(\frac{GSI-100}{9-3D})} \qquad \text{[EQ 17]}$$

$$\boldsymbol{a = \frac{1}{2} + \frac{1}{6}(exp\left(\frac{GSI}{15}\right) - exp\left(\frac{-20}{3}\right))} \qquad \text{[EQ 18]}$$

Where D is a factor that depends on the degree of disturbance to which the rock mass has been subjected by blast damage and stress relaxation. It varies from 0 for undisturbed in situ rock masses to 1 for very disturbed rock masses. Hoek (1998) provides guidelines for the selection of the factor D as shown in Table 4.

Table 4: Guidelines for the selection of the Disturbance (D) factor (Hoek, 1998)

Appearance of Rock mass	Description of Rock mass	Suggested value of D
	Excellent quality-controlled blasting or excavation by Tunnel Boring Machine results in minimal disturbance to the confined rock mass surrounding the tunnel.	D = 0
	Mechanical or hand excavation in poor quality rock masses (no blasting) results in minimal disturbance to the surrounding rock mass. Where squeezing problems result in significant floor heave, disturbance can be severe unless a temporary invert, as shown in the photograph is placed.	D = 0 D = 0.5 No Invert
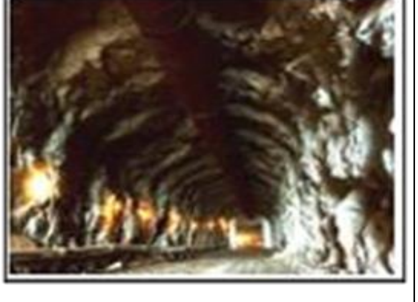	Very poor-quality blasting in a hard rock tunnel results in severe local damage, extending 2-3m into the surrounding rock mass.	D = 0.8
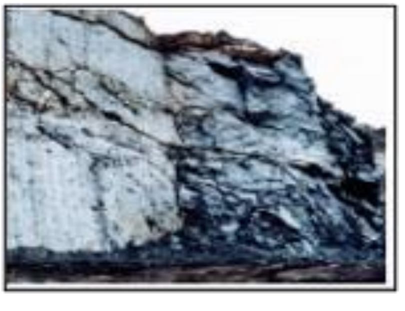	Small scale blasting in civil engineering slopes results in modest rock mass damage, particularly, if controlled blasting is used. However, stress relief results in some disturbance	D = 0.7 Good Blasting D = 1.0 Poor Blasting
	Very large open pit mine slopes suffer significant disturbance due to heavy production blasting and due to stress relief from overburden removal. disturbance due to heavy In some softer rocks, excavation can be carried out by ripping and dozing and the degree of damage to the slope is less	D = 1.0 Production Blasting D = 0.7 Mechanical Excavation

Hoek (1998), however, warns that the factor D only applies to the blast damaged zone and should not be applied to the entire rock mass.

2.5.3 Estimation of Rock Mass Properties -Mohr-Coulomb Method

Hoek (1998) advises that it is sometimes necessary to determine the equivalent angles of friction and cohesive strengths for each rock mass and stress ranges since most numerical modelling programmes are written in terms of the Mohr-Coulomb failure criterion.

Hoek (1998) suggests that this be done by fitting an average linear relationship to the curve generated by solving the generalized Hoek-Brown equation for a range of minor principal stress values. Figure 7 shows the relationship between major and minor principal stresses for Hoek-Brown and equivalent Mohr-Coulomb criteria.

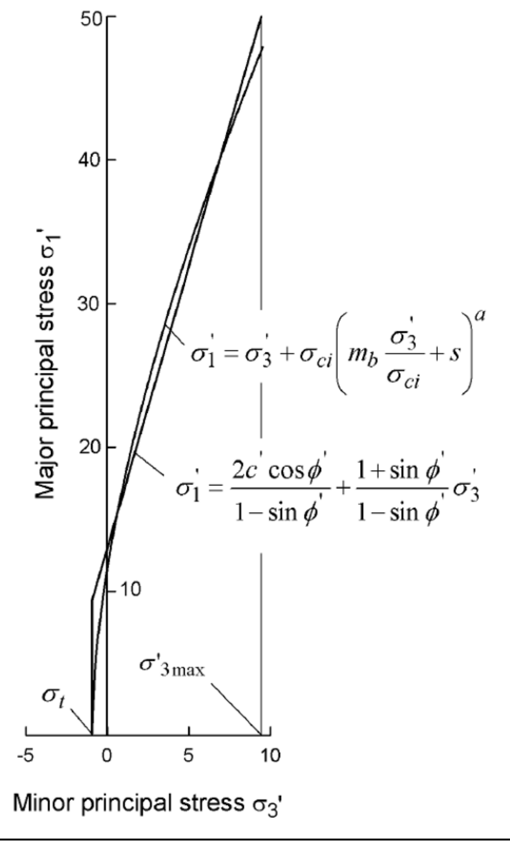

Figure 7: Relationship between major and minor principal stresses for Hoek-Brown and equivalent Mohr-Coulomb criteria (Hoek, 1998)

In the case of input parameters for numerical modelling, Hoek (1998) advises that the Hoek-Brown estimates be used rather than the Mohr-Coulomb estimates. This, he explains, will eliminate the uncertainty associated with estimating equivalent Mohr-Coulomb parameters. He elaborates that Hoek-Brown estimates are independent variables and can be treated as such in any probabilistic analysis, whereas the Mohr-Coulomb estimates are correlated, and this results in additional complication in probabilistic analyses.

2.6 Evaluation of Rock Engineering Design Methods

Design methods in rock engineering cover a full spectrum of methods and can be either empirical, analytical or numerical. Empirical and analytical models such as pillar strength equations, excavation stability charts, and classification-based support design charts are widely used in rock engineering design. These models are popular and can reduce the complexity of systems into simple charts or equations that can be readily applied (Esterhuizen, 2014).

Numerical modelling, on the other end of the spectrum, determines the most likely response of the rock surrounding the excavation. The design of excavations in rock is extremely challenging because of the variability of the rock materials, uncertainty about the loading conditions, and the need for cost-effective solutions. Most underground excavations are irregular in shape and are frequently grouped close to other excavations. These groups of excavations can form a set of complex three-dimensional shapes. Also, because of the presence of geological features such as faults and intrusions, the rock properties are seldom uniform within the rock volume of interest (Hoek, et al., 1995).

Many problems in rock engineering are limited by the imperfect knowledge of the material properties and failure mechanics of rock masses and in their seminal paper, Starfield and Cundall (1988) introduced a classification of modelling problems (Figure 8).

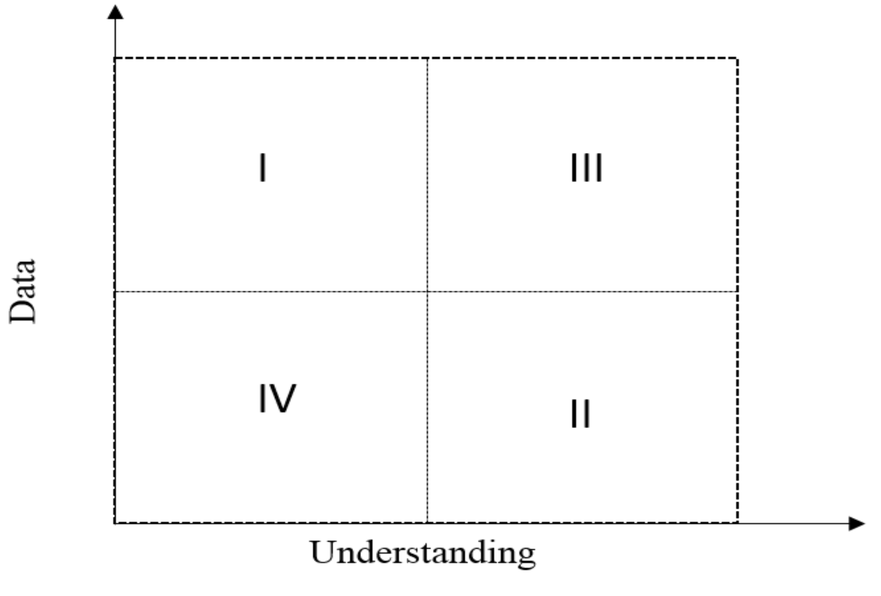

Figure 8: Classification of modelling problems (Reproduced from Starfield and Cundall, 1988)

The X-axis measures the level of understanding of the fundamental mechanics of the problem to be solved. The Y-axis refers to the quality and/or quantity of the available data, including material properties, boundary conditions, and experience. Starfield and Cundall (1988) argued that problems in rock mechanics usually fall into the data limited categories II or IV.

2.7 Evaluation of Stress Distribution in Rock mass and Support Design Methods

Before excavation of the tunnel, the state of the rock mass is assumed to be in equilibrium. When an underground opening is excavated into a stressed rock mass, the stresses in the vicinity of the new opening are re-distributed. For a horizontal circular tunnel, the re-distribution can be explained as follows:

Before the tunnel is excavated, the in-situ stresses, $\sigma_{v,}$ σ_{h1} and σ_{h2} are uniformly distributed in the slice of rock under consideration. After removal of the rock from within the tunnel, the stresses near the tunnel are changed and new stresses are induced. Three principal stresses, σ_1, σ_2 and σ_3 acting on a typical element of rock are shown in Figure 9. The convention used in rock engineering is that compressive stresses are always positive, and the three principal stresses are numbered such that σ_1 is the largest compressive stress and σ_3 is the smallest compressive stress or the largest tensile stress of the three.

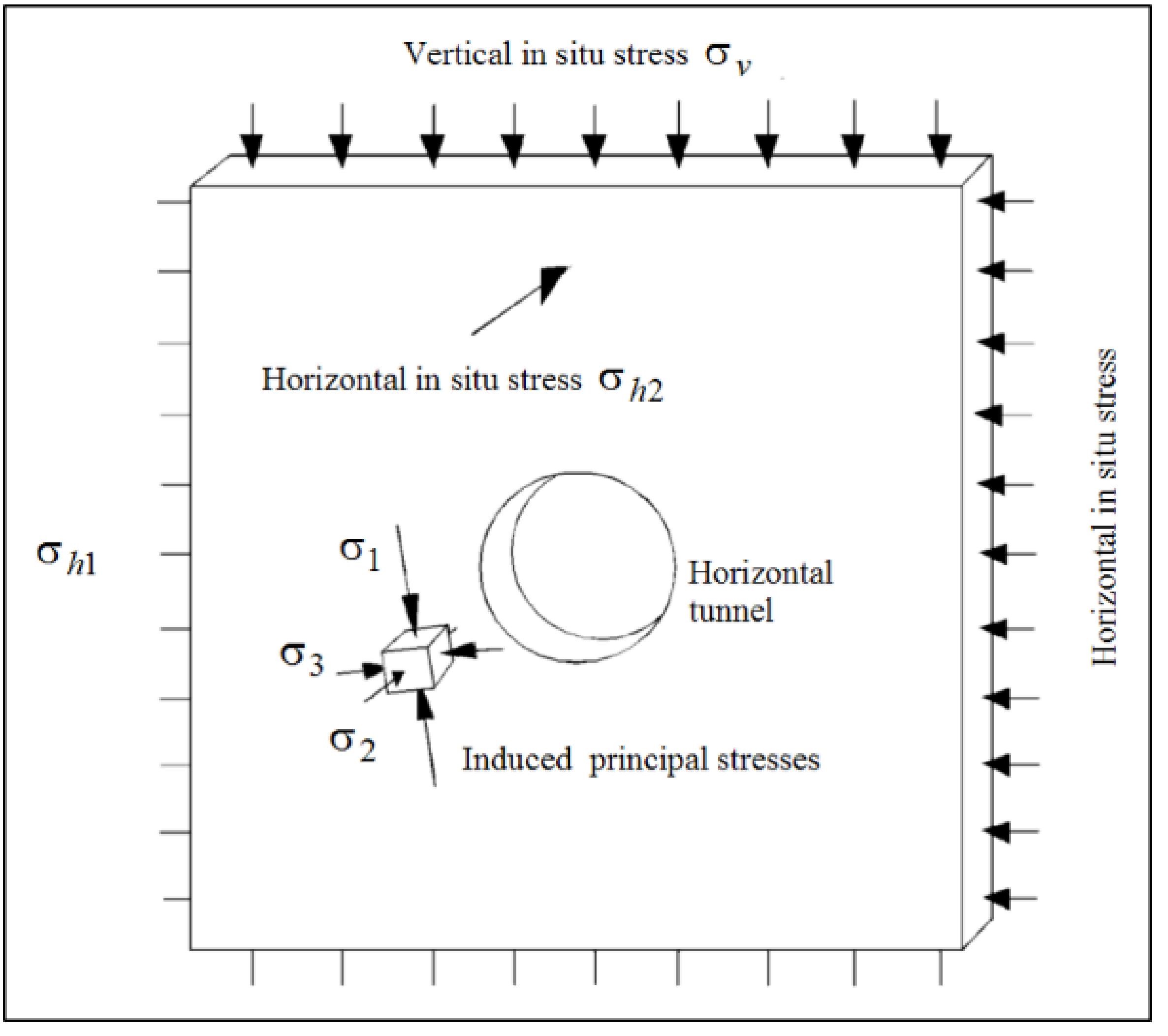

Figure 9: Illustration of principal stress induced in an element of rock close to a horizontal tunnel subjected to vertical and horizontal stresses (Hoek, 1998)

Other analyses of tunnel behaviour propose certain simplifying assumptions. The tunnel may be assumed to be circular and having a radius r_o. The tunnel is assumed to be subjected to a hydro-static stress p_o and a uniform internal pressure p_i. Failure of the rock mass surrounding the tunnel occurs when the internal pressure provided by the tunnel lining is less than a critical support pressure p_{cr}, defined by:

$$\mathbf{p_{cr}} = \frac{\mathbf{2p_o - \sigma_{cm}}}{\mathbf{1+k}} \qquad \text{[EQ 19]}$$

where,

p_o is the hydrostatic stress (MPa) k is the ratio of the horizontal stress to the vertical stress and, σ_{cm} is the uniaxial compressive strength for the rock mass (MPa)

If the internal support pressure p_i is greater than the critical support pressure, P_{cr}, no failure occurs, Hoek (1998).

A further simplifying assumption made is that the behaviour of the rock mass surrounding is elastic, and the inward radial displacement of the tunnel wall is given by:

$$\mathbf{U_{ie}} = \frac{\mathbf{r_o(1+\nu)}}{\mathbf{E_m}}(\mathbf{p_o} - \mathbf{p_i}) \qquad \text{[EQ 20]}$$

Where E_m is the deformation Modulus ν is the Poisson's ratio

When the internal pressure p_i is less than the critical support pressure, P_{cr}, failure occurs and the radius r_p of the elastic zone around the tunnel is given by:

$$\mathbf{r_p} = \mathbf{r_o}\left[\frac{\mathbf{2(p_o(k-1)+\sigma_{cm})}}{\mathbf{(1+k)(1-k)p_i+\sigma_{cm}}}\right]^{\frac{\mathbf{1}}{\mathbf{(k-1)}}} \qquad \text{[EQ21]}$$

Thus, for plastic failure, the total inward radial displacement of the walls of the tunnel is:

$$\mathbf{U_{ip}} = \frac{\mathbf{r_o(1+\nu)}}{\mathbf{E}}[\mathbf{2(1-\nu)(p_o - p_{cr})}]\left[\frac{\mathbf{r_p}}{\mathbf{r_o}}\right]^{\mathbf{2}} - (\mathbf{1-2\nu})(\mathbf{p_o} - \mathbf{p_i}) \qquad \text{[EQ 22]}$$

The intrinsic stability of any service excavation should ideally be maximized by suitable selection of its location, orientation and development profile; to minimize the demand on the support required (Jager & Ryder, 1999). This is however not always practical and support systems have to be designed for the prevailing conditions.

Safety during construction and long-term stability are factors which must be considered by the designers of the excavation in rock. It is not unusual for the requirements to lead to a need for the installation of some form of rock support (Hoek, et al., 1995). The principal objective in the design of underground excavation support is to assist the rock mass support itself.

Jager and Ryder (1999) explain the fundamental purpose of tunnel support as being to maintain the integrity and stability of rockwall under static and possibly dynamic (seismic) state of stress. The designed support system needs to be able to control slow stress-driven deformations of the rock mass. Jager and Ryder (1999) describe, that a well-chosen support system can accomplish this requirement not only by supporting the dead weight but by increasing the inter-block frictional forces, thereby containing the movement of the key blocks and preventing unravelling and differential movements of the rock mass. In the case of dynamic loading, it is explained that the requirement is for the support to be able to absorb the kinetic energy imparted on the wall rock while maintaining the integrity of the discontinuous rock structure.

2.7.1 Support Design based on Structural Analysis

In a lower stress environment, the overall state of a rock mass is generally controlled by discontinuities. The main discontinuous structural features which separate rock masses into discrete but interlocked isolated wedge pieces are bedding planes and joints. When a rock mass is excavated, a free wedge face is created. The wedge is free from the restraint of the surrounding rock. Thus, the confining stress which once contributed towards the stability of the wedge is removed thereby making it susceptible to collapse or sliding (Ongoje, 2017). Wedges fail by collapse from the roof (also called gravity falls). They are displaced and caused to slide out of the sidewalls along the weak shear planes of the discontinuities, depending on the behavioural properties of the plane (Ongoje, 2017, after Hochella, et al., 1989). The process unravels into further wedges if left unsupported until a natural arching in the rock prevents further propagation of the problem or the cavern is filled with loose wedges (Ongoje, 2017). As wedges fall or slide out of position, the overall restraint and interlocking of the rock mass is reduced, hence stability is minimized. Sliding may occur when the free wedge face is exposed and the adjoining faces are free to move because of induced strains (Ongoje, 2017, after Hoek, 2014). Shear sliding planes are usually separations of adjoining wedge faces along joints.

Theories such as Hooke's law which is a linear theory of elasticity are applied to check instability associated with sliding (Ongoje, 2017). Analysis of structurally controlled instability begins with modelling the problem. Stereographic plots are drawn indicating the average dip and dip direction of significant discontinuity sets such as joints. The structural data is obtained from borehole logs and pilot tunnel mapping (Ongoje, 2017). The stereonet (Figure 10) is a lower hemisphere plot of the three discontinuity sets including a tunnel axis plunge marked with a cross.

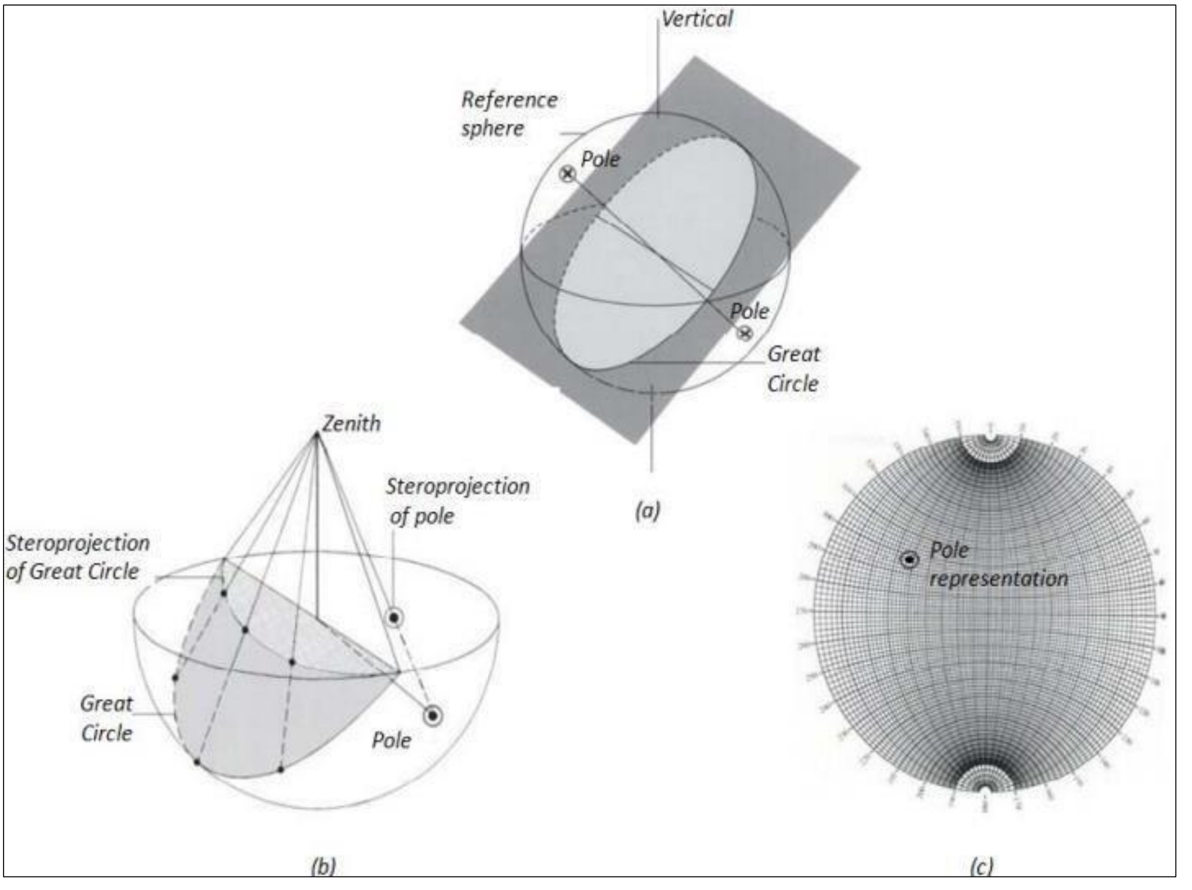

Figure 10: A strereographic projection of a pole (Ongoje, 2017)

Once the information on the significant discontinuity has been obtained, then the support requirement specific to the individual block may be determined. Figure 11 (after Stilborg, 1986) demonstrates the analysis and support determination for a key block structure.

The number of rock bolts required to support the above wedge is determined by the equation:

$$\mathbf{N} = \frac{\mathbf{w \times f}}{\mathbf{c}} \qquad \text{[EQ 23]}$$

where,

N is the required number of rock bolts

w is the weight of the wedge (kN)

f is the Factor of Safety which is between 2 and 5

c is the load-bearing capacity of the bolt (kN)

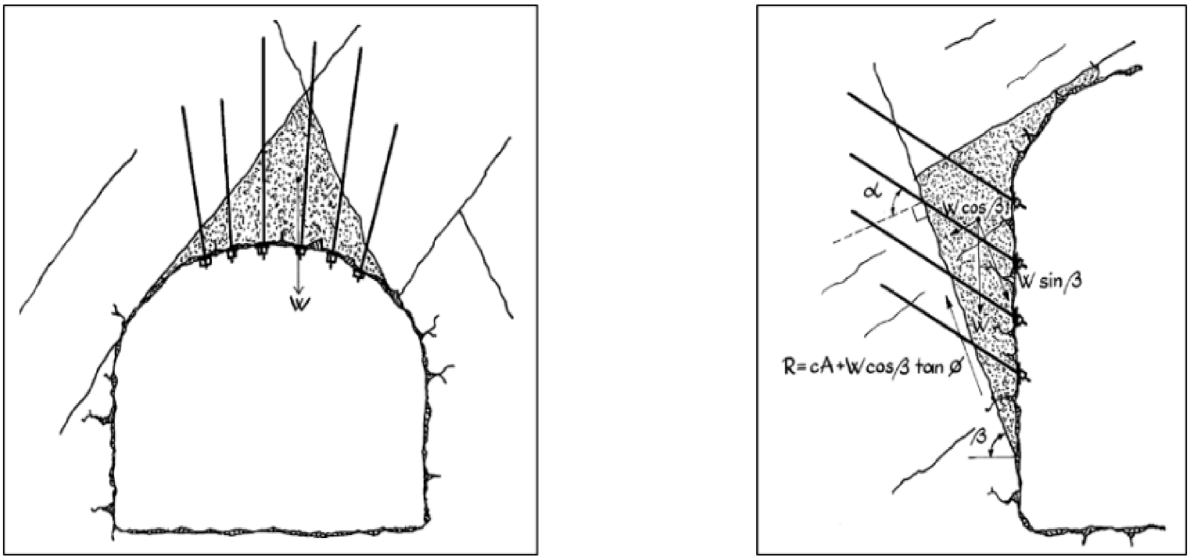

Figure 11: Analysis and support determination for a key block structure (Ryder and Jager, 2002)

According to Ryder and Jager (2002), where sliding of the block may occur (Figure 11), the influence of the discontinuity characteristics must be considered in addition to the factors discussed earlier. The development of tension within the rock bolt units will increase the normal stress on the sliding surface and thus increase its frictional resistance. The minimum rock bolt capacity required to stabilize the block can be determined by resolving the forces within the system. Equation 22 below determines the number of rock bolts required to stabilize the wedge and prevent it from sliding.

$$\mathbf{N} = \frac{\mathbf{W(fsin\beta - cos\beta tan\varphi)cA}}{\mathbf{C(cos\alpha tan\varphi + sin\alpha)}} \qquad \text{[EQ24]}$$

where,

N is the number of rock bolts

W is the weight of wedge (kN)

f is the safety factor against sliding, usually between 1.5 and 3

β (◦), φ (◦), c (MPa), A (m^2) is the dip, friction angle, cohesion, the base area of the sliding surface

C is the load-bearing capacity of the bolt (kN)

α is the angle between bolts and the normal to the sliding surface (kN).

As the frequency of discontinuities within the rock mass increases, the rock bolting requirement changes from the stabilization of individual, well-defined blocks to more systematic rock bolt patterns to reinforce and/or support the potentially unstable rock mass volume. Where the limits of rock mass instability can be defined and are within a practical depth from the excavation boundary, the rock bolt system can be designed based on suspension or containment. This will be possible where a more competent horizon occurs immediately above the unstable strata (Ryder & Jager, 2002). In this situation, the weight of the wedge to be supported is determined by:

$$\mathbf{W = fgsch\rho} \qquad \text{[EQ 25]}$$

where,

W is the weight of rock to be supported by a single bolt f is the safety factor, usually between 1.5 and 3 g is 9.8 m/s^2

s is the bolt spacing perpendicular to the axis of the excavation (m)

c is the bolt spacing along the axis of the excavation (m)

h is the thickness of the unstable layer of rock (m)

ρ is the rock density (kg/m^3).

Figure 12 shows the suspension of a laminated rock mass and the formation of an unstable zone and naturally stable arch within moderately jointed rock mass structures

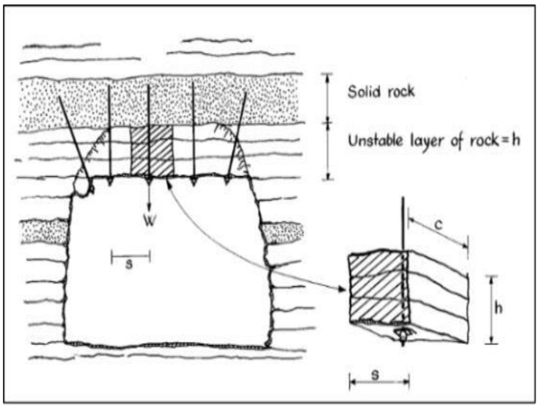

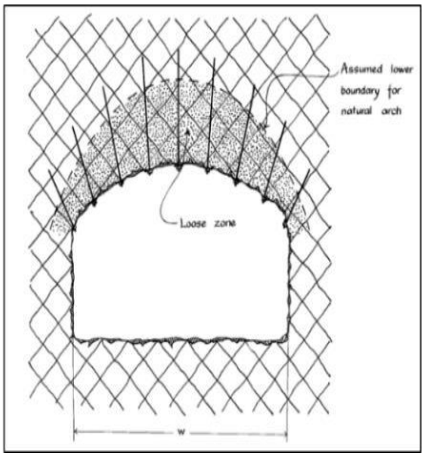

Figure 12: Suspension of a laminated rock mass and formation of a naturally stable arch within a moderately jointed rock mass structure (Ryder and Jager, 2002)

Ryder and Jager (2002) mention that under these conditions the length of the rock bolt unit must be sufficient to anchor beyond the limit of rock mass instability. In a moderately jointed discontinuous rock mass structure, the stabilization of the excavation may be based on a similar analysis. The creation of an excavation results in the formation of an unstable tensile zone in the immediate roof, above which a natural arch is formed where the rock mass loading condition is primarily compressive (Ryder & Jager, 2002). In this environment, the function of the support will be to pin the unstable rock mass into the competent natural arch. Thus, the length of the rock bolt must be sufficient to anchor into the competent rock mass. An estimation of the required rock bolt length is given by:

$$\mathbf{L = 1.40 + 0.184w} \qquad \text{[EQ 26]}$$

where,

w is the span of the excavation (m) and

L is the required rock bolt length (m) (Norwegian Institute for Rock Blasting Technique, after Stillborg, 1986).

The guidelines for the creation of a reinforced beam structure within a stratified rock mass are given by Lang and Bischoff (1982). These are based on the increase in shear resistance between layers within the rock mass and are given in the equations below:

Bolt Length

$$\mathbf{L} = \mathbf{W}^{2/3} \qquad \text{[EQ 27]}$$

Bolt Tension

$$\mathbf{C} = \frac{\mathbf{a\gamma^{AR}}}{\mathbf{1-tan\phi}}\left(\mathbf{1} - \frac{\mathbf{C}}{\mathbf{\gamma R}}\right)\frac{\mathbf{1-e_1}^{-\left(\frac{\mathbf{KO}}{\mathbf{R}}\right)\mathbf{tan\phi}}}{\mathbf{1-e_1}^{-(\mathbf{KL\backslash R})^{\mathbf{tan\phi}}}} \qquad \text{[EQ 28]}$$

where, w is the width of excavation (m)

a is the factor depending on the time of installation of bolts

γ is the unit weight of the rock (kN/m^3)

s is the bolt spacing (m)

A is the area of roof carried by one bolt (s^2)

R is the 'shear radius' of the reinforced rock unit (s/4)

k is the ratio of average horizontal to average vertical stress

φ is the angle of internal friction for the rock mass (◦)

c is the apparent cohesion of the rock mass (MPa)

D is the height of destressed zone (m).

2.7.2 Support Design based on Empirical Methods

Due to the complexities within the rock mass structure, or the lack of detailed design parameters, the design of the rock bolt system based on specific structural analysis might not be possible. Under these conditions, it is convenient to use empirical design methodologies based on the analysis of the geotechnical environment (Haile, et al., 1998).

As an initial estimate of support requirements, the US Corps of Engineers developed design rules based on case studies. These design rules are applied as the basis for rock bolt spacing in the design rock bolt support system in some mines and are tabulated in Table 5.

Table 5: Design rules developed by the US Corps of Engineers (Ryder and Jager, 2002)

Parameter	Empirical Rule
Minimum length L	Greatest of: a) 2x bolt spacing b) 3x thickness of critical and potentially unstable rock blocks c) For elements above the spring line* Spans<6m: 0.5xspan Spans between 6m and 18m: interpolate 3-4.5m d) For elements below the spring line* Height<18m: as c) above Height>18m: 0.2 x height
Maximum spacing s **Minimum spacing s**	Least of: a) 0.5 x bolt length b) 1.5 x width of critical and potentially unstable blocks 0.9-1.2m c) 2.0m (Greater spacing difficult to attach fabric support)
Minimum average pressure (support resistance)	Greatest of: a) Above spring line* Pressure = vertical rock load of 0.2 x span OR 40kN/m^2 b) Below springline* pressure = vertical rock load of 0.1 x height OR 40kN/m^2 c) Intersections: 2 x pressure determined above
*This is typically interpreted in South Africa as the point of deviation from vertical in the upper sidewall.	

Table 6 tabulates other design rules put together by Farmer and Shelton (1980) and reported by Ryder and Jager (2002) and which were specifically for rock bolting within tightly jointed rock mass structures. These design rules also considered the number of joint sets and their orientation relative to the excavation and rock bolt installation.

Table 6: Support design guidelines by Farmer and Shelton (Ryder and Jager, 2002)

Number of discontinuity sets	Rock bolt design	Comments
≤2, dipping at 0-45°	L=0.3 Span S = 0.5L (depending on the thickness and strength of strata). Install bolts perpendicular to lamination where possible with wire mesh to prevent flaking	The purpose of bolting is to create a load carrying beam over the span. Fully bonded bolts create greater discontinuity shear stiffness. Tensioned bolts should be used in weak rock, sub-horizontal tensioned bolts where vertical discontinuities occur
≤2, dipping at 45-90°	For side bolts: L>hcosΨ (If installed perpendicular to discontinuity). L>hcotΨ (If installed horizontally). Where h is the distance of installation from the point of daylight of laminations in the sidewall that defines the largest unstable wedge, and Ψ is the lamination dip.	Roof bolting as above. Side bolts designed to prevent sliding along planar discontinuities. Spacing should be such that anchoring capacity is greater than sliding or toppling weight. Bolts should be tensioned to prevent sliding
≤3 with clean tight interfaces	L=2s S=3-4x block dimension. Install bolts perpendicular to excavation periphery with wire mesh to prevent flaking.	Bolts should be installed quickly after excavation to prevent loosening and retain tangential stresses. Pre-stresses should be applied to create a zone of radial confinement. Sidewall bolting where toe of wedge daylights in sidewall

Rock mass classification systems allow one to relate one's set of conditions to conditions encountered by others. Support design for mining or civil purposes relies heavily on the use of rock mass classification procedures as a tool for empirical support assessment.

The support requirements detailed in Table 7 (Ryder and Jager, 2002) were determined for a specific civil construction and are based on the Geomechanics classification system proposed by Bieniawski. Ryder and Jager (2002) state that the application of this rock mass rating system has included a semi-empirical method for the estimation of the depth of instability around an excavation (Figure 13). This system is explained by Ryder and Jager (2002) to define an elliptical boundary around the excavation within which the rock mass is considered to require reinforcement.

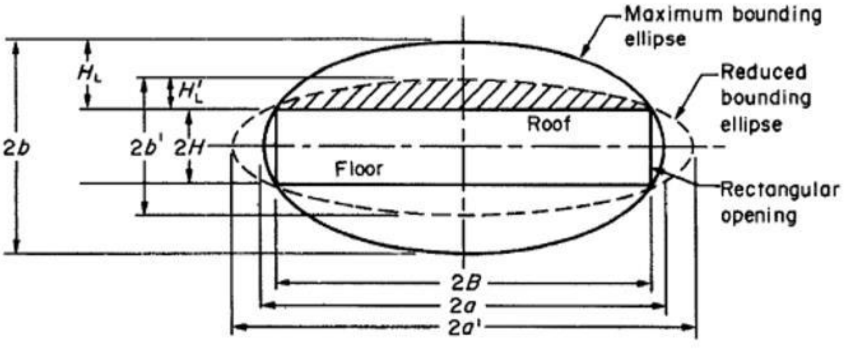

Maximum principal stress is horizontal	Maximum principal stress is vertical
$a = kb$	$a = (H^2 + k^2.B^2)^{0.5}$
$b = (B^2 + k^2.H^2)^{0.5}/k$	$b = a/k$
$a' = Bb'/(b'^2 - H^2)^{0.5}$	$a' = (1 - 0.01.RMR)a + H(0.01.RMR)$
$b' = (1 - 0.01.RMR)b + H(0.01.RMR)$	$b' = Ba'/(a'^2 - H^2)^{0.5}$
$H_L = b - H$	$H_L = a - H$
$H_L' = (1 - 0.01.RMR).H_L$	$H_L' = (1 - 0.01.RMR).H_L$

Figure 13:Semi-empirical design of the extent of instability around an excavation based on RMR (Ryder and Jager, 2002)

Table 7 gives support recommendations based on the modification of Bieniawski Geomechanics classification by Laubscher.

Table 7: Support recommendations based on the modified Geomechanics system (Ryder and Jager, 2002)

Adjusted ratings	**Original rock mass ratings, RMR**									
	90-100	80-90	70-80	60-70	50-60	40-50	30-40	20-30	10-20	0-10
60-100										
50-60		a	a	a	a					
40-50			b	b	b					
30-40				c, d	c, d	c, d, e	d, e			
20-30					g	f, g	f, g, j	f, h, j		
10-20						i	i	h, i, j	h, j	
0-10							k	k	l	l

a) Generally, no support but local joint intersections might require bolting.

b) Patterned grouted bolts at 1m collar spacing.

c) Patterned grouted bolts at 0.75m collar spacing.

d) Patterned grouted bolts at 1m collar spacing and shotcrete 100mm thick

e) Patterned grouted bolts at 1m collar spacing and massive concrete 300mm thick and only used if stress change is not excessive.

f) Patterned grouted bolts at 0.75m collar spacing and shotcrete 100mm thick.

g) Patterned grouted bolts at 0.75m collar spacing with mesh reinforced concrete 100mm thick.

h) Massive concrete 450mm thick with patterned grouted bolts at 1m spacing if stress changes are not excessive.

i) Grouted bolts at 0.75m collar spacing if reinforcing potential is present, and 100mm reinforced shotcrete, and the yielding steel arches as a repair technique if stress changes are excessive.

j) Stabilize with rope cover support and massive concrete 450mm thick if stress changes are not excessive

k) Stabilize with rope cover support followed by shotcrete to and including face if necessary, and then closely spaced yielding arches as a repair technique where stress changes are excessive.

l) Avoid development in this ground otherwise use support systems j or k.

Supplementary notes:

I. The original Geomechanics classification, as well as the adjusted ratings, must be considered in assessing the support requirements.

II. Bolts serve little purpose in highly jointed ground and should not be used as the sole support where the joint spacing rating is less than 6.

III. The recommendations contained in the above table apply to mining operations with stress levels less than 30MPa

IV. Large chambers should only be excavated in rock with adjusted total classification ratings of 50 or better.

The modifications were suggested by Laubscher so that they could cater for the differences in support requirements between the original civil environment and the mining environment. The modifications represent an alteration in terms of percentage of the individual parameters within the RMR as a function of weathering, stress environment, excavation orientation relative to the rock mass structure and the excavation method (Ryder & Jager, 2002).

The Q-system utilizes rock mass parameters to determine a value for which there is a recommended support system based on excavation dimensions and utilization. To relate the calculated Q value to the support requirement underground, Barton, et al. (1974) developed a further concept:

$$\mathbf{De} = \frac{\textbf{Excavation span,diameter or height (m)}}{\textbf{Excavation Support Ratio ESR}} \qquad \text{[EQ 29]}$$

The ESR is related to the use of the excavation and the time for which the excavation is required to be stable. Barton (1976) gives the ESR values listed in Table 8.

Table 8: ESR values for various excavations (Reproduced from Spearing, 1995)

Type or use of underground opening	**ESR**
Temporary mine openings	3-5
Vertical shafts, rectangular and circular, respectively	2.0-2.5
Water tunnels, permanent mine openings, audits, drifts	1.6
Storage caverns, road tunnels with little traffic, access tunnels, etc.	1.3
Power stations, road and railway tunnels with heavy traffic, civil defence shelters, etc.	1.0
Nuclear power plants, railroad stations, sports arenas, etc.	0.8

The relationship between the ESR, Q-value and the rock support requirements is given in Figure 14.

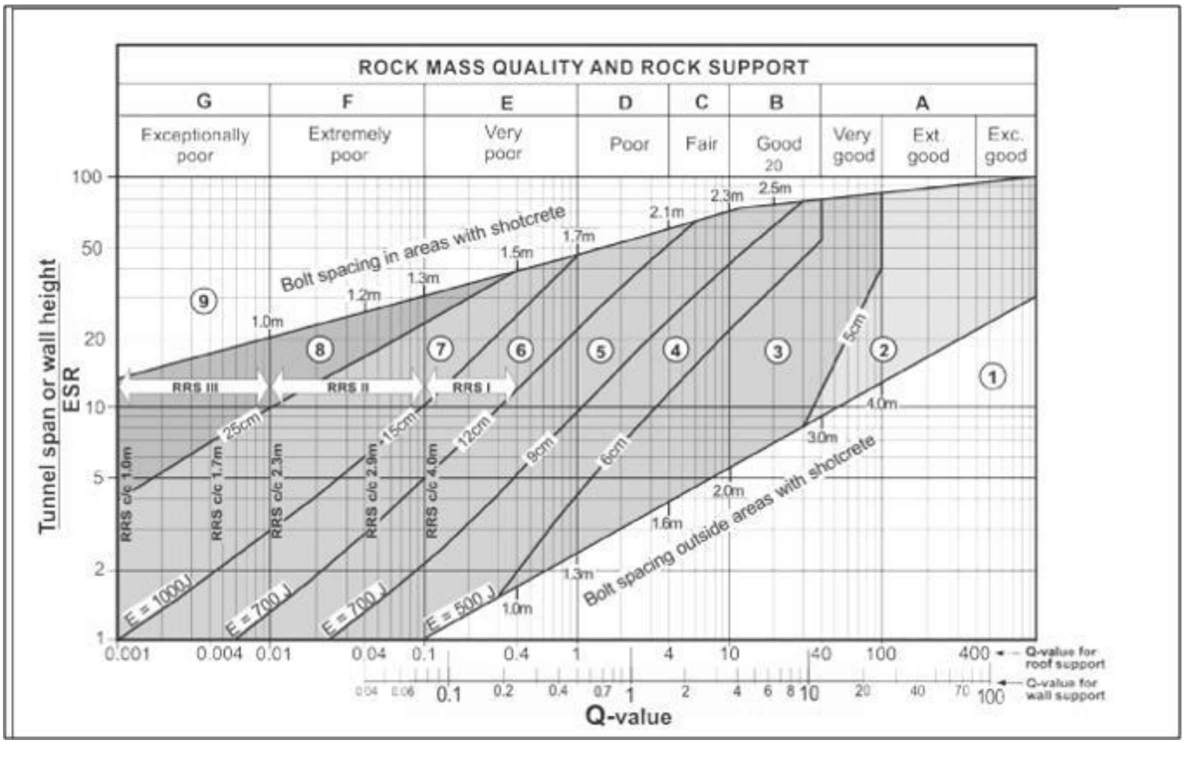

Figure 14: The Q-system chart for rock support estimates, developed by the Norwegian Geotechnical Institute (NGI) (Spearing, 1995)

2.7.3 Characteristic Behaviour of Rock Mass at Depth

Early work conducted in the analysis of rock mass behaviour at abnormal depths, revealed that tunnels are surrounded by an envelope of fracturing. The intensity of this fracturing is a function of a constant slenderness ratio, which led to the formation of more finely fractured rock at depth. This contrasted with the observations by Ortlepp (1984) that indicated that fracturing was closely spaced at the surface of the excavation and that the spacing increased with depth into the rock wall (Haile, et al., 1998).

Haile, et al. (1998) reports on the development of failure around an unsupported tunnel. The tunnel in question was investigated by Barrow (1966) and was situated in quartzite at a depth of 1600m. The tunnel was originally in virgin stress conditions but was subsequently distressed by overstoping. For this tunnel, Haile, et al. (1998) indicates that the displacement of the sidewalls increased linearly with the vertical stress and this displacement was directly associated with the development of the fracture zone.

Observations made by More O'Ferral and Brinch (1983) on the development of a fracture zone around a 5x5.5m excavation sited in quartzite indicated the presence of "bow wave" fractures up to 2m in advance of the face in a stress regime of approximately 100 MPa. Jager, et al. (1990) estimated that the deformation of a sidewall may occur up to three times the diameter behind the development face. The hangingwall fracturing was noted to be at a depth of approximately half of that in the sidewall. It was also observed that the bedding planes had a limited influence on the development of the bedding planes.

The analysis conducted by Kersten, et al. (1983) in a 10mx10m excavation situated in an argillaceous quartzite indicated a depth of fracturing of approximately 7m with a fracture intensity of 3 fractures per metre and a sidewall deformation of 90mm. Studies conducted by Ortlepp and Gay (1984) of a tunnel situated in massive siliceous quartzite of UCS 350MPa at a depth of 3075m below surface indicated that very little fracturing occurred in this competent ground in the absence of significant geological features.

Haile, et al. (1998) after Wagner (1983) indicated that the intensity of fracturing was a function of the brittleness of the rock type and the magnitude of the local stress regime which was illustrated regarding glassy or siliceous quartzite having fracture separation of approximately 10mm and argillaceous quartzite with a fracture separation of 50mm. It was also noted that the presence of bedding planes, although considered not to influence the development of the fracture zone, assisted in the slabbing of the sidewall of the excavation. Haile, et al. (1998) report that Wagner (1979) empirically determined levels of excavation deterioration due to the maximum principal stress as:

$\sigma_1 > 0.2\sigma_c$ indicates the start of scaling $\sigma_1 > 0.3\sigma_c$ indicates severe scaling $\sigma_1 > 0.4\sigma_c$ indicates heavy scaling.

Wagner (1979) advises that, where the boundary stress exceeds the rock mass strength, excavation design should consider minimization of the fracture zone.

Deep tunnel support design is often based on numerical modelling or is often arbitrary and based on general experience.

2.8 Rock Support System Interaction and Mechanism of Support

The mechanics of rock support is complex, and no models exist that can fully explain the interaction of various support components in a rock support system. Nevertheless, Kaiser, et al. (1996) summarized three key support functions as: (1) reinforce the rock mass to strengthen it and to control bulking, (2) retain broken rock to prevent fractured block failure and unravelling, and (3) hold fractured blocks and securely tie back the retaining element(s) to the stable ground (Figure 15).

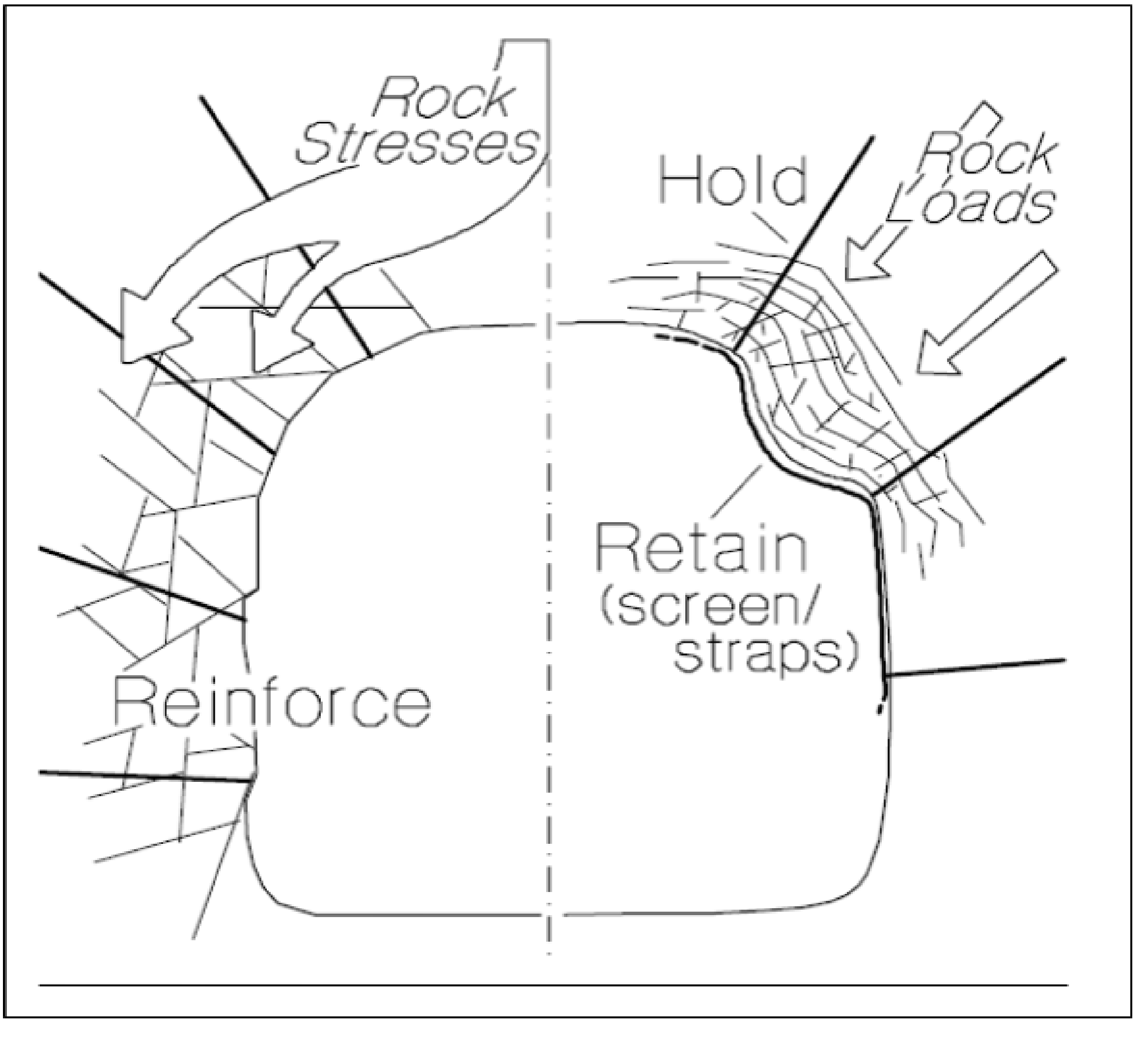

Figure 15: Three key functions (reinforce, retain and hold) of rock support (Kaiser, et al., 1996)

The purpose of a support system is to reinforce the ground, prevent deformation and support rock loads (Ongoje, 2017). Tunnel support systems typically comprise of mainly rock bolts, wire mesh reinforced shotcrete and a reinforced concrete lining. Rock bolts are installed either systematically in a pattern or at specific locations called spot bolting to limit movement and prevent unravelling by anchoring structurally unstable rock wedges as well as load transfer from an unstable excavated face to the more stable confined interior rock mass (Kristjansson, 2014).

Surface supports are placed on the surface of an excavation, and in many cases, act to truly support in whole or in part the weight of individual blocks isolated by discontinuities or zones of loosened rock.

2.8.1 Rock bolts, Dowels and Cable bolts

A wide variety of rock bolts and dowels have been developed to meet the needs for support in underground mines and civil engineering. Generally, rock bolts consist of a steel rod with a mechanical anchor on one end and a faceplate and nut on the other end. Rock bolts are always tensioned and for long term applications or use in corrosive environments are often grouted.

Mechanically anchored rock bolts (Figure 16) are usually applied as primary support and work by applying a positive force through tensioning and ensuring that all the components are in contact with the rock mass. A faceplate distributes the load from the bolt onto the rock face.

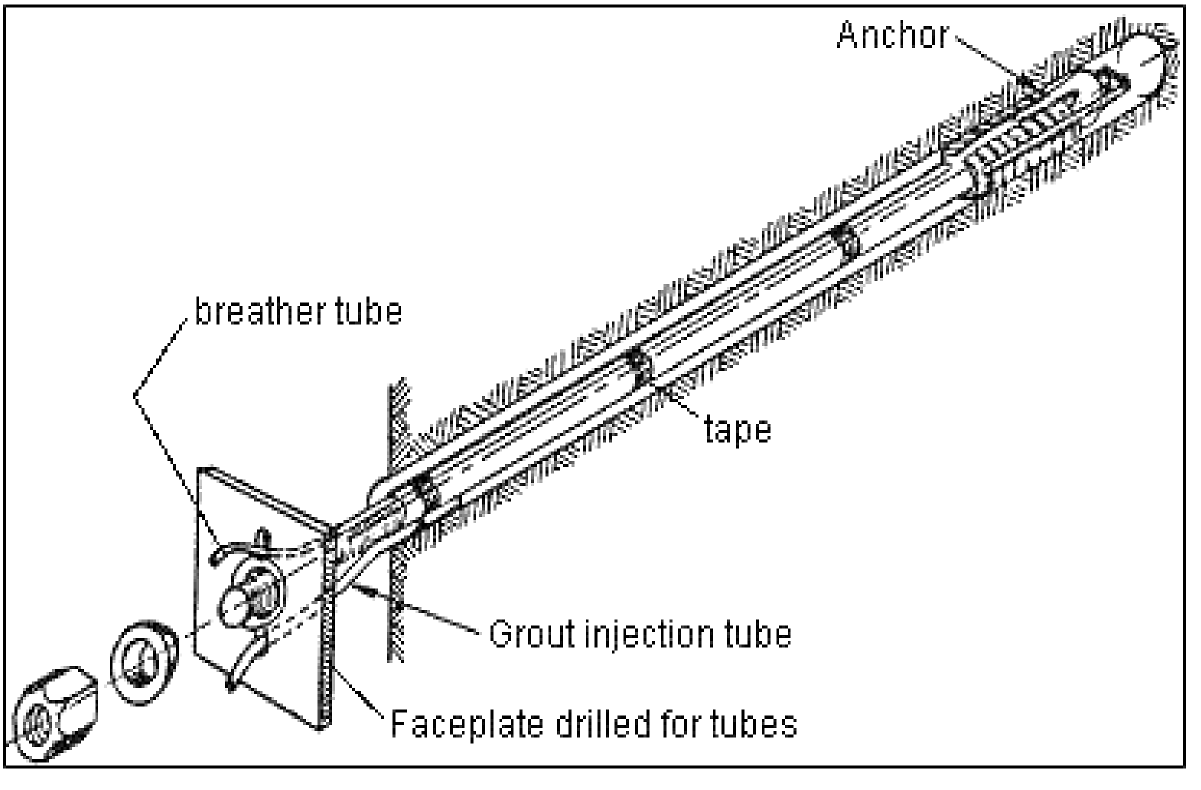

Figure 16: Mechanically anchored tendon (Ongoje, 2017)

Mechanically anchored rock bolts tend to become loose when subjected to vibrations due to nearby blasting or when anchored in weak rock. Consequently, for applications where the support load must be maintained, the use of resin anchors is considered.

Based on the initial work done by Fairhurst and Cook (1965), and reported on by Haile, et al. (1998), it was proposed that short length tendons serve to inhibit buckling and fracture formation in low-stress environments. In high-stress environments where tendons could not apply sufficient confinement to prevent fracturing, it was proposed to use longer tendons, which extend beyond the fracture zone, to inhibit buckling and thus progressive fracturing. It was further cautioned that too short tendons subjected to buckling induced tension would effectively drag out adjacent slabs and promote buckling of deeper slabs.

It was also found by Haile, et al. (1998) after Gay and Jager (1980) that fracturing along the direction of the maximum principal stress with associated dilation occurred forming slabs that tend to buckle, and if not controlled, fracturing progresses deeper into the excavation walls until scaling off and spalling of the fractured zone occurs. The inherent fractured rock mass strength is mobilized by using the confining effects of the minimum principal stress and increasing the rock strength using rock bolts.

When conditions are such that installation of support can be carried out very close to the advancing face, or in anticipation of stress changes that will occur at a later excavation stage, dowels can be used in place of rock bolts. The essential difference between these systems is that tensioned rock bolts apply a positive force to the rock, while dowels depend upon the movement in the rock to activate the reinforcing action.

Cable bolting support performs a combination of reinforcement and holding function. As reinforcement, the cables prevent separation and slip along planes of weakness in the rock mass.

2.8.2 Wire Mesh and Lacing

Wire mesh is used to support small pieces of loose rock (Figure 17) or as reinforcement for shotcrete. The wire mesh currently used is usually flexible and can be galvanized to guard against corrosion.

Figure 17: Wire mesh (Kaiser and Cai, 2012)

Weldmesh is commonly used for reinforcing of shotcrete and is usually attached to the rock using a washer. Weldmesh is susceptible to blast damage but has the advantage of not unravelling when damaged as is the case with chain link mesh. Wire mesh and lacing is also excellent as a form of rock burst-resistant support. Kaiser and Cai (2012) explain it as follows:

When brittle rock fails, it is always associated with large rock mass bulking. When a seismic event occurs, this rock may also be subjected to large impact energy, and when failing in an unstable manner, stored strain energy may be released, leading to rock ejection. Therefore, the installed rock support system must be able to absorb dynamic energy while also accommodating large sudden rock deformations due to rock failure with associated bulking. The holding function is needed to tie retaining elements of the support system and the loose rock back to stable ground, to dissipate dynamic energy due to rock ejection and rock movement, and to prevent gravity-driven falls of ground (Kaiser & Cai, 2012).

2.8.3 Shotcrete

Shotcrete was pioneered by the civil engineering industry but is used extensively in underground mining. In the underground environment, the application of shotcrete is in the secondary support of permanent openings such as haulages and other service excavations.

Shotcrete technology consists of cement, sand and fine aggregate concentrate which is applied pneumatically and compacted dynamically under high velocity. Shotcrete can be in the form of dry-crete in which dry components are fed into a hopper and agitated or wet-crete in which case the dry components are mixed with water before delivery into the pumping unit (Figure18).

Figure 18: Spraying of shotcrete on tunnel walls (Anon., n.d.)

In underground application, the addition of pozzolans to the shotcrete mixture is common. Pozzolans are cementitious materials which react with the calcium hydroxide produced during cement hydration. Silica fume, added in quantities of 8 to 13% by weight of cement, can allow shotcrete to achieve compressive strengths which are double or triple the value of plain shotcrete mixes. The result is an extremely strong, impermeable, and durable shotcrete (Hoek, et al., 1995).

2.8.4 Thin Spray-on Liners (TSLs)

Thin spray-on liners or TSLs are support types which have application in hard rock mining environments. A TSL, also referred to as a sealant, coating or membrane is defined as a thin chemical-based coating or layer that is applied to mining excavations at a thickness of 3-5mm (Jjuuko & Kalumba, 2016). The TSL sets quickly and develops an intimate and strong bond with the rock thus creating a continuous fabric that firmly adheres to the rock and provides effective rock support as shown in Figure 19. The liners can be of various properties differing by chemical composition and may include, polyurethane, cementitious material and multi-component polymeric materials.

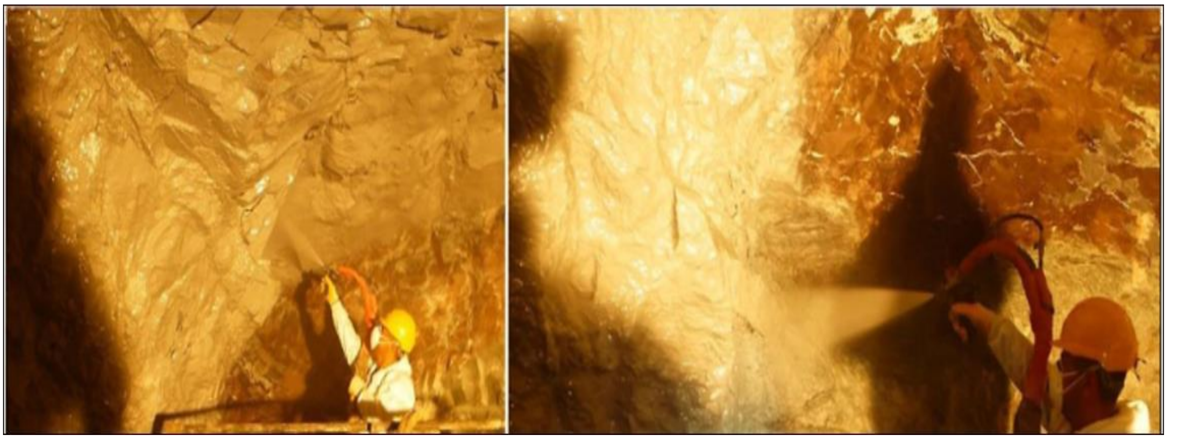

Figure 19: Application of TSL on tunnel walls (Anon., n.d.)

The history and principle of sprayed concrete dates to the early 1900s for civil engineering construction. It was adapted to tunnelling applications in the mid-1950s and mining applications in the early 1960s (Jjuuko & Kalumba, 2016).

TSLs function by firmly adhering to the rock surface and generating a continuous membrane. The continuous membrane builds up an effective support in terms of increased areal coverage and where open joints or fractures exist, the sprayed liner penetrates the loose rock (Jjuuko & Kalumba, 2016). Unlike mesh, which is effective at catching and holding small falls of rock but provides minimal resistance to the initiation of the rockfall itself, materials that are sprayed on to the rock such as liners can generate support resistance at small rock deformations (in the order of millimetres). Therefore, they possess the ability to prevent rockfalls from happening in the first place (Tannant, 2001). TSLs also can bond loose pieces of rock to adjacent competent rock and may even prevent rock mass from dilating and unravelling. This forces the fragments of the rock mass to interact with each other and create a stable beam or arch of rock. TSLs bridge the gap between rock bolts, which are favoured load carrying capabilities and mesh which is a truly passive support and requires substantial displacement before it offers a support resistance.

TSLs present many advantages when compared to other conventional support methods. The installation of conventional rock bolts and wire mesh is labour intensive, time-consuming and also, underground personnel are frequently injured while installing rock support (Tannant, 2001). TSLs, on the other hand, have the advantage of reduced labour intensity and improved safety. Other advantages of TSLs over the conventional systems include, fast application rates, rapid curing times, reduced material handling, high tensile strength with high areal coverage as well as high adhesion which enables early reduction against ground movement (Tannant, 2001).

The costs associated with the application of TSL are high, however, the economic benefits from using TSLs are realized by higher productivity and improved logistics.

2.9 Chapter Summary

This chapter presented a review on the fundamental knowledge of the research. To start, some rock mass classification methods and systems were considered. The parameters making up each method were analysed. The differences between the various rock mass classification methods as well as challenges and limitations of each method were highlighted. It was also realized that of all the classification methods considered, the Geomechanics classification system, the Q system and the modified Q system were best suited for the analysis of the footwall behaviour at Kopanang.

Various failure mechanisms of the rock mass were investigated, and it was established that certain conditions that pre-exist in a rock mass pre-empt or dictate the failure mechanism of the rock mass. It was further established that for the conditions existing at Kopanang mine, the most likely mechanism of rock failure is according to the Hoek Brown criterion. Hoek-Brown input parameters were also determined for use in numerical modelling.

Lastly, a review on support design methodologies was conducted. It was established that support design can be based on structural analysis, empirical methods, and numerical modelling. Rock-support interaction and support mechanism of various support systems used in the underground environment were also reviewed.

CHAPTER 3: METHODOLOGY

3.1 Introduction

This chapter aims to describe the methodology that was followed in conducting the research. It elaborates on the material and equipment used in conducting the research as well as the protocol that was followed.

3.2 Research Material and Equipment

First and foremost, discussions were held with mining personnel to gain an understanding of the nature and uniqueness of the problems posed by the footwall at Kopanang mine. Attention was then directed to the Geosciences department who assisted with regards to the variation of the orebody across the mine as well as the borehole core that could be used for analysis.

The core analysed had been retrieved from underground boreholes using pneumatic drills and hollow rods and had previously been utilized by the Geosciences department who had analysed it for orebody exploration and groundwater cover.

Underground stress models used in the research were obtained from routine seismic modelling, conducted by the Institute of Mine Seismology on a service rendered to Kopanang mine on a monthly basis.

3.3 Research Protocol

The method employed began with a comprehensive review of available literature on the subject. The purpose of the literature review was to establish what work had previously been done on the subject matter. The second reason for reviewing the literature was to evaluate methods previously used by other researchers to get to certain conclusions on the matter.

3.3.1 Core Logging

Core obtained from underground boreholes was logged. The purpose for the logging of the core was to determine the rock mass properties such as the quality, frequency, and nature of discontinuities as well as the influence of groundwater, if any. From core logging, a description of the lithology and stratigraphic changes with depth could also be determined. Core recovery from the different boreholes could also be established.

The information from the core logging was then used in the application of various rock mass classification systems to obtain an understanding of the strength of the rock mass and to determine whether the behaviour of the rock mass was influenced by the rock mass composition or by lateral (in terms of the different geo zones) and/or vertical variations (in terms of depth). The rock mass classification systems that were applied were:

- Geomechanics classification system
- Q-system, and
- Modified Q-system

3.3.2 Numerical Modelling

Numerical modelling was used to assess the influence of stress on the rock mass behaviour. The stress analysis was conducted on tunnels and the results inferred on polygons, under which the tunnels were classified. The tunnel stability was assessed using the Institute of Mine Seismology's (IMS) Vantage numerical modelling program. Vantage is based on the Integrated Static Stress Model (ISSM), which is IMS's implementation of the indirect boundary element method. It models the rock mass as a linear elastic continuum but can also model non-linear behaviour. Vantage modelling is conducted as routine modelling at Kopanang mine. This ensures that the mine has an up-to-date model which can then be used for planning, back analysis, and special investigations. Stress, strain, and other parameters are then calculated.

For this research, the analysis considered the major and minor principal stresses as well as the Rockwall Condition Factor (RCF), which is specifically designed for use in environments where large stress changes are expected. The formulation of the RCF is based on a simple comparison of the maximum induced tangential stress of an assumed circular excavation to the estimated rock mass strength.

3.3.3 Determination of Support Requirements

Lastly, a comparison was done in terms of the support currently installed in these areas and the support recommended by the various classification systems and the numerical modelling results.

From this study, conclusions were drawn, and recommendations were made in terms of the re-classification of the ground control districts and the most suitable support strategies for the prevailing conditions.

3.4 Chapter Summary

This chapter presented the methodology in which the research project was conducted. It was explained that the first step in conducting the research was the review of the literature to obtain an underrating of the fundamentals of the subject. The process of core logging to obtain critical information with regards to the rock mass was explained. Information from the core logging was then applied to three different rock mass classification systems and the results were compared. An explanation was also given on the numerical program that was used to analyze the underground stresses. The model used for numerical analysis was briefly introduced and it was also explained, how this modelling together with the rock mass classifications would be used in recommending support suitable for the conditions at Kopanang mine.

CHAPTER 4: ROCK MASS CLASSIFICATION ANALYSIS

4.1 Introduction

This chapter presents the findings of the rock mass classification analysis that was conducted as part of the research. The Q-System, Modified Q-system and the Geomechanics Rock mass classification system were used for this analysis. These classification systems were chosen amongst several available systems based on their suitability as well as their common use in underground mining application. For this research, a total of twenty (20) borehole core samples were analysed, and the results obtained from the different classification systems are discussed. The boreholes were recovered from different areas around the mine such that they were representative of the overall conditions in terms of lateral variation. These included the western, central and eastern portions of the mine. Figure 20 and Figure 21 shows the various boreholes as well as the locations from, which they were retrieved.

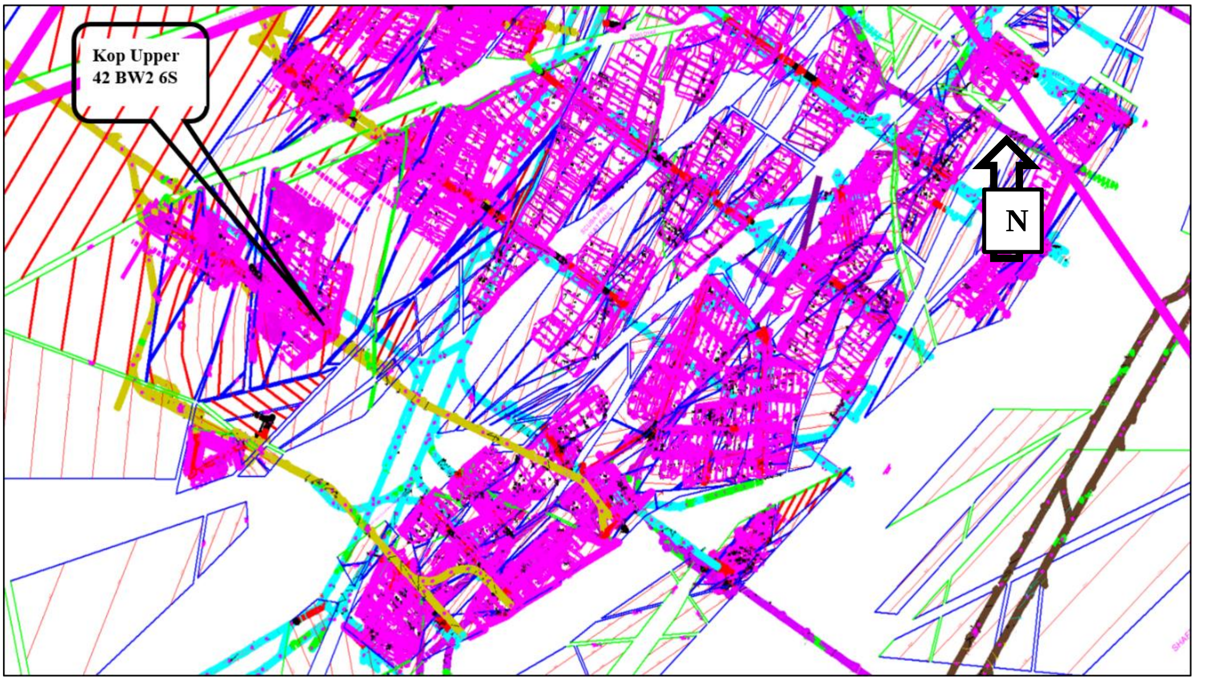

Figure 20: Borehole locations for the Kop Upper Section (West of Mine)

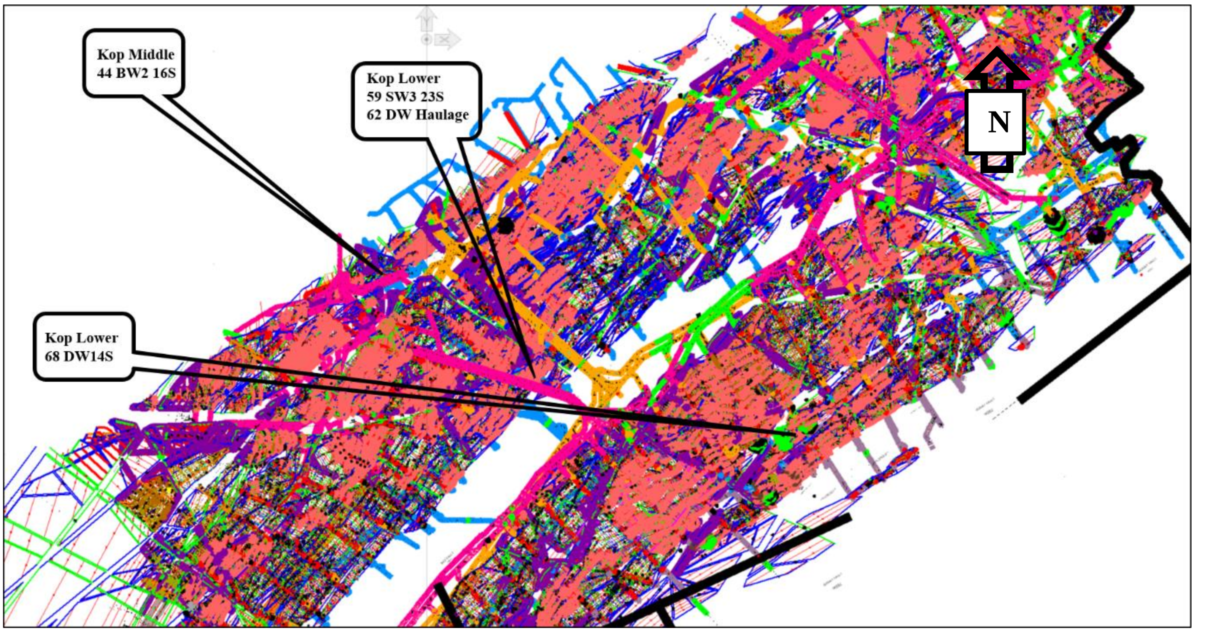

Figure 21: Borehole location for the Kop Middle and Lower Sections (Centre and East of Mine)

4.2 The Q-System

The Q-system was developed by Barton in 1974 and describes the rock mass quality by combining the six rock mass parameters described in Equation 2 of this report.

For this analysis, a value for Q was calculated for each borehole. The project study area was then split into three (3) zones based on the range of Q values that were obtained. The three segments were then labelled, Kop Upper, Kop Middle and Kop Lower and an average Q value was calculated for each of these zones. The spatial delineation of the three zones and the tunnels, which they encompassed, was as follows:

- Kop Upper - This zone represented the upper portion of the mine and covered the area from 42 level to 50 level. This is the shallowest portion of the mine with depth range being between 1247m and 1318m below surface. This zone also coincided with the western portion of the mine.
- Kop Middle - This zone represented the middle portion of the mine and covered the area from 53 level to 59 level. The range of mining depth in this zone is between 1602m and 1678m below surface. This zone coincided with the central portion of the mine.
- Kop Lower - This zone represented the deepest portion of the mine and covered the area from 62 level to 68 level. Mining depth ranges between 1850m and 2025m below surface. The naming convention at the mine is such that Kopanang does not have levels 51-52 and levels 60-61. This zone coincided with the eastern limb of the mine in term of lateral variation.

RQD values calculated from each borehole were averaged for each zone and data on discontinuities was analysed. Borehole surveying indicated that three joint sets traversed the mine lease area. The joints were rough with a separation of not more than 0.1mm. The joint surfaces had slight weathering with no infilling.

By virtue of the depth below surface from which the core was retrieved, which was well below the natural water table level and the fact that the core itself did not show any signs of water presence, an assumption was made that the joints were completely dry. No water inflow was also observed at the various sites during underground observations. It is not standard to orientate core at Kopanang mine, as such, information such as the strike of the joints could not be determined from the samples.

Other rock mass discontinuities such as faulting and stress and/or mining-induced fracturing were also observed from the core samples.

A value of 1 was assigned as the stress reduction factor (SRF). The SRF forms part of the third quotient of the equation defining the value of Q and is a crude measure of the active stress. The SRF is a difficult parameter to determine in the field (Swart, 2005) and particular care needs to be taken when assigning its rating. The SRF is divided into four broad groups (Barton, 1988):

a) Weakness zone causing loosening or fall-out
b) Rock stress problems in competent rock
c) Rock squeezing
d) Swelling (chemical effect due to water uptake)

The twenty boreholes assessed for the mine fall under category (b) and were classified as having moderate stress in essentially competent rock with $\sigma c/\sigma 1$ being less than 10.

Table 9 below presents a summary of representative Q values calculated for the three zones of the mine. The data is represented in full in Appendix E.

Table 9: Summary of representative Q-values calculated for the identified zones

Polygon	Lateral position	RQD	Q	Rock Mass Description (RQD)	Rock Mass Description (Q)
Kop Upper	West	39.38	9.84	Poor	Fair
Kop Middle	Central	30.72	7.68	Poor	Fair
Kop Lower	East	25.98	7.29	Poor	Fair

4.3 The Modified Q-System

The modified Q-system by Kirsten (1988) evaluates parameters such as the uniaxial compressive strength (UCS) of the core and the stress ratio and assigns SRF relationships for homogeneous and non-homogeneous rock masses. For this exercise, the UCS of the core was taken as the value specified in the mine's Code of Practice for rockfalls and this was taken as 172 MPa for the footwall (COP, 2017).

The value of the stress ratio was determined by dividing the value of the major principal stress, $\sigma1$ by that of the minor principal stress, $\sigma3$ in all the respective zones.

Both $\sigma1$ and $\sigma3$ were obtained from numerical modelling.

Table 10 is a summary of the representative Modified Q values calculated for the three zones. The data is represented in full in Appendix F.

Table 10: Summary of representative Modified Q values calculated for the three zones

Polygon	Lateral position	Q_n	Q_h	Rock mass Description
Kop Upper	West	12.77	0.04	Good
Kop Middle	Central	8.66	0.02	Fair
Kop Lower	East	8.02	0.02	Fair

4.4 The Geomechanics Classification System

For this exercise, the 1989 version of Bieniawski's rock mass rating system was used. This version takes the influence of joint orientation and groundwater on the rock mass into account.

Table 11 is a summary of representative RMR and GSI ratings calculated for the three zones. The data is represented in full in Appendix H.

Table 11: Summary of representative RMR and GSI ratings calculated for the three zones

Polygon	Lateral position	RMR_{89}	GSI	Rock mass Description (RMR)	Rock mass Description (GSI)
Kop Upper	West	69.4	64.4	Good	Very Good
Kop Middle	Central	70	65	Good	Very Good
Kop Lower	East	69.25	64.25	Good	Very Good

The Geological Strength Index (GSI) is a parameter that relates the rock strength parameters such as m, s and Young's modulus to the rock mass rating. The GSI is calculated from the RMR using the following equation:

$$GSI = RMR_{89} - 5 \qquad \text{[EQ 30]}$$

4.5 Discussion

The results of the rock mass classification for the core samples are presented in the earlier sections. The data from the core was analysed in terms of the RQD, Q-system, Modified Q-system and Bieniawski's rock mass rating system.

The rock quality designation (RQD) is a simple description of the condition of recovered drill core. On its own, the RQD fails to account for the condition of joint surfaces, filling material and may be overly sensitive to orientation effects. The RQD however, is a common factor in the classification systems presented earlier.

For the analysis, the mine is split into three zones according to the range of Q, modified Q and RQD values obtained. The zones were labelled Kop Upper, Kop Middle and Kop Lower and these coincided with the upper, middle and lower (depth) sections of the mine, respectively. The zones further coincided with the various lateral sections of the mine in terms of position (West, Central and East).

An analysis of the core samples and the calculated parameters indicates low RQD values across the mine. These RQD values are observed to decline with increasing depth below the surface. It is also noted that this decline seems to be more pronounced towards the eastern section of the mine.

Figure 22 is a depiction of the lateral variation of the Vaal reef and a possible explanation for the extremely poor rock mass quality in this section of the mine.

The source of the Vaal reef deposition across the mine lease area is believed to have been a braided river consisting of a network of multiple depositional channels at varying depths. Towards the centre of the channel, the river is believed to have been relatively deeper, such that the bedrock in this area would be subjected to extensive erosion when compared to the bedrock around the edges. For this reason, at the centre of the channel, some units of the bedrock would have been eliminated by erosion, but the very same units would still be preserved on the edges.

Figure 22 explains the lateral variation of the rock mass across the mine. The western side is shown to be located close to the centre or a deeper section of the channel. As such, with time, this portion of the channel would be completely eroded and the poor quality orthoquartzite would have been completely eroded in this area. In contrast, the eastern side is positioned closer to the edge of the channel. Thus, the overlying sediments, which in this case includes, the poor-quality orthoquartzites would have been preserved from erosion.

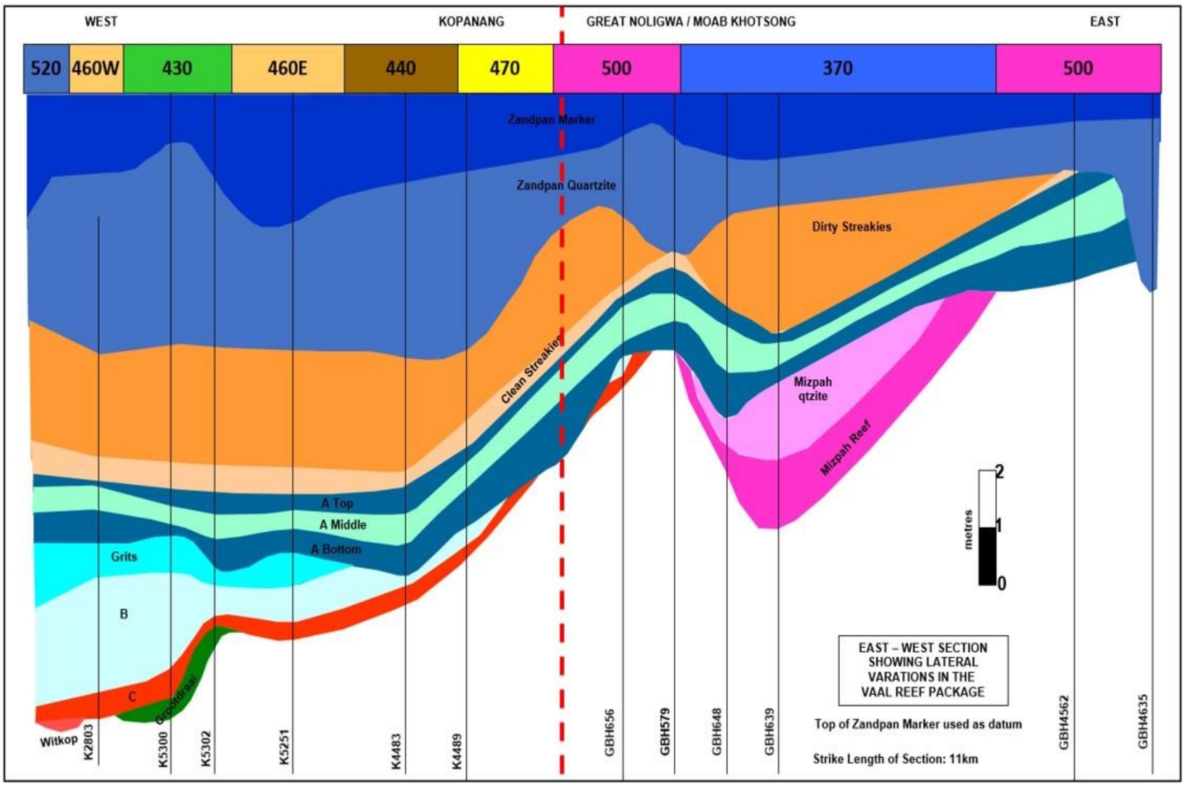

Figure 22: East-West section showing lateral variation in the Vaal reef package (COP, 2017)

The phase diagram in Figure 23 describes the variation in the footwall quartzite composition between the western and eastern sections of the mine. The orthoquartzite, which is predominantly, exposed in the eastern section of the mine, is located at the very top of the phase diagram. In this area, the composition of the quartzite is predominantly quartzerenite which is a strong rock, and which fails in a typical brittle manner. When exposed, this type of rock exhibits signs of spalling with excessive plate-like shards of rock which dislodge from the periphery of the excavations.

The argillaceous quartzite, which is encountered on the more stable western section of the mine is located further down, towards the centre of the 3-phase diagram. Towards the centre, the composition of the quartzite transitions from being purely that of quartzerenite to elements of feldspar and rock fragments. The argillaceous quartzite fails in a blocky manner when exposed. This is, in turn, easier to support and control compared to the orthoquartzite.

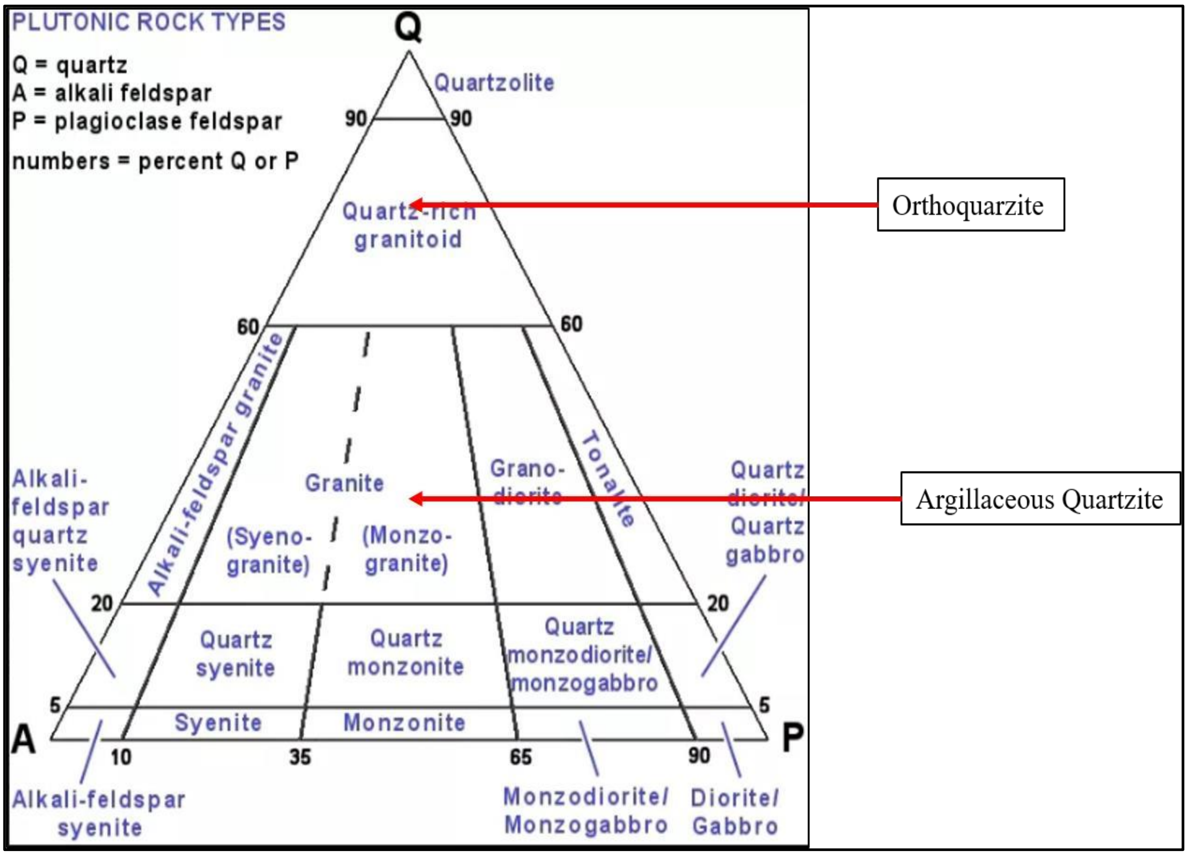

Figure 23: Three-phase diagram of footwall quartzite composition (Anon., n.d.)

It can thus be concluded that the footwall development in the eastern section of the mine has the orthoquartzite (locally referred to as the upper siliceous quartzite) still preserved. This in turn negatively affects the rock mass quality in this section of the mine.

To a large degree, there is agreement in the rock mass quality predicted by the various rock mass classification systems and possible explanations have been deduced as to why this might be the case, however, the following must still be borne in mind:

Rock mass classification systems have their limitations. These systems are often based on case histories and thus tend to be conservative in their approach. The reliability of most rock mass classification systems is another cause of concern. This is because although these systems consider similar parameters in computing the final rock mass rating, the very systems assign different weightings to similar parameters. This makes the exercise somewhat subjective and as such, the following points need to be considered for the results obtained for Kopanang mine:

- The RQD is significantly influenced by the orientation of the borehole (Swart, 2005). The core used for the analysis is not orientated and this could have influenced the results obtained from this analysis. The RQD also disregards the influence of jointing, thus it does not fully describe the rock mass.

- The Q-system does not consider joint orientation and only considers the joint condition of the most unfavourable joint. Thus, the Q-system assumes that the rock mass strength is dominated by the strength of the weakest joint.
- The RMR considers the spacing of structural features but ignores the effects of the induced stress. This may limit the use of this classification system in mining environments where the stress environment changes as mining progresses as is the case with Kopanang mine.

Also, the applied rock mass classifications show an overriding importance of discontinuities but a low importance of the rock strength.

4.6 Chapter Summary

This chapter presented the findings of the rock mass classification analysis that was conducted for the research. A total of three rock mass classification systems, namely, the Q-system, the modified Q-system and the Geomechanics rock mass classification systems were used to assess twenty bore core samples obtained from Kopanang mine.

The core samples were spread over the three different zones defined for the mine, namely the Kop Upper, the Kop Middle and the Kop Lower. These zones differentiated I terms of depth below surface as well as lateral positioning and direction (West, Central and East). The quality of the rock mass was described in terms of the RQD, Q, Modified Q and RMR value.

The results obtained using the different systems were consistent, in that all three systems plus the RQD predicted fair to poor rock mass quality across the entire mine.

The quality of the rock mass was predicted to be especially poor towards the eastern section of the mine. This observed decline in rock mass quality toward the east was attributed to the depositional process at Kopanang mine.

It was also observed that the poor rock mass quality was predicted in the areas of the mine, where orthoquartzites were still preserved and exposed. This contrasted with the western side, which was located in the centre of the river during deposition, and in which the orthoquartzite may have been completely eroded.

The conclusion was that this observation possibly explained the variation in footwall behaviour at Kopanang mine, and the reason why poor footwall conditions are being experienced on the eastern side of the mine.

However, although, agreement was achieved in the results predicted by the different systems, it was noted that the classification systems can be somewhat biased. It was also emphasised that their application be limited to the environments for which they were intended.

CHAPTER 5: NUMERICAL MODELLING ANALYSIS

5.1 Introduction

The stability of the tunnels was assessed using the Vantage numerical modelling program developed by the Institute of Mine Seismology (IMS). Vantage is based on the Integrated Static Stress Model (ISSM), which is IMS's implementation of the indirect boundary element method. It models the rock mass as a linear elastic continuum but can also model non-linear behaviour. Vantage modelling is conducted as routine modelling at Kopanang mine. This ensures that the mine has an up-to-date model which can then be used for planning, back analysis and special investigations.

The stability of tunnels and service excavations is controlled by rock mass conditions, field stress levels and quantity/quality of installed support. One of the functions of regional design is to control field stress levels as far as practically possible. This can be accomplished by placing off reef excavations sufficiently remote from highly stressed abutments and by overstoping, layout and sequences.

For this research, a case study was conducted. Four historically developed tunnels, located at varying depths were used as conceptual models. The analysis was conducted in terms of the Rockwall Condition Factor (RCF) which is specifically designed for use in environments where large stress changes are expected. The analysis results for the four tunnels were compared and the correlation of the support requirements as determined by RCF (for the prevailing stress levels and conditions) against the actual support installed in the tunnels was tested.

The formulation of RCF is based on a simple comparison of the maximum induced tangential stress of an assumed circular excavation to the estimated rock mass strength (Jager & Ryder, 1999) and is defined by:

$$\mathbf{RCF} = \frac{(3\sigma_{1-\sigma_3})}{F\sigma_c} \qquad \text{[EQ 31]}$$

where, σ_1 is the major principal stress within the plane of the excavation cross-section (MPa)

σ_3 is the minor principal stress within the plane of the excavation cross-section (MPa)

F is a factor to represent the downgrading of σ_c.

In good quality quartzites, F takes on a value of unity. In a highly discontinuous rock mass, a suitable value for F is approximately 0.5, and in large excavations (>6x6m), F may be further downgraded by 10-20%.

Based on the industry-accepted design criteria, it is anticipated that:

- RCF values lower than 0.7 should result in good excavation conditions
- RCF values between 0.7 and 1.4 should result in moderate excavation conditions.

- RCF values greater than 1.4 should result in adverse excavation conditions (Jager & Ryder, 1999).

Boundary element methods have a number of advantages in that they require less data to run efficiently, they require less time and the discretization process takes place only on the surface of the body resulting in a smaller system of equations. However, its inability to incorporate discontinuities and model non-linear problems is a disadvantage. This is particularly a concern in environments where rock mass failure is primarily driven by structure and where additional methods or modelling programs would be required to predict failure.

5.2 Case Study Background

As a result of the complex geology at Kopanang mine, the area is sub-divided into relatively small blocks of ground. Scattered mining with raise lines approximately 150m to 180m apart is conducted in this environment. The raise lines are further grouped into smaller sections known as polygons based on their spatial locations with one another.

The four tunnels considered in this research's numerical analysis are located within these polygons and the polygons fall within the Kop Upper, Kop Middle and Kop Lower sections of the mine.

All the tunnels evaluated were developed years back under virgin stress conditions before stoping in the various areas commenced. The tunnels are situated between 1247m and 2025m below surface with cross-sectional dimensions of 3.5m x 3.5m. The host rock is a well-bedded quartzite of the Main Bird Series (MB5) with an average uniaxial compressive strength of 172MPa. The long axis of the tunnels is orientated along the strike of the strata.

5.3 Input Parameters and Boundary Conditions

The input parameters for the numerical stress models were obtained from previous work conducted within AngloGold Ashanti for the Vaal River District by Hoffman and Scheepers (2010).

One material (rock type) was considered in the numerical model. The host rock mass was defined as being the MB5 Quartzite (footwall lithology). The elastic properties of the host rock both of which were determined via laboratory core testing and back analysis and model calibration (Hoffman and Scheepers, 2010) were taken as:

- Elastic Modulus – 50GPa
- Poisson's ratio – 0.2

The Great Noligwa Mine (GNM) stress state, as previously defined for the Vaal River District was used with the host rock density (ρ) taken as 2700kg/m^3, k-ratio of 0.9/0.5, σ_2 trending north and σ_1 plunging at 20°. The stress conditions are uniquely defined by three principal stress components referred to as σHmax which is the stress component most closely representing the nearest Y-axis, σHmin which is the stress component most closely representing the nearest X-axis and σVert which the stress component most closely representing the nearest Z-axis. The pre-mining stress state defines the datum, which is a reference point on the earth's surface against which positions measurements are made, for this exercise, this was taken as 519m below surface and the stress variation, Hoffman and Scheepers (2010) define the variation in σHmax to be 0.028200MPa/m, σHmin to be 0.1012500MPa/m and σVert to be 0.024100MPa/m.

For this case, an average UCS of 172MPa and a downgrading factor of 1, which was indicative of good quality quartzite, was used for all cases.

5.4 Numerical Modelling Results

The three-month RCF modelling results for the various sections are discussed in the following section.

5.4.1 42 BW2 6S Crosscut (42 BW2 Area)

The 42 BW2 6S crosscut is located at 1247m below surface and forms part of the 42 BW2 3_12 polygon in the Kop Upper area. For computing of the RCF values, σ_1 and σ_3, which are the major and the minor principal stresses, respectively for this particular polygon were used. Figure 24 shows a Vantage plot of the σ_1 values for the area. In the plot, the major principal stress values are shown as contours around the previously mined areas. For the particular area, the major principal stress values range from 65 MPa up to a maximum that is over 215 MPa, which is normal for the specified depth range.

The computed RCF value for the tunnel was in the range of 0.4 to 0.5 over an 800m stretch of the tunnel. A slight peak up to a RCF value of 0.5 is observed at a distance of 300m to 400m from the zero-reference point as indicated in Figure 25. The majority of the tunnel is situated on solid away from active stoping, however, the short portion, over which the increase in RCF is observed (shown as a blue string in Figure 25) is situated immediately below active stoping and is thus under the influence of a moving abutment. The overall RCF values predicted in this tunnel are below the critical values which would otherwise result in adverse conditions as described by Jager & Ryder (1999).

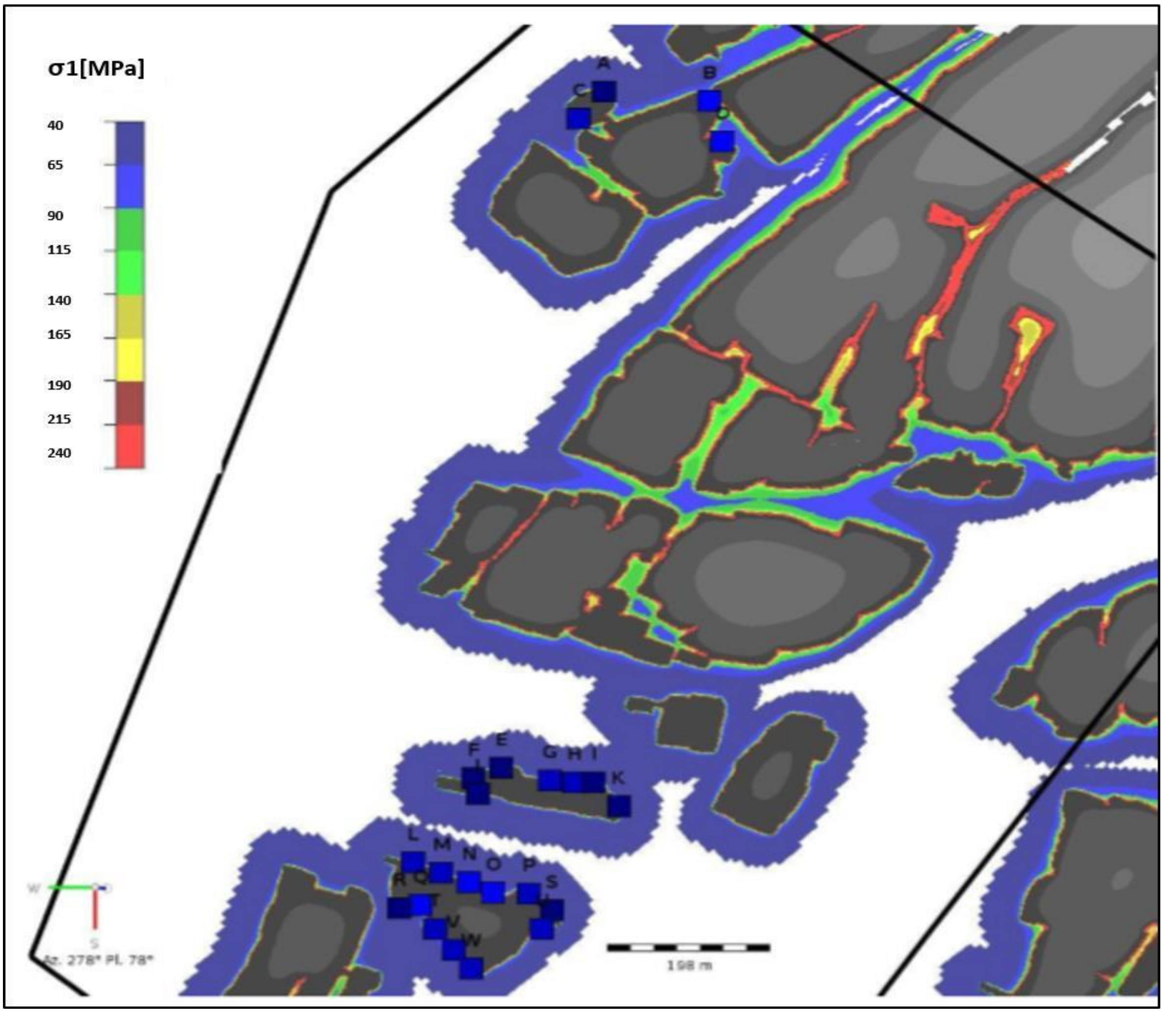

Figure 24: Sigma 1 plot of the 42 BW2 6S Crosscut Area (Vantage Modelling, 2018)

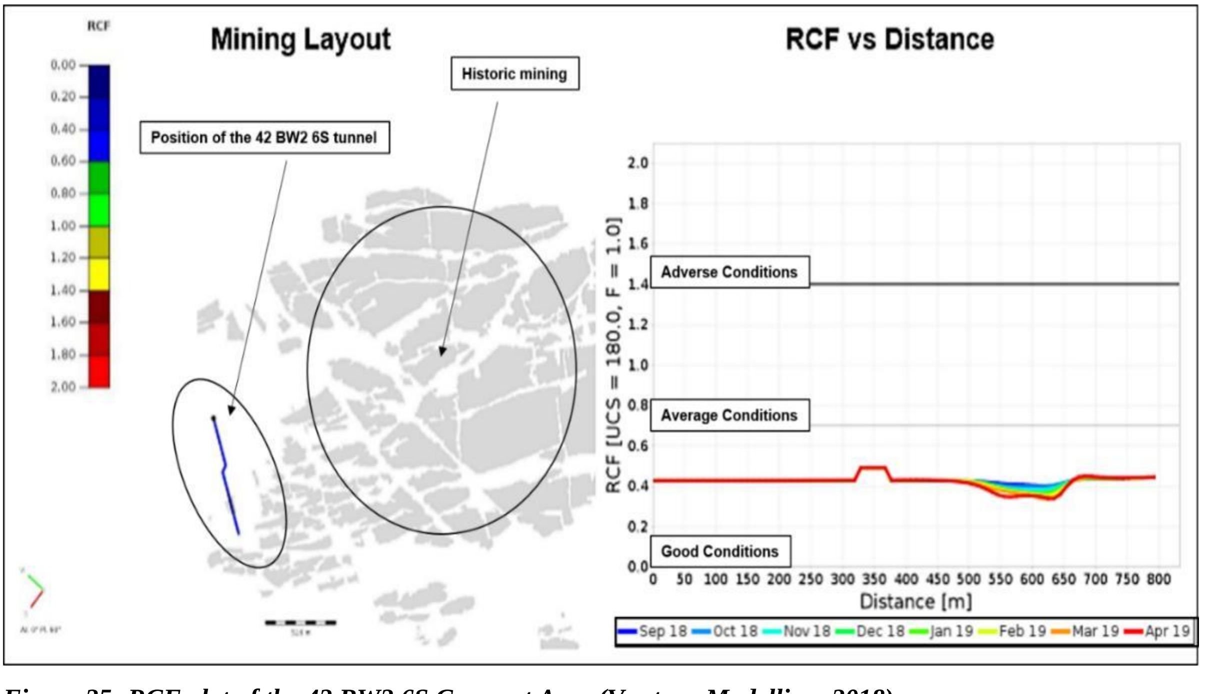

Figure 25: RCF plot of the 42 BW2 6S Crosscut Area (Vantage Modelling, 2018)

5.4.2 44 BW3 16C Crosscut (44 BW3 Area)

The 44 BW 3 16C crosscut is located at 1318m below surface and forms part of the 44 BW 2_10 polygon in the Kop Middle area. The tunnel is situated close to the main haulage on 44 level, hence, in this case, the RCF results of the 44 BW3 haulage were used. Figure 26 shows the major principal stress plot for this area. Relatively low ranges of the major principal stress are predicted in this region, with the majority being in the 40MPa-65MPa range and only a small percentage of isolated peninsulas reaching a maximum of 240MPa. RCF values in the range of 0.4 to 1.3 over a distance of approximately 3000m were obtained from modelling as shown in Figure 27. The zero reference point of the haulage starts in solid, where the RCF values are as low as 0.4. Over the distance assessed, the tunnel negotiates several static abutments which elevates the RCF to 0.8. Thereafter, the tunnel is subjected to overstoped conditions which reduce the RCF due to the associated stress relaxation. In the last portion of the haulage, the RCF levels are elevated to 1.3 which is brought about by the influence of the abutment which runs parallel to the long axis of the tunnel.

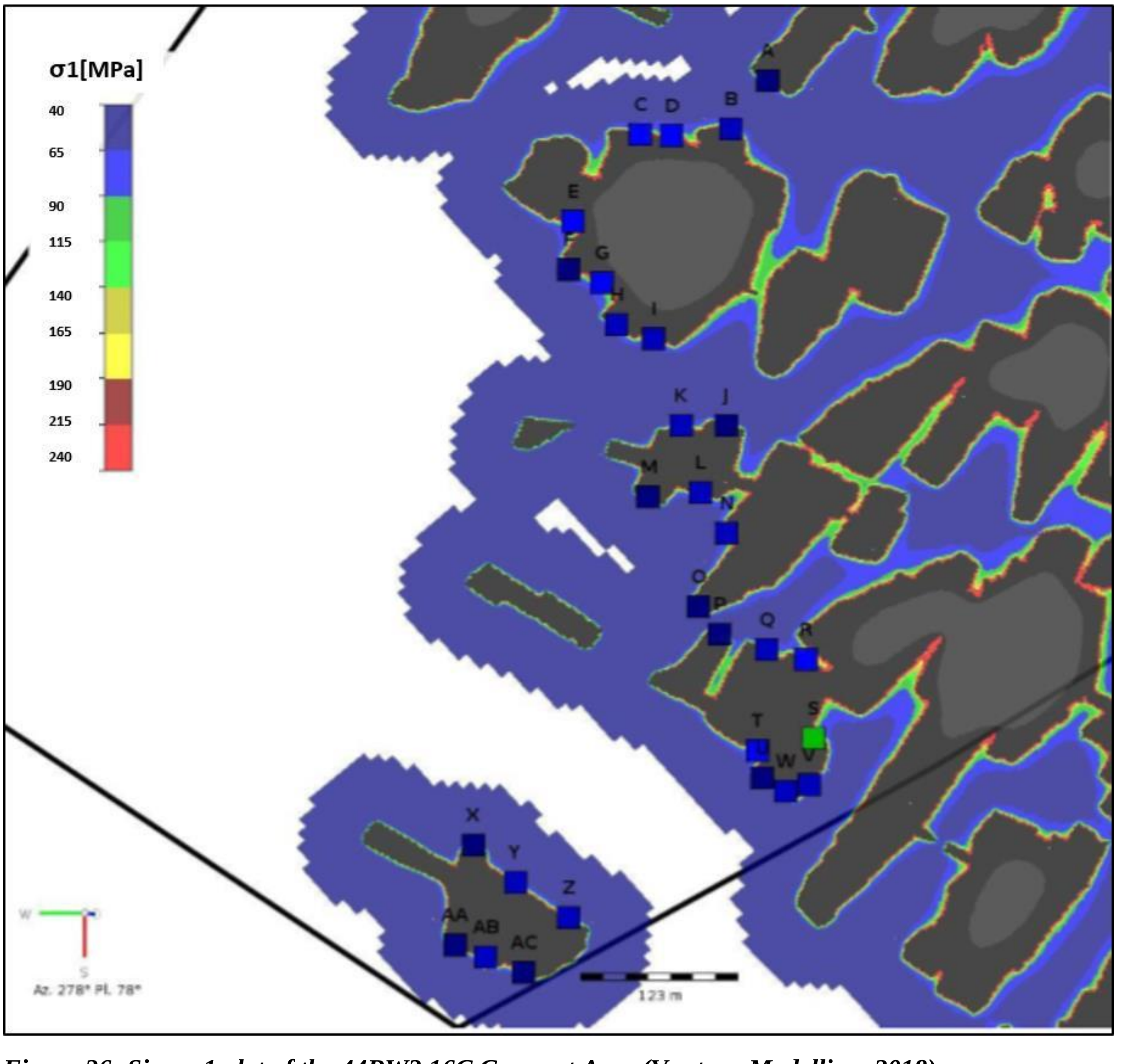

Figure 26: Sigma 1 plot of the 44BW3 16C Crosscut Area (Vantage Modelling, 2018)

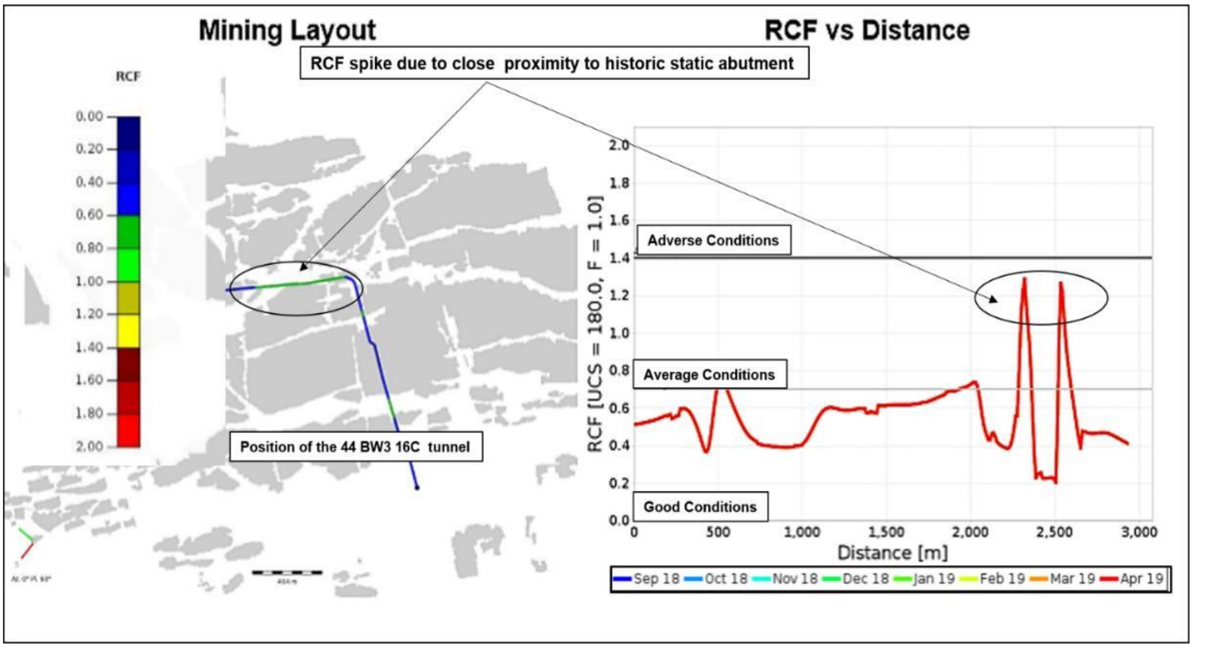

Figure 27: RCF plot of the 44 BW3 16C Crosscut Area (Vantage Modelling), 2018)

5.4.3 62 DW4 14S Crosscut (DW4 Area)

The 62 DW4 14S crosscut is located at 1850m below surface and forms part of the 6268 DW4 14-18 polygon. The major principal stress plot for this polygon is shown in Figure 28. The major principal stress in this region is predicted to be low to moderate with high-stress values concentrated around the historic stoping abutments. The RCF values are indicated to be between 0.6 and 1.3 over a tunnel distance of 340m. The tunnel negotiates static abutments on two occasions, and this is accompanied by a spike in the RCF values, almost nearing the critical value of 1.4 as shown in Figure 29. The tunnel is thereafter subjected to overstoped conditions which reduces the RCF to around 1.0 suggesting average conditions.

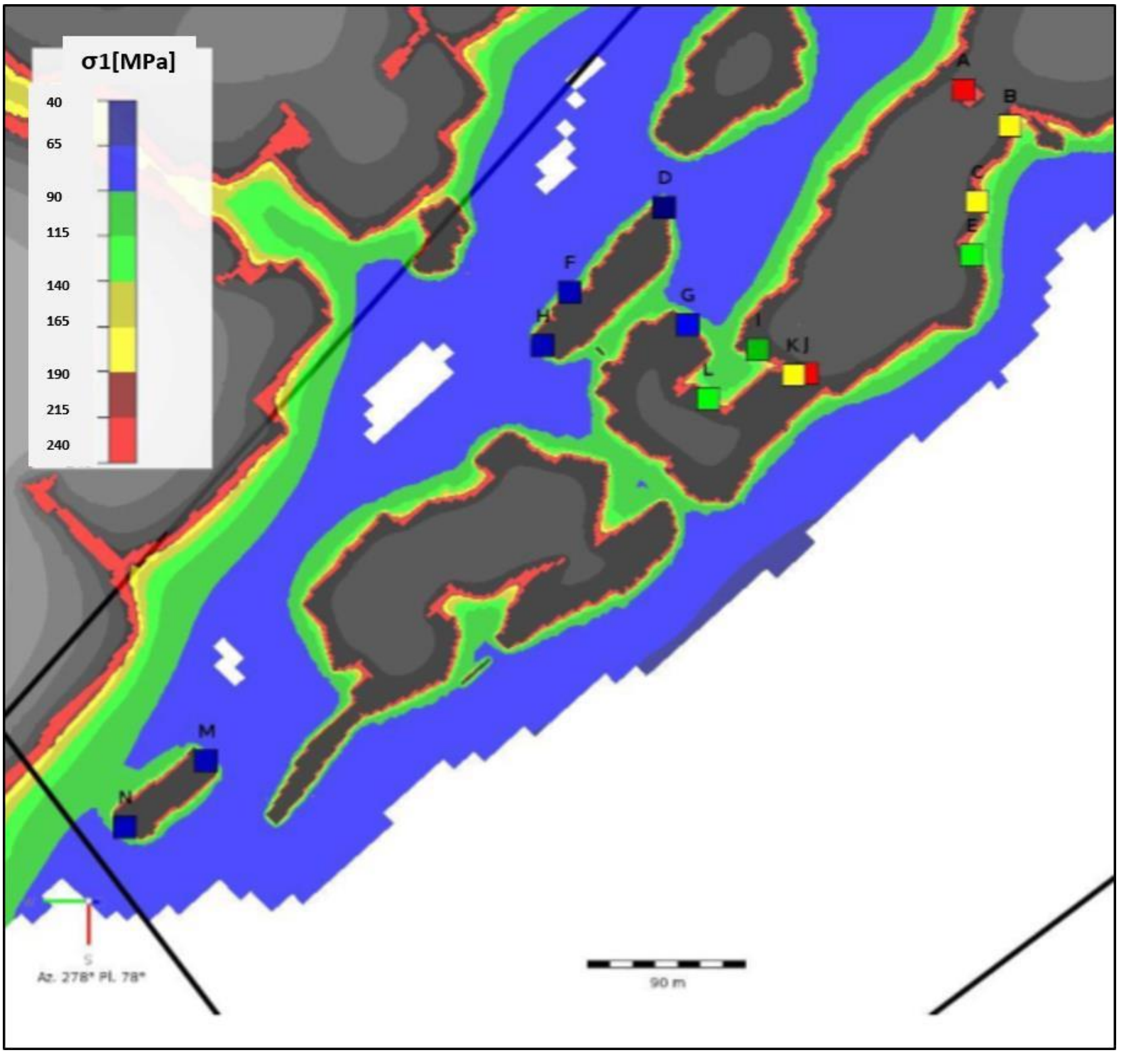

Figure 28: Sigma 1 plot of the 62 DW4 14S Crosscut Area (Vantage Modelling, 2018)

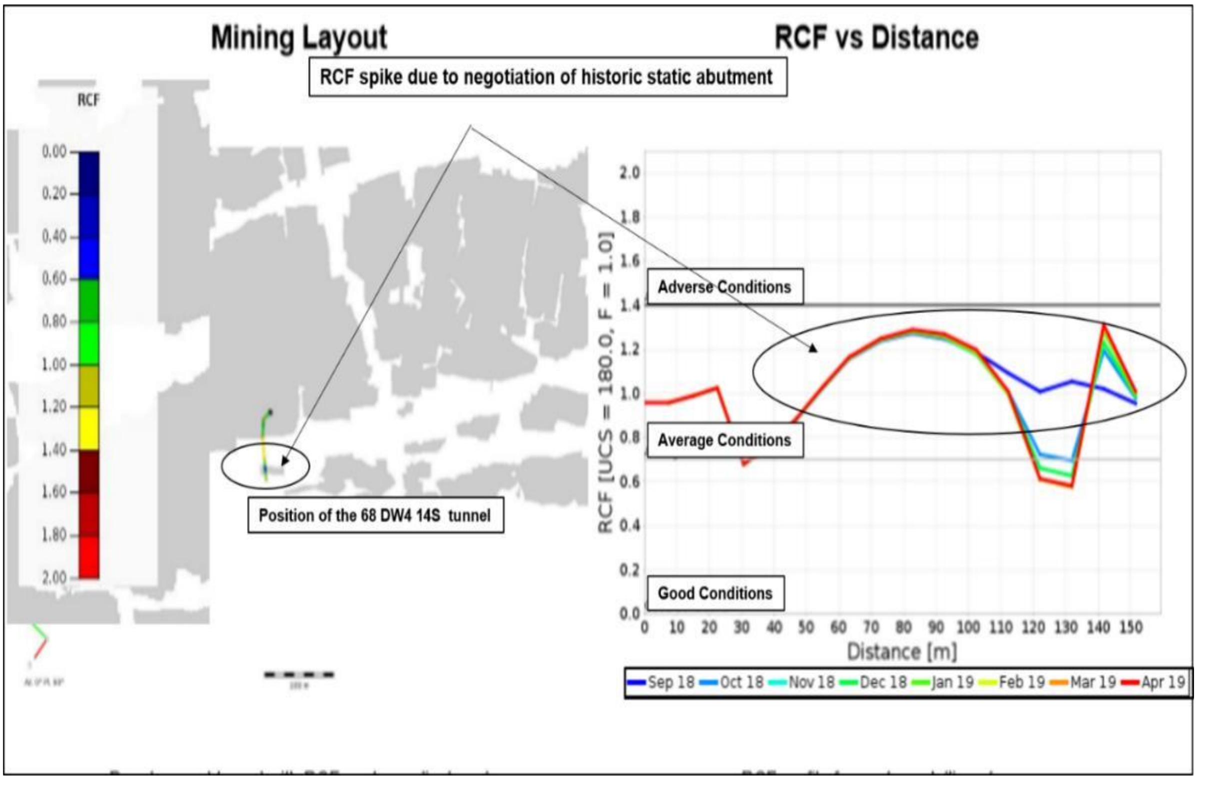

Figure 29: RCF plot of the 62 DW4 14S Crosscut Area (Vantage Modelling, 2018)

5.4.4 68 SW4 23S Crosscut (62-68_SW3/SW4 Area)

The 68 SW4 23S crosscut is located at 2548m below surface and forms part of the 62 68 SW4 18S-19A polygon in the Kop Lower area. Compared to the three other tunnels that have been analyzed, this tunnel is located in the deepest section of the mine, where the stresses are expected to be higher. The major principal stress plot for this region is shown in Figure 30. In this area, the stresses migrate from the low values observed for the other three polygons. The stresses in this area are predicted as being vastly moderate in the region of 65MPa to 140 MPa with high stresses concentrated around historic stoping abutments. The RCF values predicted for this tunnel are in the range of 0.3 to 1.9 (Figure 31). Both extremities of the tunnel are located near abutments and are hence under the influence. The majority of the tunnel is located in an overstoped area results in good to average conditions.

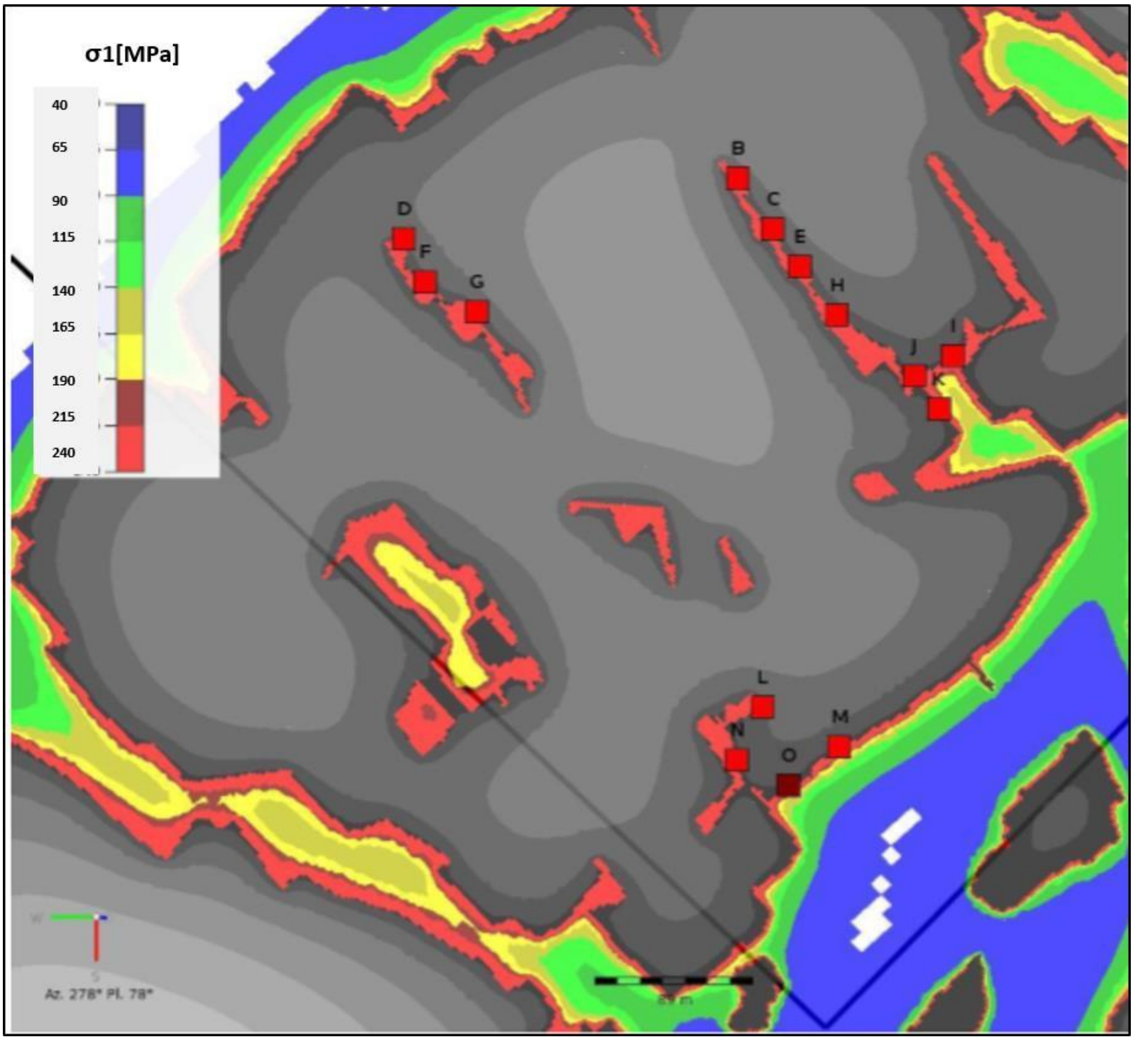

Figure 30: Sigma 1 plot of the 68 SW4 23S Crosscut Area (Vantage Modelling, 2018)

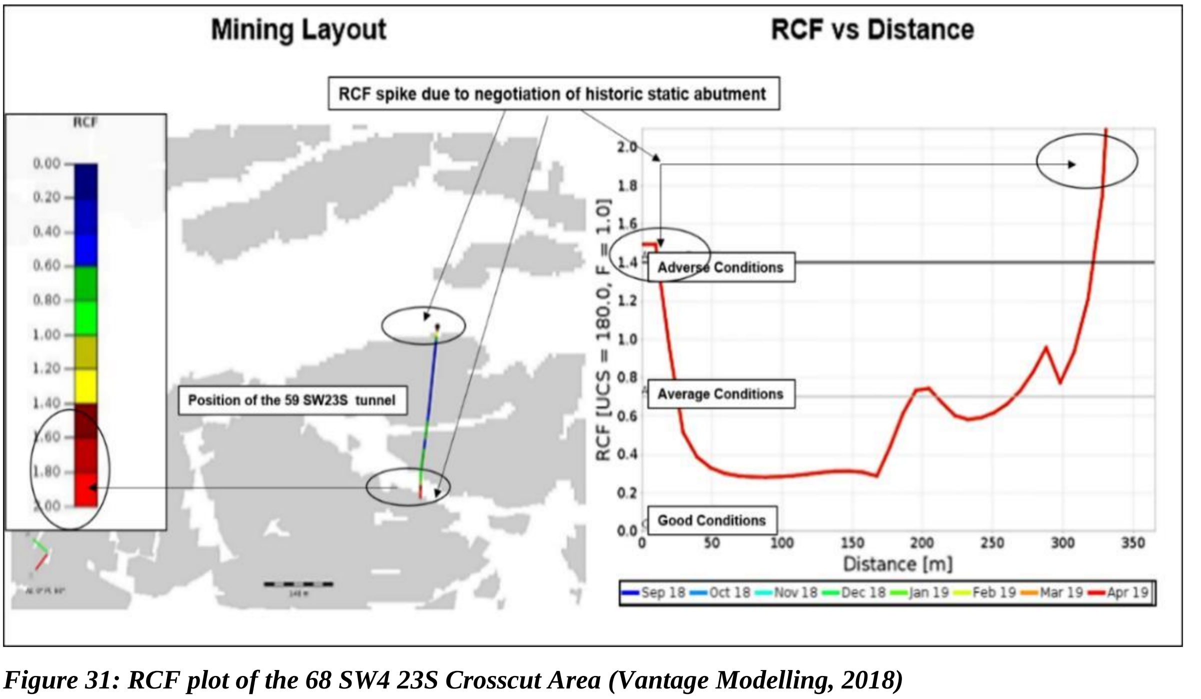

Figure 31: RCF plot of the 68 SW4 23S Crosscut Area (Vantage Modelling, 2018)

5.5 Discussion

An IMS Vantage numerical analysis was conducted for different tunnels. These tunnels are located at different mining depths but are subjected to similar mining conditions. In all the tunnels, an increase in the RCF values is observed in all areas where the tunnels negotiate static or moving mining abutments. This is testament to the fact that changes in the stress regime have an influence in the RCF values and hence in the overall tunnel conditions. It is also evident that as more abutments need to be negotiated, there is a bigger influence on the RCF and the tunnel encounters more adverse conditions, as can be seen in the case of the 68 SW4 23S crosscut and the 44 BW3 haulage.

Low values of RCF are predicted when the tunnels negotiate solid areas. From the results, it is evident that depth below surface plays a major role in influencing the RCF values.

All the tunnels analysed are subjected to and traverse various geological structures because the whole of Kopanang mine is geologically complex. Based on experience, it is universally accepted that geology will have an influence on rock mass conditions and in the case of the tunnels analysed, it can be accepted that the role played by geology was the same in all parts of the mine, although in some cases, the severity might be exacerbated by other various factors such as mining spans, depth and stress changes**.**

The RCF values are however observed to not have been influenced by lateral variations of the rock mass across the mine but purely by depth below the surface. Areas in which high RCF values are predicted are concomitant with seismic activity and rock bursting, and often require specialized support tailored for these high-stress conditions. For this analysis, however, the high RCF values were only predicted in isolated instances, where the tunnels had to negotiate abutments and were thus exposed to abrupt stress changes.

On this premise, it can be concluded that the predicted stress or RCF levels may not be used as a basis for the delineation of separate ground control districts.

5.6 Chapter Summary

This chapter presented the results of the numerical modelling that was conducted for the different polygons of the mine. The modelling was done in terms of RCF using the Vantage boundary element modelling program. The numerical modelling was also useful in obtaining σ_1 and σ_3 stresses for the calculation of stress ratios in the rock mass classification systems.

Various tunnels within the different polygons of the mine and at differing depths were assessed. From the RCF results obtained, it is evident that high RCF values prevail due to abrupt stress changes. This was particularly the case in instances where the various tunnels were subjected to high abutment stresses.

It was also found that higher RCF values are predicted in tunnels located in the deeper sections of the mine, which is evident that depth below surface plays a major role in influencing RCF values. However, it was noted that these values were not above the RCF threshold and higher values were only predicted in isolated instances, where the tunnels had to negotiate abutments and were thus exposed to abrupt stress changes.

While it is true that depth below surface influences RCF values, it is also true that other factors such as the extent of mining and proximity of stoping abutments also influence stress conditions and thus influence predicted RCF values.

For this reason, it was concluded that predicted high RCF values do not form the basis for delineation of separate ground control districts.

CHAPTER 6: DETERMINATION OF SUPPORT REQUIREMENTS

6.1 Introduction

Support requirements can be determined from rock mass classification systems and numerical modelling analyses. This chapter determines the theoretical support requirements for a tunnel based on the modified Q-system and RCF modelling. The support requirements are then compared to the actual support installed in the tunnels considered and compliance to recommendations is measured.

6.2 Support Requirements based on Numerical Modelling

The rock wall condition factor (RCF) was used to determine the support requirements for the different tunnels located in the defined polygons, i.e. Kop Upper, Kop Middle and Kop Lower. The formulation of the RCF is based on a simple comparison of the maximum induced tangential stress of an assumed circular excavation to the estimated rock mass strength (Jager & Ryder, 1999) and is defined by Equation 30 in Chapter 5.

In general, for RCF<0.7, good conditions prevail with minimum support requirements. According to Jager and Ryder (1999), an RCF value of 0.7 equates to an absolute tangential stress level of approximately 0.7 times the uniaxial compressive strength of the intact rock, equivalent to a field stress level of 0.3 times the UCS.

For 0.7<RCF<1.4, average conditions prevail with moderate support system requirements.

For RCF>1.4, poor ground conditions prevail with special support requirements. Tables 12-14, as proposed by Jager and Ryder (1999) provide support guidelines and recommendations for the different RCF spectra.

Table 12: Support recommendations for good ground conditions (RCF<0.7)

Case	Primary Support (Typical Requirements)	Secondary Support (Typical Requirements)
Static stress conditions	‘Spot’ support where necessary (rock bolts etc).	‘Spot’ support where necessary (rock bolts, etc). Light mesh where ground conditions are inherently poor.
Stress changes anticipated	‘Spot’ support where necessary (rock bolts etc).	Fully grouted tendons>1.5m in length, installed on basic 2m pattern. Support resistance: 30-50kN/m^2. Rope lacing (sidewalls only) plus light mesh where ground conditions are inherently poor.

Seismic activity anticipated	Tendons>1.2m in length, installed as close to face as possible, on a basic 2m or 1.5m: Support Resistance 305kN/m^2	Fully grouted (preferably yielding) tendons>1.5m in length, installed on basic 2m pattern. Support resistance: 50kN/m^2. Light mesh and lace (hangingwall and sidewalls).

Table 13: Support recommendations for average ground conditions (0.7<RCF<1.4)

Case	**Primary Support** **(Typical Requirements)**	**Secondary Support** **(Typical Requirements)**
Static stress conditions	Rock bolts or tendons>1.5min length, installed as close to face as possible on basic 2m pattern. Support Resistance: 30-50kN/m^2	Steel strapping or rope lacing integrated with primary support tendons; or shotcrete.
Stress changes anticipated	Fully grouted tendons or steel ropes>1.8m in length, installed as close to face as possible, on a basic 2m or 1.5m pattern. Support resistance: 40-60kN/m^2	Medium strength rope lacing and moderate strength wire mesh integrated with primary support tendons.
Seismic activity anticipated	Fully grouted (preferably yielding) tendons or steel ropes>1.8m in length installed as close to the face as possible, on a 1.5m or double 2m pattern: Support resistance:98110kN/m^2	Strong rope lacing and strong, stiff wire mesh integrated with primary support tendons, plus optional shotcrete.

Table 14: Support recommendations for poor ground conditions (RCF >1.4)

Case	**Primary Support (Typical Requirements)**	**Secondary Support (Typical Requirements)**
Static stress conditions	(If necessary) shotcrete to face, then fully grouted tendons or steel ropes, length>1.8m on basic 1.5m pattern, as close to face as possible. Support resistance: 80-110kN/m^2	Moderate strength steel wire mesh usually with additional tendons but may be integrated with primary support, optional shotcrete
Stress changes anticipated	(If necessary) reinforced shotcrete to face, then fully grouted steel ropes or yielding tendons, length>18m on basic 1m or double 2m pattern, as close to face as possible. Support Resistance: 120-203kN/m^2	Medium strength rope lacing and moderate strength wire mesh with additional tendons but may be integrated with primary support. Add integral shotcrete in long-life tunnels. If necessary, additional hangingwall support comprising grouted steel ropes

Seismic activity anticipated	(If necessary) reinforced shotcrete to face, then fully grouted steel ropes of yielding tendons, length >2.3m on basic 1m pattern as close to face as possible. Support Resistance: 220290kN/m^2	Strong rope lacing and strong, stiff wire mesh with additional tendons but may be integrated with primary support. Add integral shotcrete in long-life tunnels. If necessary, additional hangingwall support comprising grouted steel ropes.

6.3 Support Requirements based on Rock Mass Classifications

Of the commonly utilized rock mass classification methods, the Q-system as modified by Kirsten (1988) provides a more consistent method for ground quantification and support selection. The system is less open to interpretation and the difficulty in deciding whether a rock mass is homogeneous or non-homogeneous is eliminated. The system overcomes this challenge by allowing for the calculation of Q for homogeneous and non-homogeneous rock and then using the minimum of the two values (Dukes, 2002).

The rock mass Q ratings are related to support requirements by introducing an additional parameter known as the Equivalent Dimension of the excavation. This parameter was first defined by Barton (1974) and is obtained by dividing the span, diameter or wall height of the excavation by a quantity called the Excavation Support Ratio. The formula for the calculation of the Equivalent Dimension is presented in equation 29. The value of ESR is related to the intended use of the excavation and to the degree of security which is demanded of the support system installed to maintain the stability of the excavation. The ESR values have been suggested by Barton (1974) and are presented in Table 8 of this report.

The determined Q and ESR values are plotted on the support design charts developed by Kirsten (1988). From these charts, support requirements in the form of bolt spacing and shotcrete thickness can be determined for the various tunnels.

Table 15 provides a comparison of the support requirements as determined from the modified Q-system against the actual support installed in the various tunnels. Subsections 5.3.1-5.3.4 provides a detailed description of the tunnels that were analysed for this exercise.

In applying the system, both the intact and downgraded values of the uniaxial compressive strength were used. The UCS for intact rock was downgraded according to the formula:

$$\boldsymbol{\sigma_c}\,\textbf{rock mass} = \mathbf{s}\sqrt{\boldsymbol{\sigma_c}}\ \text{(MPa)} \qquad \text{[EQ 32]}$$

where s is a constant used to downgrade the intact rock and which is dependent on the properties of the rock mass

This resulted in the downgrading of the intact UCS from 172MPa to 25MPa. A minimum RMR value of 69 was obtained, resulting in an “s” value of 0.0205 for good quality rock mass.

An excavation support ratio (ESR) of 1.6, correlating to a permanent mine opening was used. The spans of the respective tunnels were taken as 3.5m. This resulted in the equivalent dimension (D_e) given by span/ESR of 2.188. The calculation table for determining the modified Q value is shown in Appendix F.

6.4 Comparison of Predicted Support Requirements vs Actual Support

Table 15 shows the support installed in tunnels in the respective areas and the support requirements as determined from the graphs developed by Kirsten (1988).

Table 15: Comparison of installed support vs, support as predicted by the modified Q- system

Tunnel	**Actual Support Installed**	**Mod. Q-System (Q = 0.03)** **UCS = 172 MPa**	**Mod. Q-System (Q = 0.03)** **UCS = 25 MPa**
42 BW 2 Area (Kop Upper)	Unibars 2.3m (100 kN) on a 1m spacing giving a support resistance of 100kN/m^2 Destranded hoist rope 2.3m (98kN), mesh (100 mm aperture) and lacing on a 1m pattern giving a support resistance of 98kN/m^2 25mm (25t) grouted cables on a 3m pattern· Total support resistance is 226kN/m^2	Mesh or fibre-reinforced shotcrete 75mm - 150 mm thick, and, Tensioned grouted rock bolts 0.7 m apart, i.e. 0.5 m^2/bolt. Assuming 100kN anchors, support resistance is 200kN/m^2	Mesh or fibre-reinforced shotcrete 150mm thick, and, Tensioned grouted rock bolts, 0.7m apart, i.e. 0.5m^2/bolt. Assuming a 100kN anchors, support resistance is 200kN/m^2
		Q = 0.02 **UCS = 172MPa**	**Q = 0.02** **UCS = 25MPa**
44 BW3 Area (Kop Middle)	Unibars 2.3m (100 kN) on a 1m spacing giving a support resistance of 100kN/m^2 Destranded hoist rope 2.3m (98kN), mesh (100 mm aperture) and lacing on a 1m pattern giving a support resistance of 98kN/m^2 25mm (25t) grouted cables on a 3m pattern· Total support resistance is 226kN/m^2	Mesh or fibre-reinforced shotcrete 175 mm thick, and, Grouted rock bolts 0.6 m apart, i.e. 0.36 m2/bolt. Assuming 100kN anchors, support resistance is 278kN/m^2	Mesh or fibre-reinforced shotcrete 175 mm thick, and, Grouted rock bolts, 0.6m apart, i.e. 0.36m2/bolt. Assuming a 100kN anchors, support resistance is 278kN/m^2
		Q = 0.02 **UCS = 172 MPa**	**Q = 0.02** **UCS = 25 MPa**

62 DW/68 DW4 and 59 SW3 Area (Kop Lower)	Unibars 2.3m (100 kN) on a 1m spacing giving a support resistance of 100kN/m^2 Destranded hoist rope 2.3m (98kN), mesh (100 mm aperture) and lacing on a 1m pattern giving a support resistance of 98kN/m^2 25mm (25t) grouted cables on a 3m pattern. Total support resistance is 226kN/m^2	Mesh or fibre-reinforced shotcrete 175 mm thick, and, Grouted rock bolts 0.6 m apart, i.e. 0.5 m^2/bolt. Assuming 100kN anchors, support resistance is 278kN/m^2	Mesh or fibre-reinforced shotcrete 175 mm thick, and, Grouted rock bolts, 0.6m apart, i.e. 0.36m^2/bolt. Assuming a 100kN anchors, support resistance is 278kN/m^2

6.5 Discussion

The support strategy currently applied on all tunnels at Kopanang mine is uniform. A similar strategy is applied on all tunnels irrespective of their lateral or vertical spatial location.

The results obtained from numerical modelling suggest that tunnels located at greater depth are subjected to higher stresses and may even be prone to seismicity and rockburst damage. High RCF values are not a widespread occurrence but rather coincide with and are limited to small sections of the tunnels which may coincidentally have been subjected to high abutment stresses because of adjacent stoping.

A comparison of the numerical modelling results to the support requirements as determined from the RCF guidelines (Tables 12-14), suggests that the support currently being installed in most tunnels at Kopanang is adequate for the prevailing conditions. However, in areas where RCF values have been predicted to be higher than 1.4., the same RCF guidelines suggest that the support installed in the tunnels is not adequate for the conditions that prevail and needs to be reviewed.

The tunnel support requirements suggested by the modified Q-system are summarized in Table 15. The variations observed in the Q values determined from using this system highlighted differences in rock mass conditions observed on the eastern side of the mine from those observed on the western side of the mine. The current support strategy in use in both these areas of the mine does not cater for this observed variation. A comparison between the tunnel support resistance suggested by the modified Q-system and the actual support installed indicates that the best correlation, albeit low, is obtained when the Q index is calculated using the intact rock UCS and the permanent support graph. For the tunnels analysed, the support resistance required by the modified Q-system was between 200kN/m^2 and 278kN/m^2, for the range of Q-values obtained. The actual support resistance of the support installed in the tunnel was calculated to be 98kN/m^2. This resulted in only 35% - 49% conformance of the actual support to that suggested by the modified Q-system. The long tendon support resistance was calculated to be 226kN/m^2 and this was close to the 278kN/m^2 predicted by the modified Q-system, attaining a conformance over 80%.

However, underground observations made in the tunnels suggested that the support installed in the hangingwall and the sidewalls performed satisfactorily, with bulging of the hangingwall and sidewall having been well contained by the mesh and lacing. This bears further testament to the possible shortcomings of overly relying on rock mass classification systems in this type of environment.

6.6 Chapter Summary

This chapter presented the results of the comparison between the support as predicted by a rock mass classification and the support installed in the tunnels. The tunnels were rated using the modified Q-system.

When applying the modified Q-system, both downgraded and intact values of the uniaxial compressive strength (UCS) were used. The intact UCS of 172MPa was downrated to 25MPa.

An excavation support ratio (ESR) of 1.6 correlating to a permanent mine opening was used. The span of the tunnel was 3.5m, and thus the equivalent dimension was taken as 2.188.

The support comparison was done using support design graphs as developed by Kirsten (1988). The results obtained were compared to the actual support installed in the tunnels. The support installed at the mine was kept constant throughout and did not differentiate based on lateral variations although the results of the Q-system predicted poor rock mass conditions towards the eastern section of the mine.

Good correlation was however observed between the actual support and the requirements as predicted by the modified Q system. The best correlation was noted to be when using the intact UCS. A support resistance correlation was observed to be between 35% and 49% for primary support, while correlation on long tendon support was 82%. Observations made underground, however, suggested that the actual support installed performed satisfactorily, thereby possibly highlighting the shortcomings of rock mass classifications in deep mining environments.

The actual support installed was further compared to the requirements as determined by numerical modelling. These results suggested a good correlation in areas where the RCF values were predicted to be low or moderate. In areas where high RCF values were predicted, the comparison suggested that the support installed was not adequate.

It was however also noted that the high RCF value predicted were only limited to shorter segments of the tunnels, which were at the time subjected to high abutment stresses.

CHAPTER 7: CONCLUSIONS AND RECOMMENDATIONS

7.1 Conclusions

A ground control district (GCD) is defined as a portion of the mine in which a given set of geological conditions, with associated rock-related hazards, permits a common set of rock engineering strategies to be employed to minimize the risks.

This research evaluated the classification and delineation of ground control districts on Kopanang mine as well as the suitability of the support methods being utilized in these areas.

The approach and methodology is two-fold: The first part examined the quality of the rock mass across the mine by applying rock mass classification systems. The second part utilized numerical modelling to assess the influence of stress on rock mass quality.

The rock mass analysis for the mine was conducted using the Q-system, the Modified Q-system and the Geomechanics system. These classification systems were chosen amongst several available systems based on their suitability as well as their common use in underground mining application as established from the literature review.

For this research, a total of twenty (20) borehole core samples were analysed. All three classification systems predicted fair to poor quality rock mass across the mine. It was also observed that there was a good correlation between the three systems in that, they all predicted the rock mass quality to worsen towards the eastern section of the mine. It could also be established that the variation in rock mass quality between the eastern and western sections of the mine could be attributed to the nature of deposition of ore at Kopanang mine. It was noted that the poor conditions encountered in the eastern portion of the mine were because of the orthoquartzite exposed in these areas.

It could be concluded that, at the time of deposition, the eastern portion of the mine was located close to the edge of the depositional river. Thus, the poor quality orthoquartzite was preserved in this area and has resulted in the challenges that are currently being experienced with the footwall. In contrast, it was concluded that the western side was deposited towards the centre of the depositional channel, hence the orthoquartzite in the western side was completely eroded. It was concluded that this lateral variation in the rock mass quality between the eastern and western side is a basis for the delineation of the eastern and western sections of the mine as two separate ground control districts.

The limitations of the rock mass classification systems were also noted. It was concluded that although a useful tool, results obtained from rock mass classifications should not be accepted at face value. The use of these classification methods should rather be restricted to environments for which they were developed.

The second part of the evaluation of the ground control districts involved the analysis of the influence of stress on the rock mass conditions across the mine. This was conducted using the Vantage program which is a boundary element program developed by the Institute of Mine Seismology (IMS). For this analysis, tunnels were selected in the different polygons and strings were put along the tunnels to calculate the RCF values along the tunnels.

From the results, it could be established, that higher RCF values were predicted with an increase in depth below the surface. It was also noted that the high RCF values predicted did not extend over the entire length of the tunnel but were rather concentrated to smaller segments of the tunnel which were particularly subjected to high abutment stresses. It was concluded that the difference in depth between the different sections of the mine could not be used as a basis for the delineations of a separate ground control district.

Lastly, a comparison was done between the actual support installed in the tunnels in the different polygons and the requirements as determined by the rock mass classification and numerical modelling.

Good correlation was found between the actuals support and the requirements as determined by the Modified Q-system, particularly when using the intact rock strength.

A support resistance correlation was calculated by comparing the actual support resistance and the required support resistance as suggested by the Modified Q-system. The correlation was observed to have been within 35%-43% for primary support, and 82% for long tendon support. Observations made underground suggested that the actual support installed performed satisfactorily.

The actual support installed was further compared to the requirements as determined by numerical modelling. These results suggested a good correlation in areas where the RCF values were predicted to be low or moderate. In areas where high RCF values were predicted, the comparison suggested that the support installed was not adequate.

It was however also noted that the high RCF value predicted were only limited to shorter segments of the tunnels which were at the time subjected to high abutment stresses.

7.2 Recommendations

The recommendation from research report is thus that Kopanang mine be re-delineated in terms of lateral variations. The result will be two ground control districts, namely:

The Kop_East - This will incorporate all the working places from the shaft area and extending to the SE3 and SW4 areas of the mine.

Kop_West - This will incorporate all the working places from the western side of the shaft and extending to the BW2 and BW3 areas of the mine.

It is recommended that the support strategies employed in this area not be altered as good correlation was observed between the actual installed support in the tunnels and the requirements as predicted by rock mass classification systems. It is however recommended that in areas where high abutment stresses are anticipated, the support be tailored to be in line with industry requirements and predictions by numerical modelling.

It is further recommended that no delineation be made based on the influence of stress, since this parameter is influenced by other factors such as surrounding mining and mining configurations.

REFERENCES

Adams, G., Jager, A. & Roering, C., 1981. Investigations of rock fracturing ahead of stope faces in deep-level gold mines. *Rock Mechanics from Research to Application. Proceedings of the 22nd US Symposium on Rock Mechanics.* Massachusetts, American Rock Mechanics Association, pp. 227-236.

Anon.,n.d. Igneous rocks classification diagrams. [Online]

Availableat:https://www.thoughtco.com/igneous-rock-classification-diagrams-4122900 [Accessed 19 May 2019].

Barton, N., 1988. "Rock mass classification and tunnel reinforcement selection using the Q-System," in *Rock* Classification Systems for Engineering Purposes, Philadelphia: American Society for Testing and Materials (ASTM).

Barton, N., Lien, R. & Lunde, J., 1974. Engineering classification of rock masses for design of tunnel support. *Rock Mechanics and Rock Engineering,* 6(4), pp. 189-236.

Bhoi, M. (2012). Creep Behaviour of Rock, Bachelor of Technology thesis, National Institute of Technology, Rourkela

Bieniawski, Z., 1978. "Determining rock mass deformability: Experience from case studies". *International Journal of Rock Mechanics and Mining Sciences & Geomechanics Abstracts,* 15(5), pp. 237-247.

Bieniawski, Z., 1989. Engineering rock mass classifications. New York: John Wiley and Sons, Inc.

Brady, B. & Brown, E., 1993. Rock mechanics for underground mining. 3rd ed. London: Chapman and Hall.

Cai, M.,Kaizer, P.K., Uno, H. & Tasaka, Y., 2004. Estimation of rock mass deformation modulus and strength of jointed hard rock masses using the GSI system. *International Journal of Rock Mechanics and Mining Sciences,* 41(1), pp. 3-19.

COP, 2017. Mandatory code of practice to combat rockfall and rockburst accidents, Klerksdorp: Kopanang Mine Internal Report.

Dukes, G., 2002. Tunnel support evaluation using a modified version of Barton's Q System, Vaal Reefs, Orkney: AngloGoldAshanti Limited, Unpublished Internal Report.

Dunn, M. & Hungwe, G., 2002. The application of a rock mass rating system at Tau Lekoa Mine, Vaal Reefs, Orkney: AngloGoldAshanti Limited, South Africa, Internal Report.

Esterhuizen, G., 2014. Extending empirical evidence through numerical modelling in rock engineering design. *The Journal of the Southern African Institute of Mining and Metallurgy,* 114(10), pp. 755-764.

Goodman, R., 1989. Introduction to rock mechanics. 2nd ed. Canada: John Wiley and Sons.

Gumede, H. & Stacey, T., 2007. Measurement of typical joint characteristics in South African gold mines and the use of these characteristics in the prediction of rockfalls. *The Journal of the Southern Institute of Mining and Metallurgy,* 107(5), pp. 335-344.

Haile, A., Grave, D., Sevume, C. & Le Bron, K., 1998. Strata control in tunnels and an evaluation of support units and systems currently used with a view to improving the effectiveness of support, stability and safety of tunnels (GAP 335), Johannesburg: Safety in Mines Research Advisory Committee.

Handley, M., 2017. Theoretical rock mechanics for professional practice. Johannesburg:

The South African Institute of Mining and Metallurgy.

Hoek, E., 1998. Rock Engineering Course Notes. [Online]

Available at: http://www.rocscience.com/hoek-corner.htm

Hoek, E. & Brown, E., 1980. Underground excavation in rock. 1st ed. London: The Institute of Mining and Metallurgy.

Hoek, E., Kaiser, P. & Bawden, W., 1995. Support of underground excavation in hard rock. Rotterdam: Balkema.

Jaeger, J. & Cook, N., 1979. Fundamentals of Rock Mechanics. 3rd ed. Great Britain:

Fletcher & Son Ltd, Norwich.

Jager, A. & Ryder, J., 1999. A handbook on rock engineering for tabular hard rock mines. 1st ed. Johannesburg: The Safety in Mines Research Advisory Committee (SIMRAC).

Jager, A., Wojno, L. & Henderson, N., 1990. "New developments in the design and supportof tunnels under high stress conditions". Johannesburg, SAIMM, pp. 1155-1171.

Jjuuko, S. & Kalumba, D., 2016. Application of thin spray-on liners for rock surface support in South African mines - A Review. *International Journal of Innovative Research in Advanced Engineering (IJIRAE),* 3(7), pp. 42-54.

Kaiser, P. & Cai, M., 2012. Design of rock support systems under rockburst conditions. Journal of *Rock Mechanics and Geotechnical Engineering,* 4(3), pp. 215-227.

Kersten, R., Piper, P. & Greef, H., 1983. Assessment of support requirements for large excavations at depth. Johannesburg, SANGORM, pp. 41-46.

Kirsten, H., 1988. Norwegian Geotechnical Institute or Q System by N Barton.

Philadelphia, ASTM STP 984.

Kristjansson, G., 2014. Rock bolting and pull-out tests on rebar bolts (Thesis), s.l.: Norwegian University of Science and Technology.

Laubscher, D., 1977. Geomechanics classification of jointed rock masses-mining applications. *Trans. Instn. Min. Metall.*, 86(1), pp. A1-8.

Lauffer, H., 1958. Gebirgskiassifiziering fur den spollenbau. *Geologie en Bauwesen,* 24(1), pp. 46-51.

Marinos, P., Marinos, V. & Hoek, E., 2006. The Geological Strength Index - A characterization tool for assessing engineering properties for rock masses, s.l.: European Social Fund and Greek National Resources.

Mark, C., 2016. Science of empirical design in mining ground control. *International Journal of Mining Science and* Technology*,* 26(3), pp. 461-470.

More O'Ferral, R. & Brinch, G., 1983. An approach to the design of tunnels for ultra deep mining in the Klerksdorp District. Johannesburg, SANGORM.

Napier, J., Malan, D. & Sellers, E., 1998. Implications of fracture zone behaviour in deep level gold mines. Johannesburg, SIMRAC.

Ongoje, J., 2017. Geotechnical engineering design of a tunnel support system - a case study of the Karuma (600MW) Hydropower project, Cape Town: University of Cape Town.

Ortlepp, W. & Gay, N., 1984. Performance of an experimental tunnel subjected to stresses ranging from 50MPa to 230MPa. Cambridge, ISRM.

Palmstrom, 1982. The volumtric joint count - A useful and simple measure of the degree of rock jointing. *Proc. 4th Congr. Int. Asse. Engng. Geol. Delhi 5*, pp. 221-228.

Palmstrom, A. & Broch, E., 2006. Use and Misuse of rock mass classification systems with particular reference to the Q-system. *Tunnels and Undergound Space Technology,* 21(6), pp. 575-593.

Palmstrom, A. & Singh, R., 2001. The deformation modulus of rock masses - Comparisons between in situ tests and indirect estimates. *Tunnelling and Underground Space Technology,* 16(3), pp. 115-131.

Piper, P., 1985. The application and evaluation of rock mass classification methods for the design and support of underground excavations at depth. Randburg, Johannesburg, ISRM.

Potvin, Y. P. & Wesseloo, J., 2012. Some pitfalls and misuses of rock mass classification systems for mine design. *The Journal of the Southern African Institute of Mining and Metallurgy,* 112(8), pp. 697-702.

Roy, M., & Rao, S. (2015, October). *Analysis of creep behaviour of soft rocks in tunneling*. Retrieved from Researchgate: http://www.researchgate.net/publication/306018025

Ryder, J. & Jager, A., 2002. A textbook on rock mechanics for tabular hard rock mines. 1st ed. Johannesburg: The Safety in Mines Advisory Committee.

Serafim, J. & Pereira, J., 1983. Consideration of the Geomechanics Classification of Bieniawski. *International Journal of Rock Mechanics and Mining Sciences & Geomechanics Abstracts,* 21(1), pp. 1133-1144.

Spearing, A., 1995. Handbook on hard-rock strata control. 1st ed. Johannesburg: The South African Institute of Mining and Metallurgy.

Starfield, A. & Cundall, P., 1988. Towards a methodology for rock mass mechanics modelling. *International Journal of Rock Mechanics and Mining Sciences & Geomechanics,* 25(3), pp. 99-106.

Stini, I., 1950. Tunnelbaugeologie, Vienna: Springer Verlag.

Swart, A., 2005. Investigation of factors governing the stability of stope panels in hard rock mines in order to define a suitable design methodology for shallow mining operations, MEng dissertation, Pretoria: University of Pretoria.

Tannant, D., 2001. Thin spray-on liners for underground rock support. Perth, Australian Centre for Geomechanics.

Terzaghi, K., 1946. Rock defects and loads on tunnel support. In: R. Procter & T. White, eds. Rock tunnelling with steel supports. Youngtown, Ohio: Commercial shearing and stamping company, pp. 17-99.

Van Aswegen, G. & Stander, M., 2012. Origins of some fractures around tabular stopes in deep South African mines. *The Journal of the South African Institute of Mining and Metallurgy*, 112(8), pp. 729-735.

Vasarhelyi, B. & Kovacs, D., 2017. Empirical methods of calculating the mechanical properties of the rock mass. *Period.Polytech.Civil Eng,* 61(1), pp. 39-50.

Watts, M., 2004. The structural evolution of Kopanang Gold Mine: A working model, Klerksdorp: AnglogoldAshanti Limited unpublished internal report

APPENDIX A: Classification of individual parameters used in the Tunnelling Quality Index Q

1. JOINT SET NUMBER (J_n)

DESCRIPTION	*VALUE*
A. Massive, few random joints	**1.0**
B. One joint set	**2.0**
C. One joint set plus random joints	**3.0**
D. Two joint sets	**4.0**
E. Two joint sets plus random joints	**6.0**
F. Three joint sets	**9.0**
G. Three joint sets plus random joints	**12.0**
H. Four or more joint sets, random heavily jointed	**15.0**
I. Crushed rock	**20.0**

2. JOINT ROUGHNESS NUMBER (J_r)

DESCRIPTION	*VALUE*		
	Discontinuous	Undulating	Planar
A. Rough or irregular	**4.0**	**3.0**	**1.5**
B. Smooth	**3.0**	**2.0**	**1.0**
C. Slickensided	**2.0**	**1.5**	**0.5**
D. +5mm thick gouges	**1.5**	**1.0**	**1.0**

3. ROCK QUALITY DESIGNATION (RQD)	
DESCRIPTION	***VALUE***
A. Very poor	**0 - 25**
B. Poor	**25 -50**
C. Fair	**50 - 75**
D. Good	**75 - 90**
E. Very good	**90 - 100**
Note 1: Where RQD<10, use value of 10	
and if RQD>100, use value of 100	

4. JOINT ALTERATION NUMBER (J_a)			
DESCRIPTION	**Fill<1mm**	**Fill 1-5mm**	**Fill>5mm**
A. Tightly healed, hard rockwall joints, (Quartz)	**0.8**	**1.0**	**2.0**
B. Unaltered joint walls	**1.0**	**2.0**	**3.0**
C. Non-cohesive mineral (Calcite)	**2.0**	**4.0**	**6.0**
D. Serpentinite/Talc Infill	**3.0**	**6.0**	**10.0**
E. Clay	**4.0**	**8.0**	**12.0**
F. Shattered Zones or crushed rock	**5.0**	**10.0**	**12.0**

5. JOINT WATER (J_w)	
DESCRIPTION	**VALUE**
A. Dry	**1.0**
B. Wet/Moist	**0.8**
C. Dripping water (< 5litres/min)	**0.5**
D. Gushing >10l/min	**0.1**

6 STRESS REDUCTION FACTOR (SRF)	
DESCRIPTION	***VALUE***
A. No shear, faults,	**1.00**
B. One shear/fault or major E-W joints with opposing dips.	**2.50**
C. One shear/fault and blocky ground	**4.00**
D. Multiple faults or dykes	**6.00**
E. Curved Low angled joints or domes	**7.50**
F. Joints sub // to advance direction (same/opposing dips)	**8.00**
H. Multiple faults/Wide shears mylonite zones	**10.00**

APPENDIX B: Rock mass Rating System (Bieniawski, 1989)

A. CLASSIFICATION PARAMETERS AND THEIR RATINGS

	Parameter		Range of values						
1	Strength of intact rock material	Point-load strength index	>10 MPa	4 - 10 MPa	2 - 4 MPa	1 - 2 MPa	For this low range - uniaxial compressive test is preferred		
		Uniaxial comp. strength	>250 MPa	100 - 250 MPa	50 - 100 MPa	25 - 50 MPa	5 - 25 MPa	1 - 5 MPa	< 1 MPa
	Rating		15	12	7	4	2	1	0
2	Drill core Quality *RQD*		90% - 100%	75% - 90%	50% - 75%	25% - 50%	< 25%		
	Rating		20	17	13	8	3		
3	Spacing of discontinuities		> 2 m	0.6 - 2 . m	200 - 600 mm	60 - 200 mm	< 60 mm		
	Rating		20	15	10	8	5		
4	Condition of discontinuities (See E)		Very rough surfaces Not continuous No separation Unweathered wall rock	Slightly rough surfaces Separation < 1 mm Slightly weathered walls	Slightly rough surfaces Separation < 1 mm Highly weathered walls	Slickensided surfaces or Gouge < 5 mm thick or Separation 1-5 mm Continuous	Soft gouge >5 mm thick or Separation > 5 mm Continuous		
	Rating		30	25	20	10	0		
5	Ground water	Inflow per 10 m tunnel length (l/m)	None	< 10	10 - 25	25 - 125	> 125		
		(Joint water press)/(Major principal σ)	0	< 0.1	0.1, - 0.2	0.2 - 0.5	> 0.5		
		General conditions	Completely dry	Damp	Wet	Dripping	Flowing		
	Rating		15	10	7	4	0		

B. RATING ADJUSTMENT FOR DISCONTINUITY ORIENTATIONS (See F)

Strike and dip orientations		Very favourable	Favourable	Fair	Unfavourable	Very Unfavourable
Ratings	Tunnels & mines	0	-2	-5	-10	-12
	Foundations	0	-2	-7	-15	-25
	Slopes	0	-5	-25	-50	

C. ROCK MASS CLASSES DETERMINED FROM TOTAL RATINGS

Rating	100 ← 81	80 ← 61	60 ← 41	40 ← 21	< 21
Class number	I	II	III	IV	V
Description	Very good rock	Good rock	Fair rock	Poor rock	Very poor rock

D. MEANING OF ROCK CLASSES

Class number	I	II	III	IV	V
Average stand-up time	20 yrs for 15 m span	1 year for 10 m span	1 week for 5 m span	10 hrs for 2.5 m span	30 min for 1 m span
Cohesion of rock mass (kPa)	> 400	300 - 400	200 - 300	100 - 200	< 100
Friction angle of rock mass (deg)	> 45	35 - 45	25 - 35	15 - 25	< 15

E. GUIDELINES FOR CLASSIFICATION OF DISCONTINUITY conditions

Discontinuity length (persistence) Rating	< 1 m 6	1 - 3 m 4	3 - 10 m 2	10 - 20 m 1	> 20 m 0
Separation (aperture) Rating	None 6	< 0.1 mm 5	0.1 - 1.0 mm 4	1 - 5 mm 1	> 5 mm 0
Roughness Rating	Very rough 6	Rough 5	Slightly rough 3	Smooth 1	Slickensided 0
Infilling (gouge) Rating	None 6	Hard filling < 5 mm 4	Hard filling > 5 mm 2	Soft filling < 5 mm 2	Soft filling > 5 mm 0
Weathering Ratings	Unweathered 6	Slightly weathered 5	Moderately weathered 3	Highly weathered 1	Decomposed 0

F. EFFECT OF DISCONTINUITY STRIKE AND DIP ORIENTATION IN TUNNELLING**

Strike perpendicular to tunnel axis		Strike parallel to tunnel axis	
Drive with dip - Dip 45 - 90°	Drive with dip - Dip 20 - 45°	Dip 45 - 90°	Dip 20 - 45°
Very favourable	Favourable	Very unfavourable	Fair
Drive against dip - Dip 45-90°	Drive against dip - Dip 20-45°	Dip 0-20 - Irrespective of strike°	
Fair	Unfavourable	Fair	

APPENDIX C: Support design chart for determining shotcrete thickness and bolt spacing for temporary support (reproduced from Kirsten, 1988)

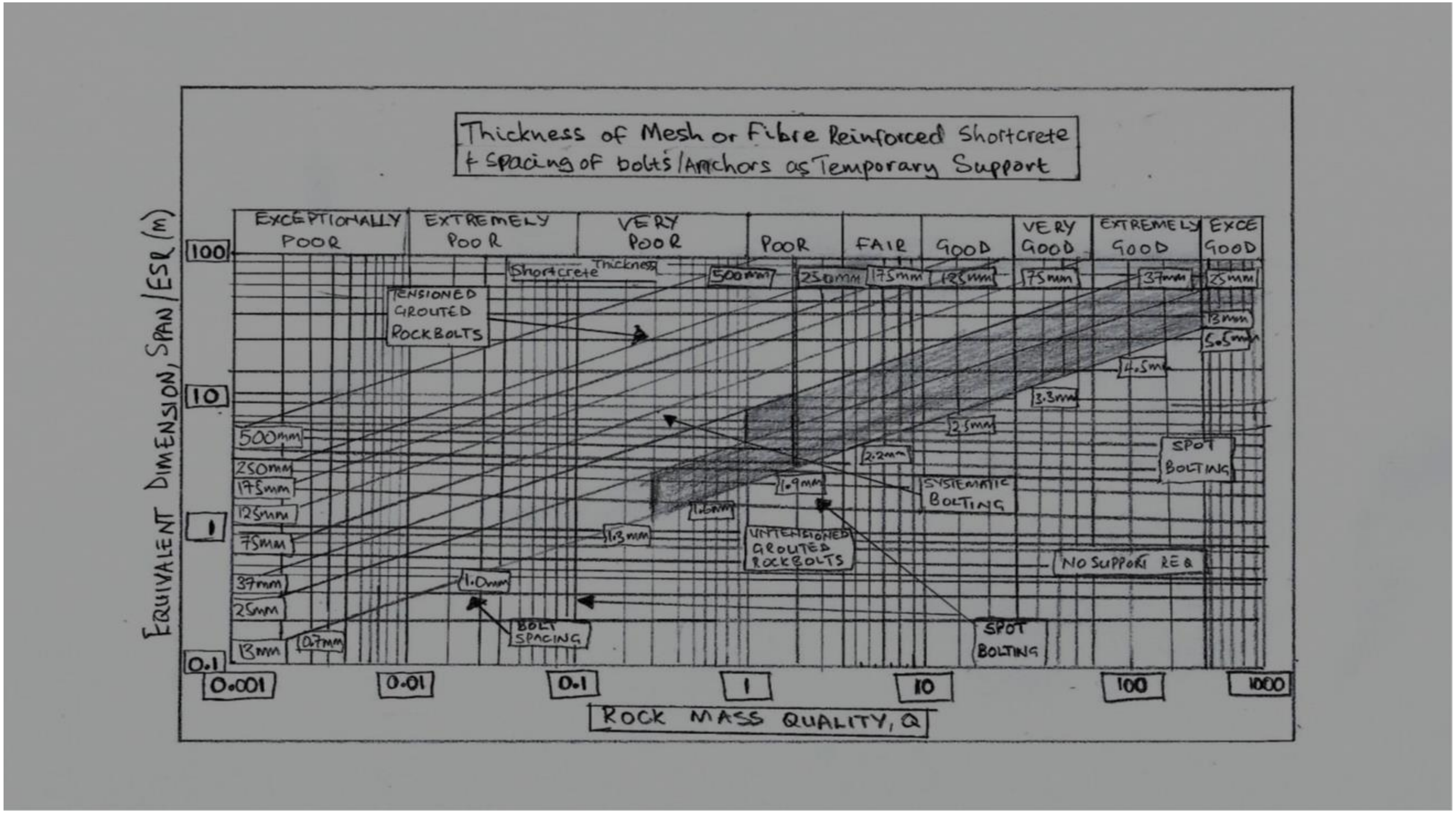

APPENDIX D: Support design chart for determining shotcrete thickness and bolt spacing for permanent support (Kirsten, 1988)

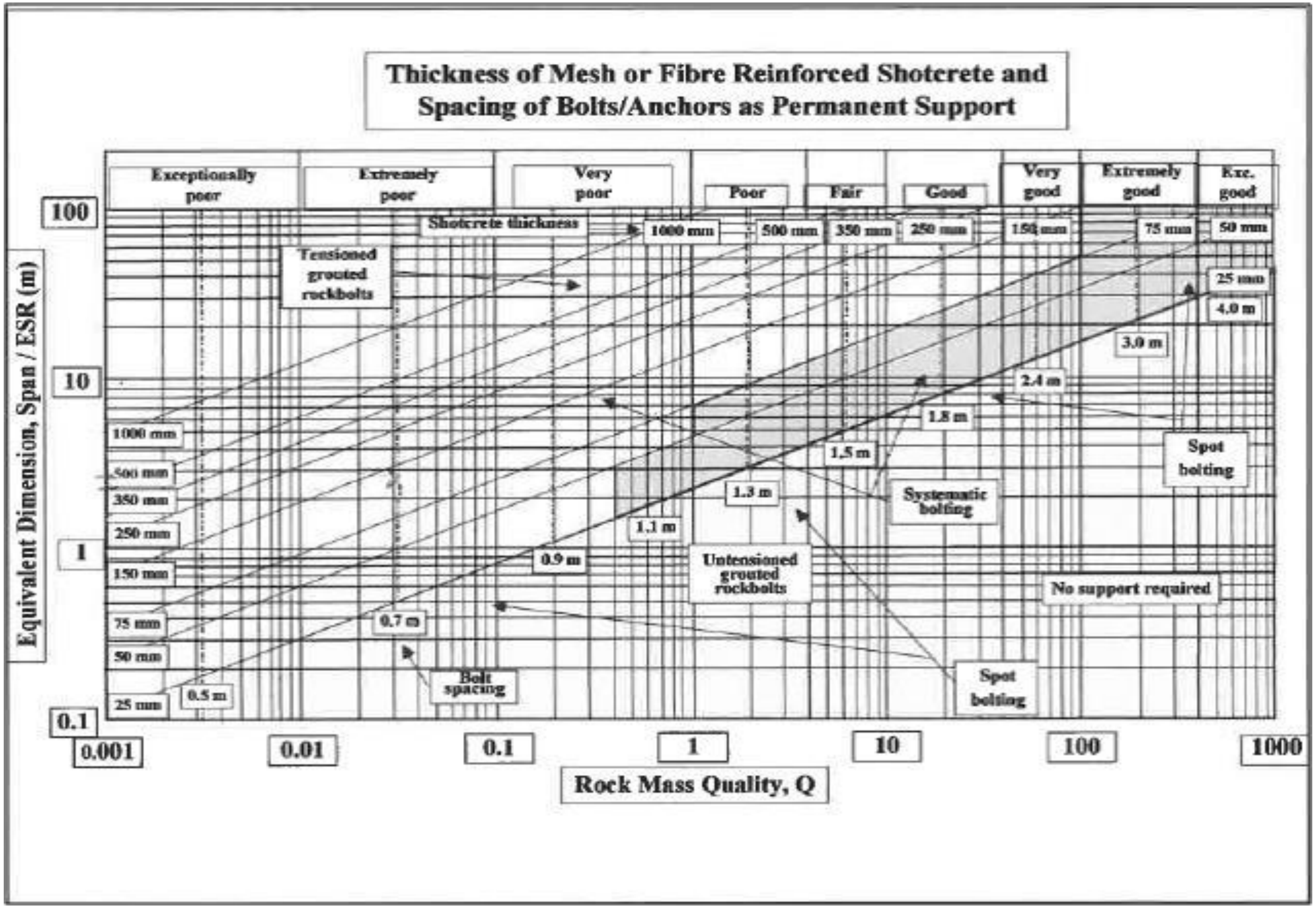

APPENDIX E: Input Data and Calculations for Q Values

					Project Data Input Sheet					
Borehole ID	Working Place	Core Length(m)	Intact length(m)	RQD	Jn	Jr	Ja	Jw	SRF	Q
K10403	42 BW2 6S	86	39	45.34884	6	1.5	1	1	1	11.33721
K10411	42 BW2 6S	91	42	46.15385	6	1.5	1	1	1	11.53846
K10431	42 BW2 6S	69	35	50.72464	6	1.5	1	1	1	12.68116
K10412	42 BW2 6S	95	40	42.10526	6	1.5	1	1	1	10.52632
K10408	42 BW2 6S	87	40	45.97701	6	1.5	1	1	1	11.49425
K10287	42 BW2 16C	90	28	31.11111	6	1.5	1	1	1	7.777778
K10269	44 BW3 16C	82	38	46.34146	6	1.5	1	1	1	11.58537
K10265	44 BW3 16C	71	16	22.53521	6	1.5	1	1	1	5.633803
K10325	44 BW3 16C	83	20	24.09639	6	1.5	1	1	1	6.024096
K10317	59 SW3 23XC	65	21	32.30769	6	1.5	1	1	1	8.076923
K10318	59 SW3 23XC	35	9	25.71429	6	1.5	1	1	1	6.428571
K10306	59 SW3 23XC	41	14	34.14634	6	1.5	1	1	1	8.536585
K10313	62 DW Haulage	53	15	28.30189	6	1.5	1	1	1	7.075472
K10311	62 DW Haulage	68	22	32.35294	6	1.5	1	1	1	8.088235
K10301	68 DW4 14 XC	27	8	29.62963	6	1.5	1	1	1	7.407407
K10416	68 DW4 14 XC	84	35	28	6	1.5	1	1	1	7
K10426	68 DW4 14 XC	64	24	37.5	6	1.5	1	1	1	9.375
K10468	68 DW4 14 XC	72	18	25	6	1.5	1	1	1	6.25
K10472	68 DW4 14 XC	59	16	27.11864	6	1.5	1	1	1	6.779661
K10445	68 DW4 14 XC	63	16	25.39683	6	1.5	1	1	1	6.349206

APPENDIX

APPENDIX F: Input Data and Calculations for Modified Q Values

Borehole ID	Working Place	Depth Below Surface(m)	Core Length(m)	Intact length(m)	RQD	σ_c	H	Q	SRF_n	SRF_h	K	Q_n	Q_h
K10403	42 BW2 6S	1769	86	39	45.34884	172	1769	11.33721	77.18651	262.4351	2.179385	15.39122	0.0432
K10411	42 BW2 6S	1769	91	42	46.15385	172	1769	11.53846	76.73962	262.4351	2.179385	15.80008	0.0439669
K10431	42 BW2 6S	1769	69	35	50.72464	172	1769	12.68116	74.38511	262.4351	2.179385	18.1872	0.0483211
K10412	42 BW2 6S	1769	95	40	42.10526	172	1769	10.52632	79.10014	262.4351	2.179385	13.78005	0.0401102
K10408	42 BW2 6S	1769	87	40	45.97701	172	1769	11.49425	76.83689	262.4351	2.179385	15.70997	0.0437985
K10287	44 BW3 16C	1769	90	28	31.11111	172	1769	7.777778	87.40698	262.3985	2.146725	8.77877	0.029637
K10269	44 BW3 16C	1841	82	38	46.34146	172	1841	11.58537	76.63695	262.7722	2.146725	15.89588	0.0441456
K10265	44 BW3 16C	1841	71	16	22.53521	172	1841	5.633803	97.22186	262.7722	2.146725	5.429419	0.0214674
K10325	44 BW3 16C	1841	83	20	24.09639	172	1841	6.024096	95.09641	262.7722	2.146725	5.999263	0.0229546
K10317	59 SW3 23XC	2286	65	21	32.30769	172	2286	8.076923	86.32514	265.636	2.44636	9.286571	0.0307768
K10318	59 SW3 23XC	2286	35	9	25.71429	172	2286	6.428571	93.07878	265.636	2.44636	6.609209	0.0244959
K10306	59 SW3 23XC	2286	41	14	34.14634	172	2286	8.536585	84.76268	265.636	2.44636	10.08492	0.0325284
K10313	62 DW Haulage	2371	53	15	28.30189	172	2371	7.075472	90.17978	266.1371	2.44636	7.624203	0.0269608

K10311	62 DW Haulage	2371	68	22	32.35294	172	2371	8.088235	86.28528	266.1371	2.44636	9.305957	0.0308199
K10301	68 DW4 14 XC	2548	27	8	29.62963	172	2548	7.407407	88.82569	266.5916	2.101058	8.163222	0.0282257
K10416	68 DW4 14 XC	2548	84	35	28	172	2548	7	90.49948	266.5916	2.101058	7.503347	0.0266733
K10426	68 DW4 14 XC	2548	64	24	37.5	172	2548	9.375	82.18223	266.5916	2.101058	11.59568	0.0357231
K10468	68 DW4 14 XC	2548	72	18	25	172	2548	6.25	93.94811	266.5916	2.101058	6.337532	0.0238154
K10472	68 DW4 14 XC	2548	59	16	27.11864	172	2548	6.779661	91.45971	266.5916	2.101058	7.154163	0.0258337
K10445	68 DW4 14 XC	2548	63	16	25.39683	172	2548	6.349206	93.46113	266.5916	2.101058	6.488001	0.0241934

APPENDIX G: Input Data and Calculations for Stress Ratios

Sigma 3						Sigma 1				
42 BW2 _3-12						42 BW2_3-12				
	Jul	Aug	Sep				Jul	Aug	Sep	
	52	54	54				131	144	144	
	39	42	43				77	82	89	
	42	45	46				81	89	92	
	44	44	45				97	98	98	
	44	44	45				96	96	97	
	36	36	37				85	85	87	
	34	42	47				74	90	94	
	45	49	37				92	102	107	
	37	38	44				86	89	91	
	33	39	37				64	79	85	
	43	44	51				81	82	84	
	39	39	39				79	84	91	
	32	34	42				78	81	85	
	36	38	45				80	88	93	

Mean	39.71429	42	43.71429	**41.80952**

Mean	85.78571	92.07143	95.5	**91.11905**

Sigma 3				
44 BW1_2-10				
	Jul	**Aug**	**Sep**	
	33	34	34	
	41	33	33	
	47	47	48	
	92	94	92	
	33	36	38	
	35	34	29	
	44	37	36	
	48	45	39	
	34	37	46	
	57	34	56	
	33	58	40	
	32	34	45	
Mean	44.08333	43.58333	44.66667	**44.11111**

Sigma 1				
44 BW1_2-10				
	Jul	**Aug**	**Sep**	
	84	86	86	
	104	91	91	
	113	114	115	
	165	169	166	
	71	76	79	
	71	77	81	
	87	89	89	
	102	76	109	
	75	77	92	
	103	104	112	
	72	73	75	
	73	80	82	
Mean	93.33333	92.66667	98.08333	**94.69444**

Sigma 3				
62 SW4_18S-19A				
	Jul	Aug	Sep	
	555	557	558	
	381	383	384	
	202	481	481	
	374	376	377	
	185	312	313	
	235	270	270	
	259	260	262	
	137	138	125	
	111	111	113	
	243	371	391	
	100	112	202	
Mean	252.9091	306.4545	316	**291.7879**

Sigma 1				
62 SW4_18S-19A				
	Jul	Aug	Sep	
	1217	1223	1225	
	890	894	895	
	502	953	953	
	832	835	838	
	489	746	747	
	539	582	583	
	620	622	626	
	332	333	281	
	262	263	265	
	462	693	732	
	2389	268	465	
Mean	775.8182	673.8182	691.8182	**713.8182**

Sigma 3				
68 DE4_14S-18A				
	Jul	Aug	Sep	
	149	179	95	
	114	103	102	
	86	87	88	
	51	55	59	
	54	56	57	
	56	56	56	
	56	59	58	
	75	67	72	
Mean	80.125	82.75	73.375	**78.75**

Sigma 1				
68 DE4_14S-18A				
	Jul	Aug	Sep	
	305	346	369	
	193	173	185	
	171	172	175	
	99	102	111	
	115	117	119	
	110	110	110	
	125	134	135	
	172	155	168	
Mean	161.25	163.625	171.5	**165.4583**

APPENDIX H: Input Data and Calculations for Rock Mass Ratings

						Project Data Input Sheet						
Borehole ID	**Working Place**	**UCS**	**Rating**	**RQD**	**Rating**	**Spacing**	**Rating**	**Condition of Discontinuity**	**Rating**	**Groundwater Condition**	**Rating**	**Adj.for discontinuity**
K10403	42 BW2 6S	172	12	45.34884	8	200mm	10	Rough, Separation <0.1mm, No infilling, Slightly weathered	27	Completely Dry	15	Favourable
K10411	42 BW2 6S	172	12	46.15385	8	200mm	10	Rough, Separation <0.1mm, No infilling, Slightly weathered	27	Completely Dry	15	Favourable
K10431	42 BW2 6S	172	12	50.72464	13	200mm	10	Rough, Separation <0.1mm, No infilling, Slightly weathered	27	Completely Dry	15	Favourable
K10412	42 BW2 6S	172	12	42.10526	8	200mm	10	Rough, Separation <0.1mm, No infilling, Slightly weathered	27	Completely Dry	15	Favourable
K10408	42 BW2 6S	172	12	45.97701	8	200mm	10	Rough, Separation <0.1mm, No infilling, Slightly weathered	27	Completely Dry	15	Favourable
K10287	44 BW2 16C	172	12	31.11111	8	200mm	10	Rough, Separation <0.1mm, No infilling, Slightly weathered	27	Completely Dry	15	Favourable
K10269	44 BW3 16C	172	12	46.34146	8	200mm	10	Rough, Separation <0.1mm, No infilling,	27	Completely Dry	15	Favourable

								Slightly weathered				
K10265	44 BW3 16C	172	12	22.53521	3	200mm	10	Rough, Separation <0.1mm, No infilling, Slightly weathered	27	Completely Dry	15	Favourable
K10325	44 BW3 16C	172	12	24.09639	3	200mm	10	Rough, Separation <0.1mm, No infilling, Slightly weathered	27	Completely Dry	15	Favourable
K10317	59 SW3 23XC	172	12	32.30769	8	200mm	10	Rough, Separation <0.1mm, No infilling, Slightly weathered	27	Completely Dry	15	Favourable
K10318	59 SW3 23XC	172	12	25.71429	8	200mm	10	Rough, Separation <0.1mm, No infilling, Slightly weathered	27	Completely Dry	15	Favourable
K10306	59 SW3 23XC	172	12	34.14634	8	200mm	10	Rough, Separation <0.1mm, No infilling, Slightly weathered	27	Completely Dry	15	Favourable
K10313	62 DW Haulage	172	12	28.30189	8	200mm	10	Rough, Separation <0.1mm, No infilling, Slightly weathered	27	Completely Dry	15	Fair
K10311	62 DW Haulage	172	12	32.35294	8	200mm	10	Rough, Separation <0.1mm, No infilling, Slightly weathered	27	Completely Dry	15	Fair
K10301	68 DW4 14 XC	172	12	29.62963	8	200mm	10	Rough, Separation <0.1mm, No infilling,	27	Completely Dry	15	Favourable

								Slightly weathered				
K10416	68 DW4 14 XC	172	12	28	8	200mm	10	Rough, Separation <0.1mm, No infilling, Slightly weathered	27	Completely Dry	15	Favourable
K10426	68 DW4 14 XC	172	12	37.5	8	200mm	10	Rough, Separation <0.1mm, No infilling, Slightly weathered	27	Completely Dry	15	Favourable
K10468	68 DW4 14 XC	172	12	25	8	200mm	10	Rough, Separation <0.1mm, No infilling, Slightly weathered	27	Completely Dry	15	Favourable
K10472	68 DW4 14 XC	172	12	27.11864	8	200mm	10	Rough, Separation <0.1mm, No infilling, Slightly weathered	27	Completely Dry	15	Favourable
K10445	68 DW4 14 XC	172	12	25.39683	8	200mm	10	Rough, Separation <0.1mm, No infilling, Slightly weathered	27	Completely Dry	15	Favourable